ABSTRACT

Title of Dissertation: EFFECT OF RELATIVE SPECTRAL RESPONSE ON MULTI-SPECTRAL MEASUREMENTS AND NDVI FROM DIFFERENT REMOTE SENSING SYSTEMS

David James Fleming, Doctor of Philosophy, 2006

Dissertation Directed By: Professor Samuel N. Goward
Department of Geography

Spectrally derived metrics from remotely sensed data measurements have been developed to improve understanding of land cover and its dynamics. Today there are an increasing number of remote sensing systems with varying characteristics that provide a wide range of data that can be synthesized for Earth system science. A more detailed understanding is needed on how to correlate measurements between sensors. One factor that is often overlooked is the effect of a sensor's relative spectral response (RSR) on broadband spectral measurements.

This study examined the variability in spectral measurements due to RSR differences between different remote sensing systems and the implications of these variations on the accuracy and consistency of the normalized difference vegetation index (NDVI). A theoretical model study and a sensor simulation study of laboratory and remotely sensed

hyper-spectral data of known land cover types was developed to provide insight into the effect on NDVI due to differences in RSR measurements of various land cover signatures.

This research has shown that the convolution of RSR, signature reflectance and solar irradiance in land cover measurements leads to complex interactions and generally small differences between sensor measurements. Error associated with cross-senor calibration of signature measurements and the method of band radiance conversion to reflectance also contributed to measurement discrepancies. The effect of measurement discrepancies between sensors on the accuracy and consistency of NDVI measurements of vegetation was found to be dependent on the increasing sensitivity of NDVI to decreasing band measurements. A concept of isolines of NDVI error was developed as a construct for understanding and predicting the effect of differences in band measurements between sensors on NDVI. NDVI difference of less than 0.05 can be expected for many sensor comparisons of vegetation, however, some cases will lead to higher differences. For vegetation signatures used in this study, maximum effect on NDVI from measurement differences was 0.063 with an average of 0.023. For sensors with well aligned RSRs such as Landsat 7 ETM+ and MODIS, NDVI differences in the range of 0.01 are possible.

EFFECT OF RELATIVE SPECTRAL RESPONSE ON MULTI-SPECTRAL MEASUREMENTS AND NDVI FROM DIFFERENT REMOTE SENSING SYSTEMS

By

David James Fleming

Dissertation submitted to the Faculty of the Graduate School of the
University of Maryland, College Park, in partial fulfillment
of the requirements for the degree of
Doctor of Philosophy
2006

Advisory Committee:
Professor Samuel N. Goward, Chair
Dr. Gregory T. Koeln
Professor Shunlin Liang
Professor John Townshend
Professor Richard Weismiller

Dedication

In loving memory of my mother Helene for her inspiration and belief in me, and to my wife Nina for her undying support and everlasting encouragement that made this endeavor possible.

Acknowledgements

I would like to thank and recognize those that have helped me through this academic journey. I must first thank Rory Shefferman and Dr. Gary Roggin who were instrumental in providing the encouragement to return to graduate school to pursue a doctorate degree. Without my wife, Nina, this degree would not have been possible. She provided the encouragement and support to pursue and complete this degree through a cross country move, job changes, house selling and buying, home remodeling, long hours at work, and the addition of two wonderful children to our family. She has been dedicated to my completion of this degree, and has sacrificed to ensure my commitment to the program. My son Brayden and daughter Bryce have also been a tremendous inspiration to succeed.

I thank Samuel Goward for giving me the opportunity to work on the CRESS program and more importantly, for being my mentor. Sam's wisdom and guidance were instrumental to the development of this research. His enthusiasm about Earth System Science has been motivating and his encouragement was fundamental to completing the degree. I thank John Townshend for helping me focus my interest in high-resolution satellite imagery and for his guidance and insight, and Shunlin Liang for his enthusiasm to help me learn the technical aspects of remote sensing. I would also like to thank Greg Koeln and Richard Weismiller for their guidance in the proposal to implementation phase of this research. In addition, I must thank the CRESS program team Paul Davis, Lee Miller, and Clay Baros who all shared in the original work comparing the IKONOS and

Landsat 7 ETM+ radiometry, and Jeff Masek who provided mathematical and scientific expertise early in the CRESS program.

Finally, I am truly grateful to Dr. John Craven for his vigilance to keep me on the path to completion. He has spent endless hours in discussion and review of this research and provided invaluable guidance, encouragement, enthusiasm, and wisdom. He has been a great inspiration.

Table of Contents

List of Tables

List of Figures

List of Equations

Chapter 1: Introduction

Remote Sensing of NDVI

Vegetation land cover monitoring and characterization is important in ecological research (Qin et al., 2002). Vegetation is diagnostic of the photosynthetic life process and characteristics of vegetation have a fundamental and profound relationship with physical and biological Earth processes at all scales. Remote sensing provides a primary means of conducting this monitoring, since vegetation dominates remotely sensed measurements for most land areas of our planet.

Photosynthetic processes are generally consistent and common across Earth vegetation types. Studies of vegetation spectral reflectance properties began as early as the late 1920's (Billings & Morris, 1951). These same processes also underpin the formation of vegetation solar wavelength spectral reflectance properties and are amenable to monitoring by electro-optical remote sensing systems. Over the last three decades, spectrally derived metrics from remotely sensed data measurements have been developed to improve understanding of land cover and its dynamics. For example, Jordan (1969) used near infrared vs. red ratio for estimating biomass. The normalized difference vegetation index (NDVI), a contrast of red and near infrared spectral measurements, first used with Landsat MSS data (Rouse et al., 1973), has served as the primary metric used to evaluate green vegetation properties such as canopy closure, leaf area index, and biomass because its relation to green vegetation photosynthetic properties.

Today there are an increasing number of remote sensing systems with varying characteristics (Bailey et al., 2001) available that provide a wide range of Earth system science data for the scientific community (Kramer, 1996). As the number and diversity of remote sensing systems has increased, so has the use of data synthesized from multiple sensor sources. These sensors vary in spatial resolution, radiometric precision, temporal coverage, and spectral characteristics.

These factors, combined with the dynamic condition of the Earth and the atmosphere, produce complex measurements that vary with sensor characteristics. This necessitates the need for a clearer understanding of the effects of variations in sensor characteristics and their ultimate effect on measurements and NDVI. Various researchers have addressed at least some of these complexities. Given the large number of multi-spectral sensors that have been and will continue to be used for Earth observations, a more detailed understanding is needed on how to correlate measurements between sensors (Chilar, 2000; Goward et al., 2003).

Relative Spectral Response

One factor that is often overlooked is the effect of a sensor's relative spectral response (RSR), or spectral response function (SRF), on broadband spectral measurements. The RSR describes the quantum efficiency of a sensor at specific wavelengths over the range of a spectral band. Currently, general descriptors, such as bandwidth and average band pass, are often the only spectral characteristics considered in analysis of sensor spectral

measurements. However, cross-sensor wavelength variations in RSR can lead to measurement discrepancies between sensor measurements that make them not directly comparable (Teillet et al., 1997). In order to provide consistent quantitative spectral measurements of vegetation land cover and derived metrics, such as spectral vegetation indices, the effect of a sensor's SRF must be considered and understood.

The main problem with comparing spectral measurements between sensors is that the magnitude of the RSR effect varies with spectral signatures of land features observed. The result is variability in measurements between different sensors even after inter-calibration techniques are applied. This variability may lead to reduced accuracy, precision, and consistency of land cover measurements.

Research Conducted

The research in this dissertation develops relationships between red and near infrared spectral band measurements and NDVI due to differences in relative spectral responses of different remote sensing systems. This study examines, quantitatively, the magnitude and significance of the effect of sensor RSR on multi-spectral measurements of vegetation and the comparability of these measurements between sensor systems. This effect was evaluated with a spatially independent theoretical model, followed by a sensor simulation study that uses specific sensor RSRs to determine measurement discrepancies of land cover signatures from different sensors. The Theoretical Model explores the effect RSR in relation to land cover characteristics and is based on band spectral characteristics of land cover signatures and theoretical RSRs that include a square wave and Gaussian

response plus two opposed extreme wavelength biased responses. The square wave response function was based on the Landsat Data Continuity Mission (LDCM) data specification bandwidths (NASA, 2003). The RSRs used for the simulation study include the square wave response used in the Theoretical Model as well as the relative spectral responses of IKONOS, Landsat 7 ETM+, Moderate Resolution Imaging Spectrometer (MODIS), and the Advanced Very High Resolution Radiometer (AVHRR). Particular attention was placed on vegetation signature characteristics in relation to the RSR. For both the Theoretical Model and Sensor Simulation Study, cross-sensor responses of reflectance were evaluated to determine differences between spectral responses and effect on NDVI.

Chapter 2: Background

Spectral Vegetation Indices

Healthy green vegetation displays a characteristic (Figure 1) spectrum across the visible, near and shortwave infrared wavelengths, because of variations in internal leaf structure, pigment composition, water content, surface roughness, and in cellular refractive indices (Tucker & Garratt, 1977).

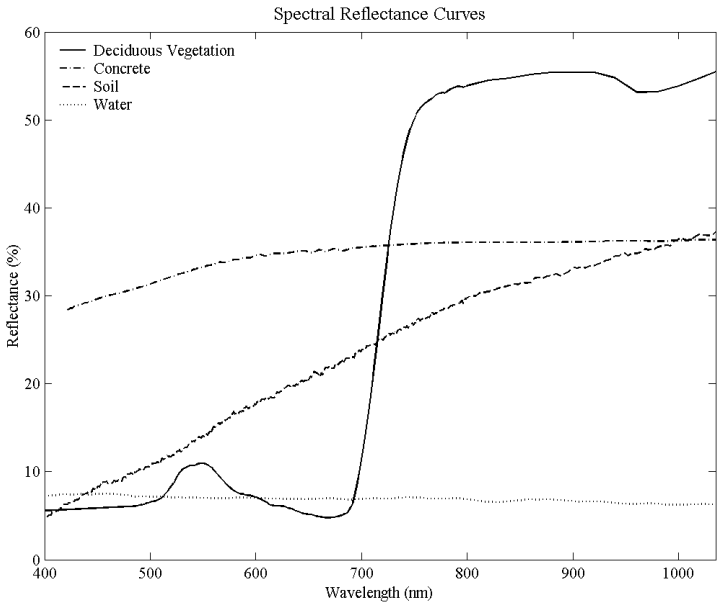

Figure 1. Spectral reflectance characteristics of a range of land cover types: vegetation, concrete, soil, and water.

Most all healthy living vegetation share a characteristic contrast in reflectance between the visible region just below 700nm and near infrared wavelengths just above 700nm (Figure 2). This contrast has become an important vegetation metric since its discovery. Remotely sensed spectral data used to derive vegetation indices (VI) have become one of the primary information sources to characterize the surface of the Earth (Teillet et al.,

1997) and employed as a measure of green vegetation density (Steven et al., 2003). This is because vegetation indices are most commonly combinations of visible and near infrared spectral information, which can be used as a strong indicator of active photosynthetic green biomass (Tucker, 1979) and to monitor the status and quantity of green foliage vegetation across the globe (Goward et al., 2003).

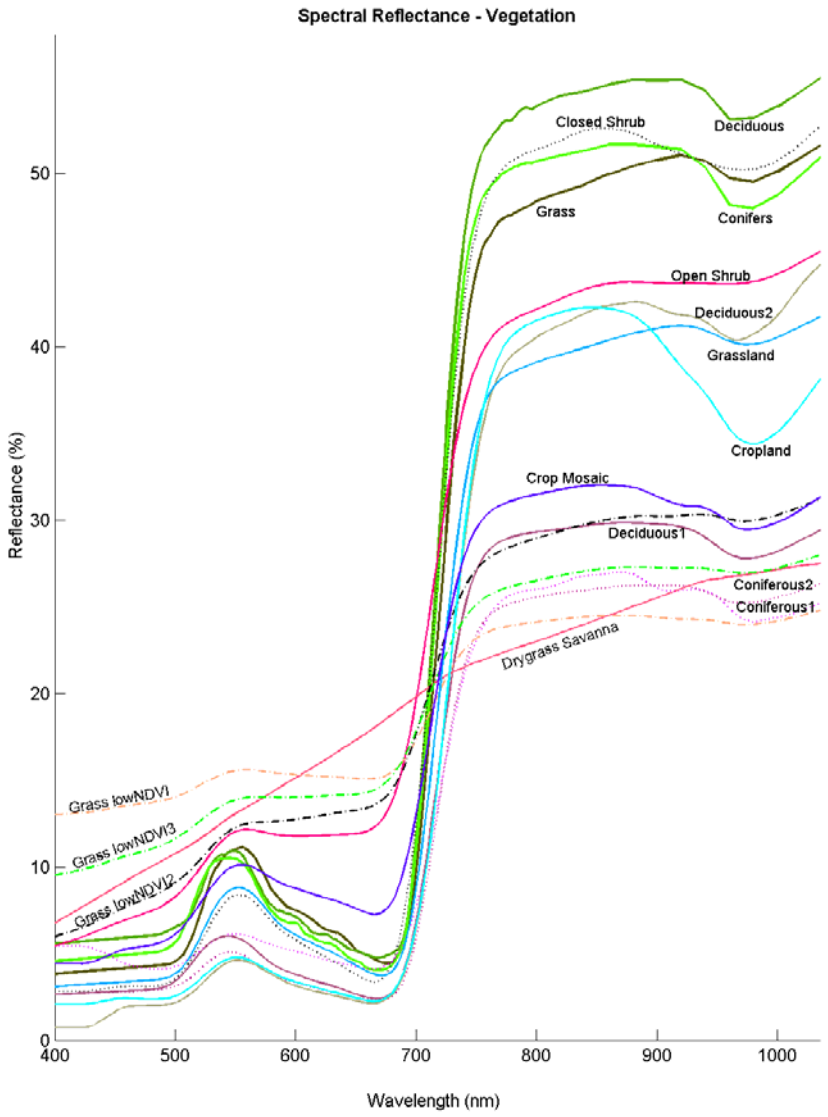

Figure 2. Spectral signatures for a variety of vegetation types from ASTER (Hook, 1998) and Probe 1 (Secker et al., 1999) data.

Vegetation indices have been used to make quantitative estimates of leaf area index, percent ground cover, plant height, biomass, plant population, and other biophysical parameters (Perry & Lautenschlager, 1984). They have additionally been applied to a wide range of studies at various scales ranging from continental scale vegetation dynamics, global plant responses to climate change, regional crop yield predictions, and to local scale precision farming (Steven et al., 2003).

There have been a multitude of vegetation index transformations proposed for monitoring vegetation using visible and near infrared spectral measurements (Deering et al., 1975; Huete, 1988; Jackson, 1983; Kaufman & Tanré, 1992; Wiegand & Richardson, 1984). Other transforms using additional spectral measurements, such as the tassel cap transformation (Kauth & Thomas, 1976) have also been proposed and employed. Many of these transforms have been developed in an attempt to compensate for variable background (e.g. soil & litter) reflectance and some forms of atmospheric attenuation, while emphasizing vegetation spectral features (Trishchenko et al., 2002).

The normalized difference vegetation index (NDVI), a red and near infrared band combination vegetation index, originally developed by Rouse for the Landsat MSS sensor (Jensen, 1996; Tucker, 1979), has remained the prevalent index used to measure vegetation characteristics (Trishchenko et al., 2002). NDVI is defined as:

$$NDVI = \frac{\rho_{nir} - \rho_{vis}}{\rho_{nir} + \rho_{vis}} \qquad \text{Equation 1}$$

ρ_{vis} = Visible band reflectance
ρ_{nir} = Near infrared band reflectance

Vegetation indices are designed around high red band energy absorption by chlorophyll in contrast with high near infrared reflectance due to scattering from plant cell walls of green plants (Turner et al., 1999). High absorption in the red band results in a non-linear inverse relationship with biomass (Figure 3) and a characteristic low band reflectance (Tucker, 1979).

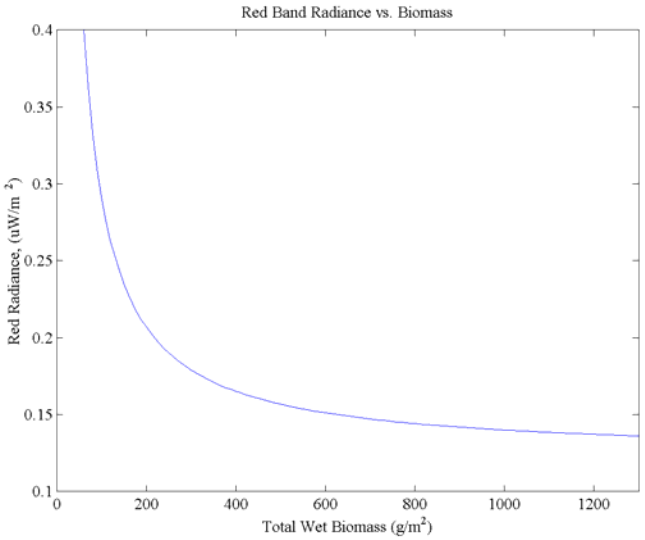

Figure 3. Red radiance vs. biomass (Tucker, 1979).

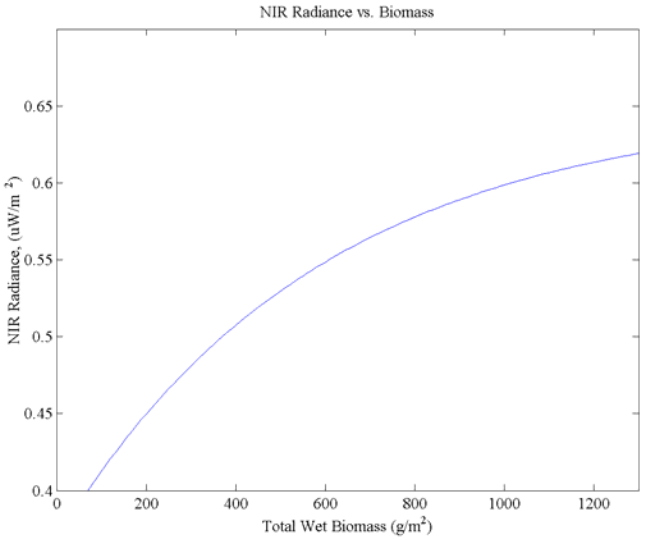

Figure 4. Near infrared radiance vs. biomass (Tucker, 1979).

Although there are various forms of chlorophyll, chlorophyll a and chlorophyll b are the most frequent in higher plants and absorb in the vicinity of 645 nm (Gates et al., 1965) in the red band. The near infrared band, on the other hand, exhibits a nonlinear direct relationship with biomass (Figure 4) (Tucker, 1979). This is due to the absence of absorption in this wavelength region and, therefore, high spectral reflection in the infrared region above approximately 700 nm (Sinclair et al., 1971). This leads to an enhanced or increased level of reflected radiance over background materials (Tucker, 1979). The "red edge" at approximately 720nm is where scattering dominates and absorption ceases (Goward et al., 2003; Wooley, 1971).

NDVI is related to vegetation biophysical phenomena including leaf area index (LAI), biomass, percent ground cover, and fraction of photosynthetically active radiation absorbed (f_{APAR}) (Hummrich & Goward, 1997). These vegetation attributes are used in various models to study photosynthesis, carbon budgets, water balance, and terrestrial processes (Goward et al., 1991). The accuracy and precision of measured vegetation indices will, therefore, effect the estimations of these parameters. The sensitivity of a particular parameter will depend on its relationship to spectral vegetation indices and upon the application or model to which these parameters are applied.

NDVI and Photosynthetically Active Radiation

Biomass accumulation (Figure 5) is nearly linearly related to NDVI (Deering & Haas, 1980) and to the amount of incident solar radiation intercepted by the vegetation canopy. NDVI has a one-to-one relation with percentage photosynthetically active radiation

(PAR) absorbed by the canopy and an error of .01 NDVI leads to an approximately 1% error rate in estimating PAR absorption.

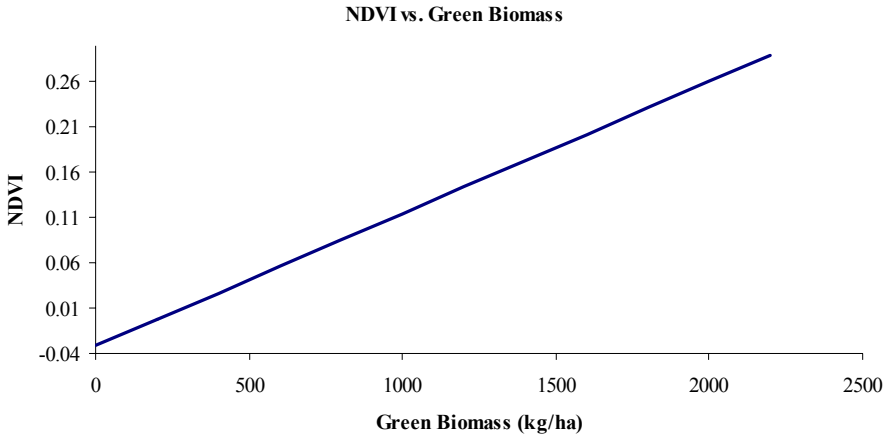

Figure 5. NDVI vs. green biomass (Deering & Haas, 1980).

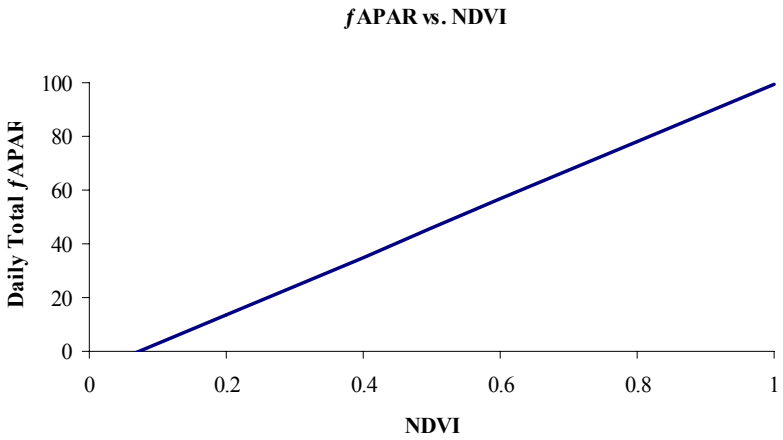

Figure 6. SAIL modeled *f*APAR vs. NDVI (Goward & Hummerrich, 1992).

Small errors such as this in NDVI can produce large errors in inferred processes, particularly those which are cumulative, such as primary production. Kaufman and Holben's 1990 study of tropical grassland production estimates varied by as much as 30% when using NDVI for PAR estimations due to drift in calibrations of only 0.05

NDVI units (Goward et al., 1991). For typical observing conditions NDVI is also near linearly related to both instantaneous and daily total f_{APAR}. A 0.1 change in NDVI (Figure 6) will result in an approximate change of 10% in f_{APAR} (Goward & Hummerrich, 1992).

NDVI and Leaf Area Index

LAI is an important parameter in a number of models related to ecosystem functioning, carbon budgets, climate, hydrology, primary productivity, and others. A number of approaches have been employed to estimate LAI including the use of empirical spectral/vegetation indices and physically based canopy inversion models. The complexity of inversion techniques makes them unpopular and has driven the need for more simplistic approaches using spectral indices- LAI relationships (Chaurasia & Dadhwal, 2004).

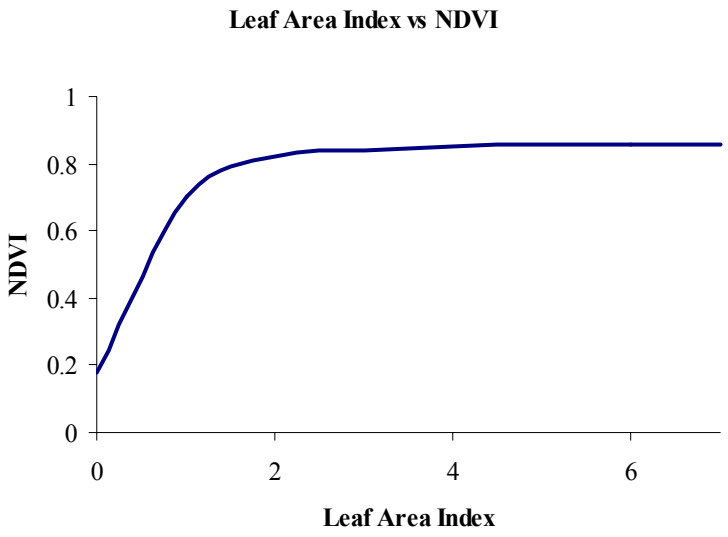

Figure 7. Leaf Area Index vs. NDVI (Choudhury, 1987).

Many studies have shown that vegetation indices reach a saturation level with increasing LAI values and can be fitted to an exponential equation or set in the form of simple semi-empirical Beer's Law (Baret & Guyot, 1991). Choudhury (1987) showed that at low LAI values this leads to a relatively small linear increase in LAI with increasing NDVI until an asymptote is reached, at which point, high values of NDVI result in a relatively large range of LAI values (Figure 7).

Different Sources of Remote Sensing Measurements

The diversity of sensors that have been used since the beginning of space-acquired land multi-spectral measurements is substantial. For example, The Landsat series of satellite sensors (Table 1), operated from 1972, have flown on 7 separate satellite platforms and employed 3 generations of sensor systems (RBV, MSS and TM). There have been 3 RBV sensor versions, 5 MSS sensor and 4 TM sensors. These sensors operate at the scale of tens of meters (Teillet et al., 2001) with varying visible, near infrared, and thermal spectral bands.

Platform	Sensor	Spectral Range	Spectral Bands	Spatial Resolution	Sensor	Spectral Range	Spectral Bands	Spatial Resolution	Sensor	Spectral Range	Spectral Bands	Spatial Resolution
Landsat 1	RBV	.5-.75um	1	40m	MSS	.5-11 um	4	79m				
Landsat 2	RBV	.5-.75um	1	40m	MSS	.5-11 um	4	79m				
Landsat 3					MSS	.5-12.6um	5	79m				
Landsat 4					MSS	.5-11 um	4	79m	TM	.45-12.5 um	7	30m, 120m (band 6)
Landsat 5					MSS	.5-11 um	4	79m	TM	.45-12.5 um	7	30m, 120m (band 6)
Landsat 6			Never Reached Orbit						ETM	.45-12.5 um	7	30m, 120m (band 6)
Landsat 7									ETM+	.45-12.5 um	7	30m, 60m (band 6)

Table 1. Landsat satellite series sensors (Kramer, 1996; Sample, 2004).

The AVHRR sensors (Table 2), flown on the NOAA polar orbiter satellites have operated since 1978 (NOAA, 2004), collect infrared and thermal spectral information at the spatial scale of kilometers, and have been used for global monitoring of terrestrial environments.

There have been three series of AVHRR instruments that include the four-channel radiometers AVHRR/1 onboard the Tiros-N, NOAA-6, -8 and –10; the five-channel radiometers AVHRR/2 deployed on NOAA-7, -9, -11, -12, and –14; followed by a six-channel radiometer AVHRR/3 aboard NOAA-15 and –16. Though the spectral bands of these systems are similar, they differ in shape, central wavelength location, and bandwidth, especially in the transition area (0.68-0.72 um) from chlorophyll absorption to foliage reflection (Trishchenko et al., 2002).

Platform	Sensor	Spectral Range	Spectral Bands	Spatial Resolution
Tiros-N	AVHRR/1	.58-11.3 um	4	1.1 km
NOAA-6	AVHRR/1	.58-11.3 um	4	1.1 km
NOAA-8	AVHRR/1	.58-11.3 um	4	1.1 km
NOAA-10	AVHRR/1	.58-11.3 um	4	1.1 km
NOAA-7	AVHRR/2	.58-12.5um	5	1.1 km
NOAA-9	AVHRR/2	.58-12.5um	5	1.1 km
NOAA-11	AVHRR/2	.58-12.5um	5	1.1 km
NOAA-12	AVHRR/2	.58-12.5um	5	1.1 km
NOAA-14	AVHRR/2	.58-12.5um	5	1.1 km
NOAA-15	AVHRR/3	.58-12.5um	6	1.1 km
NOAA-16	AVHRR/4	.58-12.5um	6	1.1 km

Table 2. AVHRR series sensors (Hastings & Emery, 1992; Kramer, 1996)

In addition to differences among sensors within the same series of satellites, a large increase has been seen this last decade in the number and types of sensors that provide a range of data and information content never before seen by the earth system scientific community (Richards & Jia, 1999; Liang, 2004). A wide range of operating scales of satellite sensors is necessary to capture the complex nature and dynamics of the phenomena at the surface of the Earth. This is evident in new remote sensing programs that use smaller spacecraft with very specific objectives that allow for greater flexibility, accountability, and responsiveness of a program to serve specific needs (Kramer, 1996).

In recent years, sensors such as IKONOS and Quickbird are operating at the finest spatial scale publicly available from space (Zanoni & Goward, 2003) at sub-meter to meter scale over the visible and near infrared spectral region (Digital-Globe, 2004; Space-Imaging, 2004).

The complexity of questions being addressed with the use of remotely sensed data along with the availability of numerous and different data from different sensors covering a geographic region has fostered an increasing focus on studies that incorporate data from multiple sensors. The value of multi-scale remote sensing (Colwell, 1960; Reeves, 1975; Goward et al., 2003) and the strong incentive to utilize data from more than one observing system is well accepted (Steven et al., 2003). For example, the Boreal Ecosystem Atmosphere Study, BOREAS, designed to improve the understanding of the boreal forest biome and its interactions with the atmosphere, biosphere, and the carbon cycle in the face of global warming, incorporated data from numerous (Table 3) remote sensing systems (Gamon et al., 2004). Data collected in 1962 from the Central Intelligence Agency's Corona Satellite was used along with Landsat Thematic Mapper data from 1987 for water resource monitoring (USGS, 2004) to determine the reduction in the size of the Aral Sea due to diversion of the Amu-Darya and the Syr-Darya Rivers for irrigation and other factors. Chilar (2000) recognized the increasing need to use data from different sensors interchangeably with the objective of producing mosaics of the same consistency as from one sensor. Use of multi-temporal and multi-sensor data in regional and global land cover classifications also offers a richness of information and potentially improved classification accuracies (DeFries & Belward, 2000).

Sensor	Platform	Measurement
Advanced Verry High Resolution Radiometer (AVHRR)	satellite	multi-band spectral radiance, thermal emittance
Landsat Thematic Mapper (TM)	satellite	multi-band spectral radiance, thermal emittance
SPOT	satellite	spectral radiance
GOES	satellite	spectral radiance (irradiance, PAR, and albedo)
ERS-1	satellite	radar backscatter
NASA scattometer (NSCAT) SIR-C/XSAR	space shuttle	radar backscatter (C and L bands, polarimetric)
AIRSAR	DC-8	radar backscatter (C, L, and P bands, polarimetric)
Scanning Lidar Imager of Canopies by Echo Recovery (SLICER)	C-130	lidar tree heights and surface microtopography
Polarization and Directionality of Earth's Radiation (POLDER)	helicopter and C-130	spectral radiance and BRDF
Advanced Solid-State Array Spectrometer (ASAS)	C-130	spectral radiance and BRDF
Airborne Visible-Infrared Imaging Sepctrometer (AVIRIS)	ER-2	hyperspectral radiance
Compact Airborne Spectrographic Imager (CASI)	Piper Chieftan)	spectral radiance
PARABOLA	suspended cables	BRDF
Modular Multispectral Radiometer (Barnes)	helicopter	spectral radiance
SE-590 (Spectron Engineering)	helicopter	spectral radiance
Various portable spectroradiometers	ground-based (handheld or tripod)	spectral reflectance of canopy and stand elements

Table 3. Sensors employed in BOREAS (Gamon et al., 2004).

The use of data from different sensors with varying characteristic raises a number of important questions. What is the variability in measurements between sensors? Is the variability between sensors in studies that incorporate data from a number of different systems significant and how does it affect analysis, results, and conclusions? To answers these questions, an understanding of factors that cause the variation, must first be understood.

Measurement Variation

The quality of information derived from remotely sensed data is dependent upon many factors, including data quality, analysis techniques and interpretations, and numerous temporal/phenological considerations (Vogelmann et al., 2001). Measured values will also vary with soil background effects as well as the heterogeneity and scale of terrestrial surfaces in relation to sensor pixel size (Teillet et al., 1997). Processing of imagery for the purpose of obtaining physical measurements requires many steps including adjustments for intervening effects of the atmosphere, observational geometry, and specific sensor properties (Guyot & Gu, 1994; Steven et al., 2003; Trishchenko et al., 2002). Although a detailed discussion of these many factors is beyond the scope of this paper, the most critical items that effect remote sensing system measurements are reviewed briefly below.

Radiometry

Comparing measurements from different sensors requires consistent solar input and proper radiometric calibration (Price, 1987) because measurements values are dependent on whether digital numbers, radiance units, or reflectance values (Steven et al., 2003) are used. The methodology for using imagery data can contribute to significant error in many studies. The use of digital numbers (DNs) for comparative analysis purposes is not valid and can produce to seriously misleading conclusions (Goward et al., 1993). Conversion to calibrated physical units is required. Conversion to spectral radiance is a substantial improvement over use of DNs in analyses; however, its use is limited because observations taken at differing times of day, year, or at differing latitudes vary inversely

with solar zenith angle. The differences in acquired electro-magnetic energy between sensors are also not accounted for in radiance measurements. To account for these effects, conversion to reflectance values is required. These values are more easily compared to ground measurements and between sensors. Reflectance is the ratio of sensor-measured spectral radiance from the Earth to spectral radiance incident at the sensor altitude (LPSO, 1998). Planetary reflectance is calculated as follows:

$$\rho_p = \frac{\pi * L_{band} * d^2}{ESUN_{band} * \cos(\theta s)} \qquad \text{Equation 2}$$

ρ_p = planetary reflectance (%)
L_{band} = spectral radiance at sensor's aperture (W m^{-2} $sr^{-1}\mu m^{-1}$)
$ESUN_{band}$ = band dependent mean solar exo-atmospheric irradiance (W $m^{-2}\mu m^{-1}$)
θs = solar zenith angle (Usually in radians for Image Processing Applications)
d = earth-sun distance (astronomical units)

L_λ is calculated for remotely sensed data using sensor specific calibration methods, and $ESUN_{band}$ also referred to as the band pass, is calculated using Equation 3.

$$ESUN_{band} = \frac{\Sigma(RSR_\lambda * \text{Solar Irradiance}_\lambda) * \Delta\lambda}{\Sigma (RSR_\lambda) * \Delta\lambda} \qquad \text{Equation 3}$$

$ESUN_{band}$ = band average solar spectral irradiances (W m^{-2} μm^{-1})
RSR_λ = wavelength dependent radiance spectral response (W m^{-2} μm^{-1})
$\Delta\lambda$ = wavelength spectral interval (μm)
$\text{Solar Irradiance}_\lambda$ = exo-atmospheric solar spectrum (W m^{-2} μm^{-1})

Planetary reflectance, as a top of the atmosphere measurement, includes the effects of the atmosphere and thus will vary with atmospheric conditions even when nothing changes on the land surface observed. Exo-atmospheric reflectance values can be used for valid cross-sensor comparisons and other analyses if intervening atmospheric effects are recognized (Goward et al., 2003). When the effects of the atmosphere on planetary

reflectance values are considered, the resulting conversion to surface reflectance (Guyot & Gu, 1994) provides a sound basis for comparison of sensor measurements.

Solar Spectrum

Exo-atmospheric solar illumination varies with time and a number of different solar spectra data are available for use in calculations of target radiance values in this study as well as for determination of average band pass, or ESUN, values used in calculating planetary reflectance values of remotely sensed data. There are a number of reference solar spectra available today that vary throughout wavelength on the order of 1-2 %. Differences between solar spectra data sets are due to a number of factors including uncertainty in solar activity and in the experimental measurements of the data (Nieke & Fukushima, 2001). Although these spectra are similar, differences between them can affect the results of multi-sensor studies through variations in calculated reflected surface irradiance and in the determination of sensor band average spectral response. For example, the use of Thekaekara's solar spectrum versus the values of Neckel and Labs results in differences in albedo values of 5.2% in Channel 1 and 1.7% in Channel 2 for Tiros-N through NOAA9 (Price, 1987). To eliminate this error, reflectance values derived from different systems should be based on calibration and band pass values determined from common solar illumination spectrum.

The new MODTRAN 4 based "newkur" values (Figure 8) correspond closely to the accepted solar constant of 1367 W/m2 (Harrison et al., 2003) and is used in the Landsat 7

ETM+ published values of solar constant for each band (ESUN) (LPSO, 1998), and was used in this study.

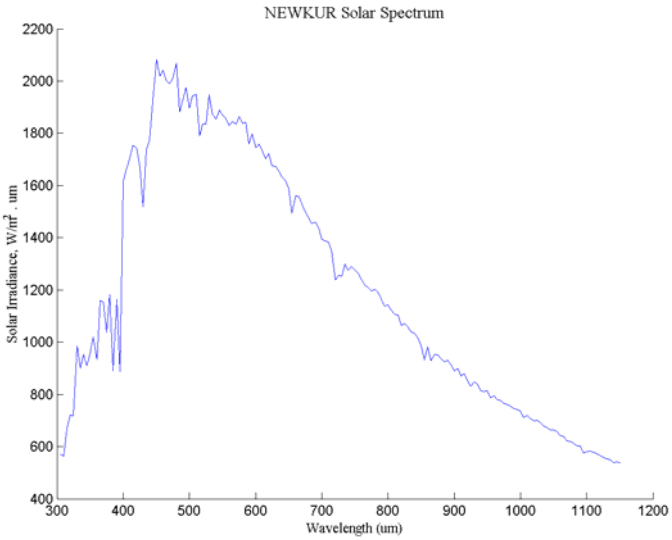

Figure 8. NEWKUR exo-atmospheric solar spectrum (AFRL, 1999).

Acquisition Geometry

Scene data acquired from different systems at different times consequently differ and depict their instantaneous view of the dynamic condition on the Earth's surface. The acquisition geometry along with terrain relief can result in displacement and may potentially be a significant source of error in acquired imagery (Goward et al., 2003). It is, therefore, important to understand scene characteristics, scene-sensor-sun geometry, and dynamic changes that occur on the Earth's surface and in the atmosphere (Steven et al., 2003; Teillet et al., 1997; Trishchenko et al., 2002). The solar zenith angle, time of day and year, and geometry of the satellite sensor in relationship to the area of observation (Curran, 1983) may also result in error due to bidirectional reflectance factor (BDRF) which is a function of both viewing direction and sun position (Dymond et al., 2001).

Spatial Resolution and MTF

A common and misused measure of image quality is spatial resolution, which often presents a significant challenge in studies that are based on data from multiple sensors. Pixel size is often used to describe spatial resolution, but is rather only a measure of the spatial sampling rate and is usually not identical to the instrument's instantaneous fields of view (IFOV), which is a valid measure of its resolution (Forshaw et al., 1983). Typically, the integrated energy from a "footprint" surface area on the ground is used to define corresponding pixel values that are represented as a non-overlapping mosaic of data points (Cahoon et al., 2000). However, a significant problem with remotely sensed image data occurs because a substantial proportion of the signal apparently coming from the land area represented by a pixel comes from surrounding pixels. This is a consequence of many factors including the optics of an instrument, its detectors and electronics, as a well as, atmospheric effects. The Modular Transfer Function (MTF) describes these effects, and its inverse Fourier transform, the Point Spread Function (PSF), depicts how the intensity of a point of light is spatially represented (Townshend et al., 2000).

In a typical sensor design, only about fifty percent of the spectral energy recorded for a given pixel comes from within the pixel dimension (Goward et al., 2003). For example, although the resolution of AVHRR is commonly referred to as 1.26m, only 28 percent of the total energy recorded for the pixel comes from within the corresponding surface area (Cahoon et al., 2000). For the Landsat 7 ETM+ sensor, data is often reported in 30m increments; however, energy from up to approximately 90m from the center of each pixel

contributes to the pixel value. This means that the information extracted from individual pixels is substantially corrupted by the signal contribution from surrounding pixels, and therefore, either land cover properties should be used at spatial resolutions coarser than the individual pixel or that pixel values be deconvolved (Townshend et al., 2000).

Atmosphere

The atmosphere can have a significant, if not dominant, effect on electromagnetic radiation and the observed irradiance recorded by electro-optical imaging sensors. A good knowledge of the atmosphere and its effects are required for many remote sensing studies, and radiative transfer codes may be used to account for the effect of the atmosphere on absorption, scattering, MTF, adjacency, directional effects, and more (Dinguirard & Slater, 1999). Without clouds, atmospheric effects will render somber a bright surface (sand, vegetation) in the NIR and render bright a dark object (water, vegetation) in the visible (Bannari et al., 1995). Obvious clouds in imagery must also be accounted for along with the subtle and difficult to detect cloud contamination in terrestrial observations (Goward et al., 2003).

Aerosol, water vapor content, and ozone columnar amounts (Jacobsen et al., 2000; Kaufman & Tanré, 1992; Trishchenko et al., 2002), in particular, may have a strong effect on band measurements and can limit the quantitative interpretation of physical and biophysical properties derived from vegetation indices (Pinty et al., 1993). Increasing water vapor will result in declining NDVI measurements, which can be seen as a periodicity in season and an increase in noise from period to period if no correction is

applied (Brown et al., 2005). The effect of atmosphere has more influence at low reflectance values and greater effects the near infrared channels because of water absorption bands located in this region (Chilar et al., 2001).

Sensor Data Comparability

In order to overcome or account for potential errors due to factors previously described, techniques must be employed that improve the comparability of data acquired from different sensors, thereby allowing them to be used interchangeably or to augment spatial and temporal observation quality (Goetz, 1997). This will require knowledge of how sensor responses compare (Dinguirard & Slater, 1999; Rao & Chen, 1995). In addition, systems must be well calibrated and validated in order to obtain high quality and consistent data sets of known accuracy (Justice et al., 2000) It is commonly agreed that for satellite sensors lacking onboard calibration in the solar spectrum, the total relative uncertainties of calibration are within 5% (Trishchenko et al., 2002), while well calibrated sensors such as Landsat 7 ETM+ have a radiometric calibration uncertainty of ± 3% (Teillet et al., 2001).

With the above limitations addressed, Vogelmann (2001) found that monitoring activities initiated using Landsat 5 data can be continued with a minimal amount of caution using Landsat 7 data. Masek (2001) also found that the much-improved Landsat 7 ETM+ sensor continues the heritage of the Landsat 5 TM mission. However, even when all these factors are taken into account vegetation indices (Steven et al., 2003) and band measurements from different sensors may not match. This occurs because different

sensors receive different components of the reflectance spectra (Gallo & Daughtry, 1987b) as defined by the relative spectral response of each sensor. For example, Teillet (2001) attributed top-of-atmosphere NDVI differences of 4% to differences in spectral band measurements of surface reflectance spectrum between Landsat 7 ETM+ and Landsat 5 TM.

Relative Spectral Response

While many factors effect, to varying degrees, the accuracy and comparability of data acquired from different remote sensing systems, variances in the relative spectral response are too often neglected or not well understood. Earth observing remote sensing systems detect and record the electromagnetic radiation that is reflected or emitted from the Earth's surface (Bailey et al., 2001). The relative spectral response function (Figure 9 and 10) of an electro-optical sensor describes the responsivity at each wavelength the signal output per unit flux incident for the sensor (Schott, 1997).

The effect of spectral band pass differences on top of atmosphere (TOA) reflectance depends on spectral variations in exo-atmospheric solar illumination, surface reflectance, and atmospheric transmittance (Teillet et al., 2001). Few radiative transfer models incorporate sensor spectral response functions in their software packages (Liang, 2004). As pointed out by Trishchenko (2002), the effect of the spectral response function has not been carefully considered, at least in most AVHRR studies. This lack of consideration of the effect of the RSR also extends to the numerous sensors aboard satellites today.

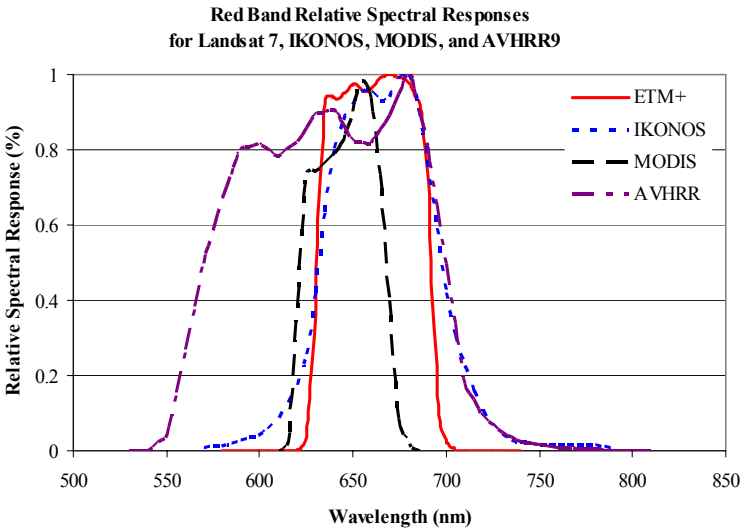

Figure 9. Red Band relative spectral response for Landsat 7 ETM+, IKONOS, MODIS, and AVHRR9

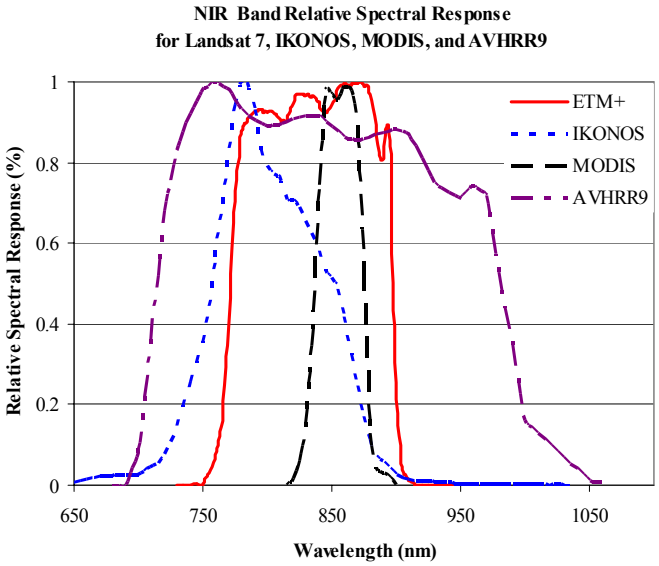

Figure 10. Near Infrared relative spectral response for Landsat 7 ETM+, IKONOS, MODIS, and AVHRR9

Band placement in terms of bandwidth and position has been considered by a number of authors for selecting ideal bands for vegetation monitoring (Steven et al., 2003). Spectral bands are often generalized (Pagnutti et al., 2003) in terms of full width at half maximum

bandwidth and central wavelength corresponding to the maximum value of the response function (Liang, 2004) as shown in Figure 11.

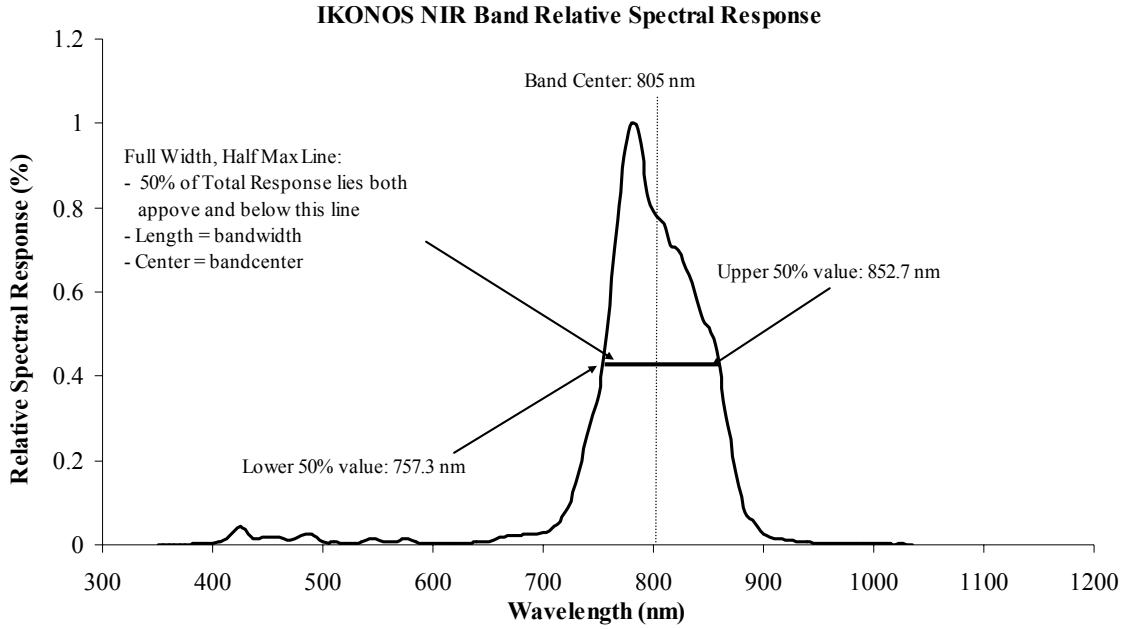

Figure 11. Full width at half maximum bandwidth and band center.

Consideration of these characteristics alone can be misleading. Variations in an instrument's RSR within each band may have a significant effect on measured data and derived metric values even when bandwidth and band center values are similar and, therefore, their use may not be appropriate (Liang, 2004). The effect of RSR on red band and near infrared red band measurements and the resulting NDVI of a range of land cover signature types can be seen in comparison of simulated ETM+ and AVHRR band measurements (Figure 12). This variability is generally true even within the same series of sensors, such as the Thematic Mapper on Landsat (Slater, 1979) and the AVHRR sensors aboard the NOAA polar orbiting satellites (Trishchenko et al., 2002).

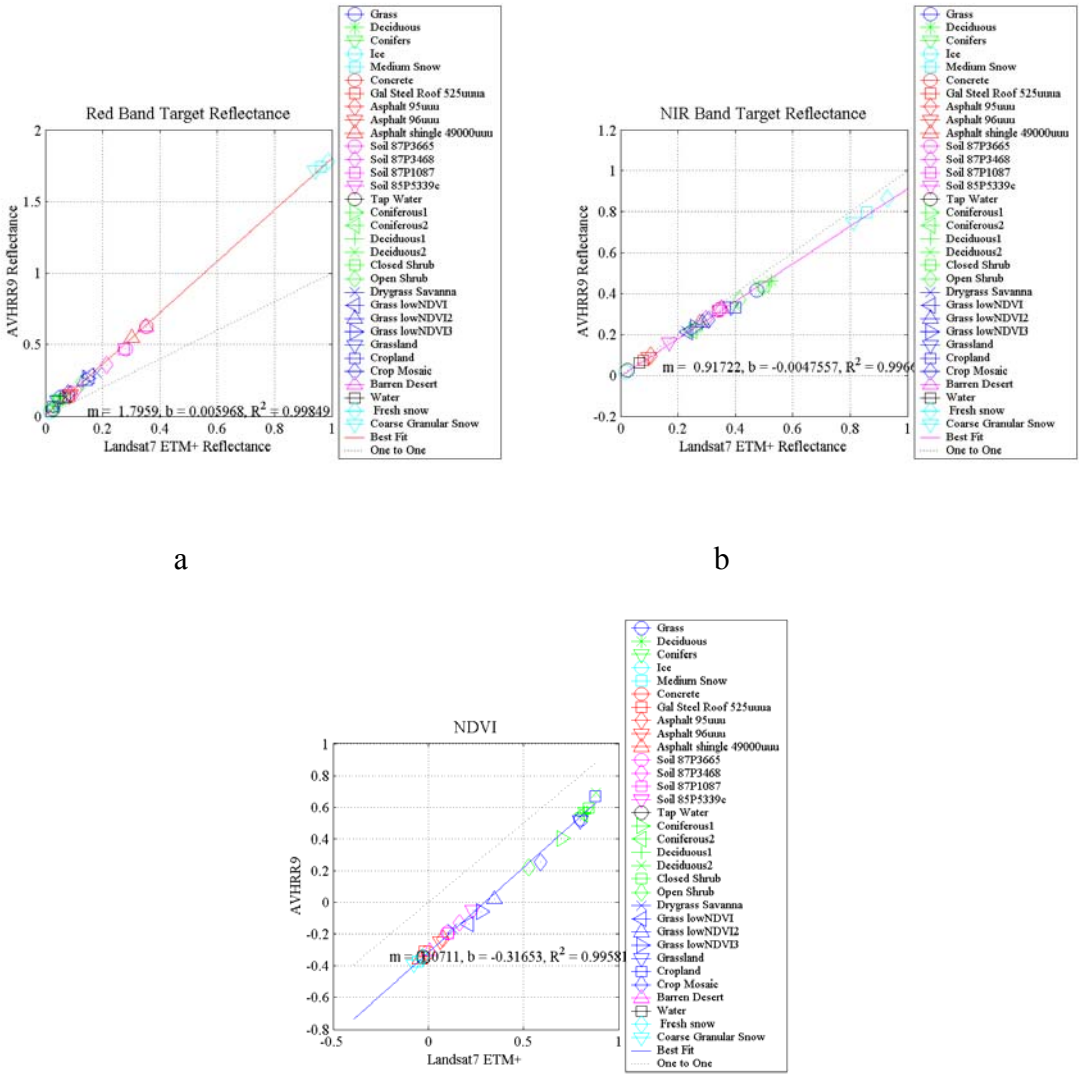

a b

c

Figure 12. Surface reflectance of Landsat 7 ETM+ vs. AVHRR9 for (a) Red, (b) NIR, and (c) NDVI values.

A regression line and associated variability describe the relationship between measurements between two different sensors and can be used as the basis for adjusting the gain and offset of one data set to the other in sensor inter-calibration. The remaining variation is due to the coupled effect of the different RSRs in response to different land cover signatures. Variation will differ for different sets of sensors. For example, relative

to the RSR of AVHRR/NOAA-9, differences in reflectance measurements among the different AVHRR sensors range from -25% to 12% in the red channel and –2% to 4% for the near infrared channel (Trishchenko et al., 2002).

Linear Regression

Standard statistical methods for determining the linear relationship between two or more data sets generally consists of the ordinary least square method (OLS). Errors in only one coordinate, usually the y axis, are considered in the standard OLS method (Bruzzone & Moreno, 1998). However, determining linear relationships between remotely sensed data sets using standard methods may not be appropriate because of resident errors in both coordinates. These data sets also do not meet the associated classical linear regression model assumptions (Kahane, 2001) and may result in line-fit biases due to measurement error in both data sets. Although methods for considering errors in both coordinates have been known for a long time, only the standard OLS version seems to be at the core of current, easily available, methods for curve fitting (Bruzzone & Moreno, 1998). This has been recognized in principal component analysis for imagery data as initial measure coordinates may not be the best arrangement in multi-spectral feature space to analyze remote sensor data (Jensen, 1996). The more appropriate method is a two-directional estimated line fit, but as Press (1992) notes, fitting a straight line model to data that are subject to error in both coordinates is considerably more difficult. The solution used in this study for scene comparisons was derived from algorithms supplied by Peltzer (2000) that are based on original derivation by Pearson (1901). This two-directional approach is consistent with principle component analysis, which provides the best-fit line that

explains the greatest variance between data sets and has the regression intersecting the mean of both data sets in the original scatter of points (Jensen, 1996).

Previous Studies of the RSR

Differences in measured equivalent radiances due to differences of spectral responsiveness of sensors in homologous bands has been recognized in a number of studies (Chander et al., 2004). There is also acceptance of the influence of surface reflectance variation on the magnitude of the RSR effect. An increasing number of studies are examining the influence of the spectral response on remotely sensed data of vegetation.

Gallo and Daughtry (1987b) studied the differences in vegetation indices for simulated Landsat5 MSS and TM, NOAA-9 AVHRR and SPOT-1 sensor systems. They found that variability in NDVI measurements between the four sensors was nearly constant for most of the growing season and concluded that AVHRR-9 data could estimate NDVI and agronomic variables as effectively as direct use of the vegetation indices of MSS. They also noted that some of the variability may be attributable to sensitivity of the different sensor bands to the observed scene.

Goetz (1997) found that calibrated, atmospherically corrected, multi-temporal, and multi-resolution imagery from a suite of sensors are not statistically significant between sensors, despite different radiometric and observational acquisition characteristics. This

investigation included examination of the AVHRR-9, Landsat 4 and 5 TM, and SPOT1 HRV1 and HRV2 sensors.

Teillet (1997) modeled various theoretical and actual sensor characteristics to understand the effect of spectral, spatial and radiometric characteristics on measured vegetation index values of forested regions between sensor systems. They found that bandwidths greater than 50nm, particularly in the red band, had a significant effect. This was attributed to the spectral band capture of the red edge and a portion of the green edge. The study was limited in signature types and analysis was focused primarily on bandwidths and band centers.

Teillet (2001) performed a cross calibration of Landsat 7 EMT+ and Landsat 5 TM using tandem data sets. Their study results clearly indicate that atmospheric and illumination conditions generally contribute significantly less to the spectral band difference than does surface reflectance spectrum for all target types investigated. The tandem cross calibration approach provided a valuable contemporary calibration update for Landsat 5 TM.

Trishchenko (2002) examined the effect of the spectral response function on surface reflectance and NDVI with moderate resolution satellite sensors. They modeled actual sensor spectral response functions for a number of sensors under a number of atmospheric and observational geometries. The main results of the study were bulk polynomial fits for NDVI between sensors for operational considerations. Their modeled

expected results are generally similar to satellite observations, but are only first order approximations and higher accuracies may be achieved.

Steven (2003) investigated the effect of relative spectral response on vegetation indices from different sensor systems. They used spectro-radiometric measurements over a range of crop densities, soil backgrounds, and foliage color convoluted with spectral response functions of a range of satellite images to simulate sensor measurements. Sensors modeled in this study spanned a large range of sensors from AVHRR at 1km resolution to Quickbird at 2.5m resolution. This inter-calibration study had a restrictive data set of only two cultivated crop types with no natural vegetation examined. The relationship between SPOT vs. TM and ATSR-2 vs. AVHRR were validated for OSAVI (Optimized Soil Adjusted Vegetation Index) by comparison of atmospherically corrected image data. OSAVI is a form of soil adjusted vegetation index introduced by Huete (1988) with L equal to 0.16(Rondeaux et al., 1996; Steven et al., 2003). The authors conclude that vegetation indices may be inter-converted to a precision of 1-2%.

Goward et al. (2003) performed an empirical cross examination of IKONOS and Landsat 7 ETM+ imagery of a number of Earth Observation System validation sites across the east to west moisture gradient of the United States. The IKONOS sensor generally produced higher reflectance values in the red band and lower reflectance values in the near infrared band than Landsat 7 ETM+. This results in lower spectral vegetation index measurements for IKONOS relative to Landsat 7 ETM+. The pre-calibration differences

between sensors in band measurements and spectral vegetation indices were attributable to differences in RSR between sensors. (Goward et al., 2003).

Research Questions

The importance of metrics derived from vegetation indices in geographic studies, along with their potential inconsistencies when derived from different systems (Teillet et al., 2001) has been widely recognized and provides the motivation for this research. While some studies suggest that appropriately calibrated and corrected data from different sensors can be used interchangeably, variability in measurements from different remote sensing systems may result in inconsistencies interpreting relationships between biophysical parameters and NDVI. Even when calibration techniques are employed to compensate for most factors of variation, the question of the contribution to the magnitude and significance of variability due to sensor RSR on measurements of varying land cover types remains. This study examined these variations and their effect on the accuracy and consistency of NDVI measurements from different remote sensing systems. Specific questions addressed in this research are:

1. What are the factors that contribute to the variation in red and near infrared band measurements of land cover and vegetation due to relative spectral response?
2. What are the quantitative effects of these factors on the accuracy and consistency of NDVI measurements of vegetation from different remote sensing sensors?
3. How significant are differences in RSR to measurement variability of NDVI between a range of standard Earth observation sensors in use today as well as systems in the future?

To address these questions, a number of theoretical and actual response functions and theoretical and actual surface reflectance characteristics were analyzed to characterize the effects of variations in RSRs on land cover and ultimately NDVI. To quantitatively determine the significance of these effects, a null hypothesis is proposed: the magnitude of the effect of differing RSR on NDVI measurements of vegetation derived from different sensors is within 0.050 uncertainty; similar to the 5% radiometric calibration uncertainty in sensors (Teillet et al., 2001). Additionally, since a 1% change in NDVI can lead to significant variation in some study results as pointed out above by Goward (1991), NDVI differences between sensors greater than 0.010 were also used in evaluating data results.

Chapter 3: Theoretical Model of the Relative Spectral Response

Introduction

How do differences in RSR lead to measurement discrepancies between different sensors? To investigate this question, a theoretical model was developed and explored based on exaggerated forms of spectral response functions and a range of target signatures that represent characteristics found in various land cover types. A key consideration in the design of this study was to isolate and evaluate the effect of RSR free from errors introduced by other factors in remotely sensed data. For this reason, the study is focused on specific land cover spectra, not on remotely sensed imagery. Other researchers (Gallo & Daughtry, 1987a; Steven et al., 2003; Teillet et al., 2001; Trishchenko et al., 2002) have looked at the effect of RSR on sensor data and have empirically shown that relatively similar comparable measurement estimates can be obtained from different sensors under certain conditions. This theoretical study fills the gap in understanding of the mechanisms that lead to measurement discrepancies and their effect on NDVI. Because NDVI is derived from red and near infrared band values, RSR comparisons for each band were conducted separately. Effects of RSR on NDVI are inherently a result of discrepancies in these bands between sensors.

Analyses were performed in a manner so that Theoretical Model results could be used to predict the effect of different RSRs on band measurements and NDVI of different land cover types. This was accomplished by modeling signature characteristics with step and

linear functions in red and near infrared bands since these functions can generally be used to describe signatures of different classes of land cover. These functions varied in reflectance magnitude and slope within each band. Each signature type has a distinct effect on the resulting integrated wavelength dependent irradiance obtained by different RSRs when convolved with solar irradiance. The effect of differences between RSRs was examined in this context before the data was calibrated between sensors. Pre-calibrated data varied depending on the integrated wavelength dependent effect of RSR, solar irradiance, and target reflectance signatures, which made generalizations about the sole effect of RSR on measurement differences between sensors for the range of target signature intractable. Explanations are provided in each section that describe the differences between sensors due to these effects. Calibrated data was then analyzed to understand how cross-sensor equivalent data compare and to determine the quantitative effect of RSR differences on NDVI.

Methods

The analysis was conducted as a function of signature characteristic because differences in RSRs are signature dependent and so that Theoretical Model results could be used to predict effects of RSR on band measurements and NDVI in the Sensor Simulation Study. Typical land cover types were examined to determine the theoretical basis of signature characteristics. Almost all signatures can be simulated with linear or step functions within a band. Signatures also vary in the slope and magnitude of reflectance over the width of each band and these factors were incorporated into the study. In some cases, signatures may be a combination of these functions. For example, vegetation has a

decrease in reflectance, a decreasing linear function, from the green to red region of the electro-magnetic spectrum and a sharp increase in reflectance, a step function, transitioning from the red to near infrared region. Signature functions were quantitatively examined to determine measurement dependency of different RSRs on different signature characteristics. In addition, because reflectance levels of land cover vary, theoretical signatures were developed at varying levels of reflectance. The location of step functions, such as the red edge of vegetation, is located at different points within sensor spectral bands, and therefore, step function locations were varied in the model as well.

While both red and near infrared regions of the solar spectrum experience decreasing irradiance with increasing wavelength, the wavelength dependent magnitude in the two regions differs. For this reason, Theoretical Model analyses were conducted separately for each band. These band independent analyses provided insight into the relationship between differences in RSR, signature characteristics, and their effect on NDVI.

Initial analyses focused on relative differences of band measurements and NDVI. This method is consistent with previous studies and allows differences between sensors to be expressed in terms of percent change. However, the results from these analyses between sensors on a band by band measurement or NDVI basis does not provide the necessary insight into the effect of RSR on NDVI. This is because the effect on NDVI is dependent on the precision of absolute difference between band measurements. Relative differences can become large even when absolute differences are small, especially at lower levels of red and near infrared band reflectance. A preferred approach was employed that allowed

quantitative absolute band differences between sensors to be evaluated in relation to the effect on NDVI. The combined effect of differences in both bands was then investigated. This was accomplished by developing quantitative isolines of NDVI error in a red and near infrared coordinate space. The concept of isolines is conceptually similar to isolines of NDVI as depicted by (Liang, 2004). However, the isolines of NDVI error depict the quantitative effect on NDVI from differences in red and/or near infrared band measurements and is dependent on red and near infrared values themselves. The isolines of NDVI error can also be used to determine the precision of red and near infrared band measurements required to meet a defined level of NDVI error.

In the first red band comparison an analysis of relative differences between sensors as well as the use of absolute differences in relation to NDVI error was conducted. This was the only case where both approaches were included in this text in order to demonstrate the differences of utility between these two approaches. Analyses of relative differences between sensors were not included in the remaining comparisons.

Cross-sensor Calibration

In order to take advantage of multi-spectral data, data must be self-consistent and not significantly affected by artifacts of the measurement system. Different relative spectral responses obtain energy from different parts of the electromagnetic spectrum and lead to fundamental differences between sensors. To account for the gain and offset differences between sensors, cross-calibration can be performed and based on pre-launch measurements or near-simultaneous images of common targets (Teillet et al., 2001).

These differences, if uncorrected, would lead to significant biases between sensors (Steven et al., 2003). Cross-sensor calibration was performed in this study between each sensor for each band in order to provide equivalent values between sensors that could be compared. For each sensor comparison, linear regressions that account for error in both data sets were determined to quantitatively define relationships for both the red and near infrared responses. Linear calibration equations were determined based on the regression slope and offset to calibrate the first RSR to the other for the red band and near infrared band for each comparison (Equation 4):

RSR1 calibrated band = (RSR1* band intercept)/ band slope Equation 4

The new calibrated RSR values were used to determine relative differences between sensors as follows (Equation 5):

(RSR2 band - RSR1 calibrated band) / RSR2 band Equation 5

Statistics were employed to determine how the calibrated RSR measurement values compare. A standard deviation of plus or minus one was used as a threshold to identify discrepancies between sensors to be examined in detail to identify characteristics that resulted in measurement variance. Variance between sensors was then evaluated in relation to its effect on NDVI.

Cross-sensor calibration induces data transformations that may mask the true effect of RSR on measurements. The effect of differing RSRs is apparent in comparisons of data prior to calibration. For this reason, pre-calibrated data is referred to in this study when discussing the effect of RSR on measurements between sensors. Calibration leads to improved correlation between sets of data, however, for certain data it leads to increased error between different sensor measurements.

Relative Spectral Responses

Four different response functions were used in this theoretical model for visible red and near infrared spectral bands: square wave, Gaussian, shorter wavelength biased, and longer wavelength biased (Figure 13). The RSRs were developed based on the same FWHM band specifications. This isolated the effect on measurements due to differing RSRs without substantially complicating the analysis with the effect of additional variables such as differing bandwidth and band center. The square wave response, which captures one-hundred percent of signature radiance within the defined spectral band, serves as a standard for comparison throughout this theoretical model, as well as for the simulation study that follows. This square wave response was defined in accordance with the accepted Landsat Data Continuity Missions (LDCM) community standard for continuing the Landsat data record (NASA, 2003), and was therefore, used as the measurement standard of land cover signatures.

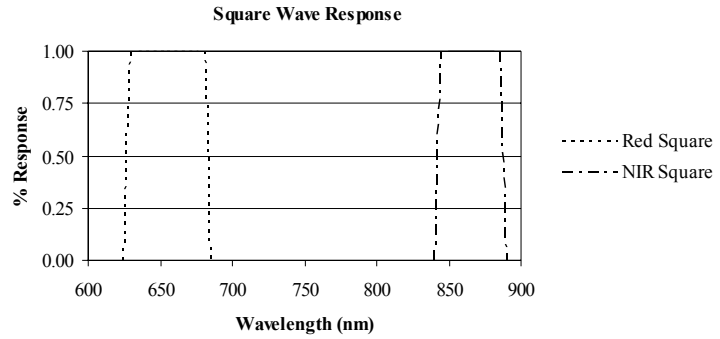

a

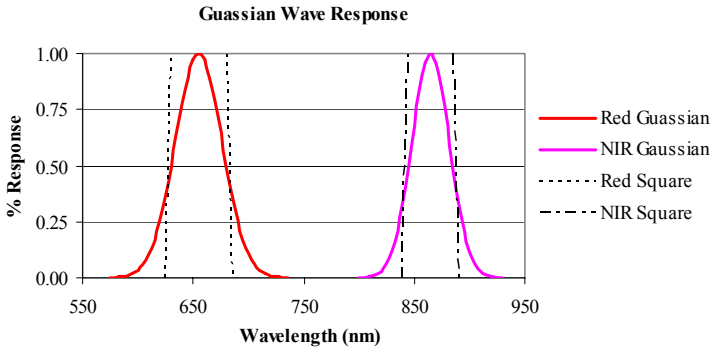

b

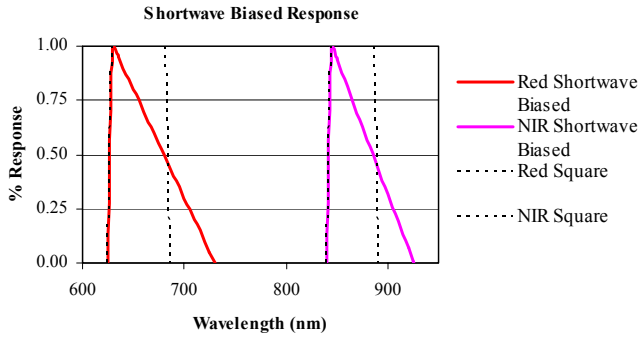

c

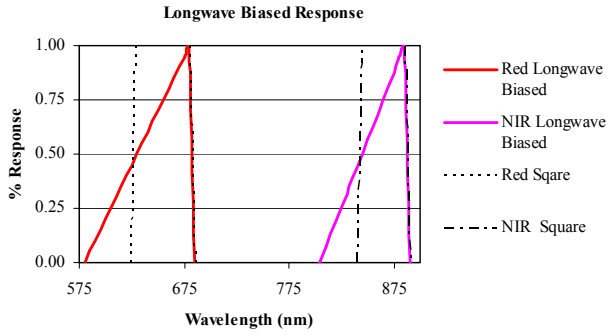

d

Figure 13. Theoretical spectral response functions: a, square wave; b, Gaussian; c, shorter wavelength biased; d, longer wavelength biased

The square wave response function is based on the LDCM, Section 4.1; Spectral Band Widths minimum lower and maximum upper band edge data specification (NASA, 2003). The goal of LDCM is to maintain Landsat's legacy of continual, comprehensive medium resolution coverage of the Earth's surface (Marburger III, 2004). The LDCM specifications include NASA's determination of defined spectral characteristics of systems that will best suit Earth observation needs in the future, and were, therefore, chosen as the basis of the square wave response. The lower and upper band edge is 630 nm and 680, respectively, for the red band, and 845nm and 885nm, respectively, for the near infrared band. The Gaussian, shorter wavelength biased, and longer wavelength biased responses are determined based on similar full width at half maximum (FWHM) values of the square wave band, which can be seen in Figure 13 and in combined plots (Figure 14).

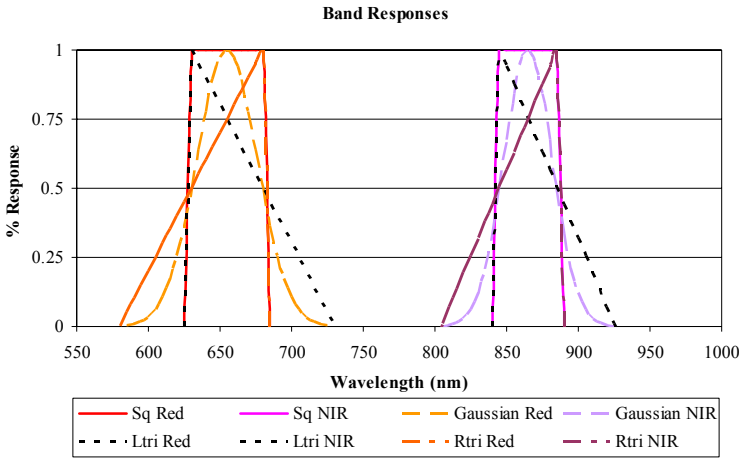

Figure 14. Theoretical model spectral response functions with similar FWHM band values

The Gaussian band represents typical sensor responses that have deficiencies in precisely capturing the beginning and ending portions of a spectral band. The shorter wavelength

biased response is biased with a one-hundred percent response in the beginning of the band with a linear decrease throughout the band. The longer wavelength biased response has a linear increase from the beginning of the band until it reaches one-hundred percent at the end of the band. The shorter and longer wavelength biased responses capture the extreme range in maximum band response of relative spectral responses that lead to target signature irradiance values that are primarily obtained from different parts of the electro-magnetic spectrum within a band.

Surface Object Reflectance Characteristics

As surface object reflectance varies with wavelength across multi-spectral bands, signatures generally have an increasing slope, decreasing slope, no slope, or a step function within the band (Figure 15). For example, water and concrete have a flat signature, or similar reflectance values throughout much of the visible and near infrared region (Figure 2). Drygrass Savannah has an increasing slope throughout much of the visible and near infrared region while green vegetation has a decrease in reflection with wavelength from the green to red region of the electro-magnetic spectrum and a strong increase (step function) in reflection from the red absorption region to the near infrared plateau. The range of target reflectance signature characteristics was simulated in this Theoretical Model using standard linear functions and step functions. Since land cover types also differ in the magnitude and slope of reflectance through spectral bands, the no slope, increasing slope, and decreasing slope functions were modeled at three different slopes and levels of reflectance.

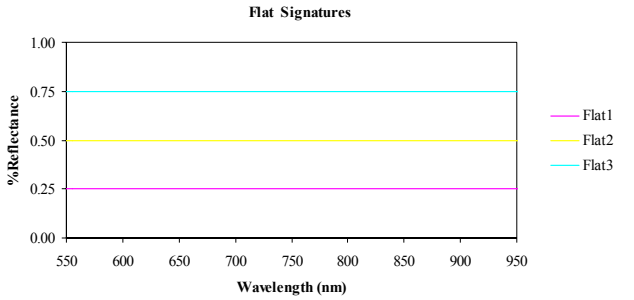

a

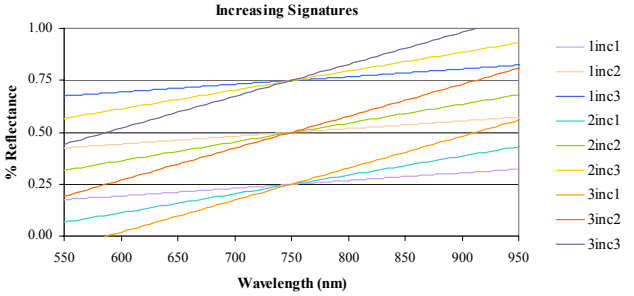

b

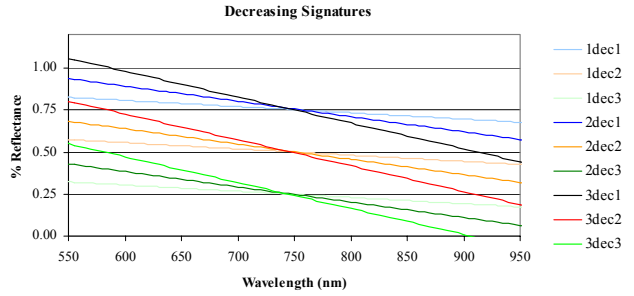

c

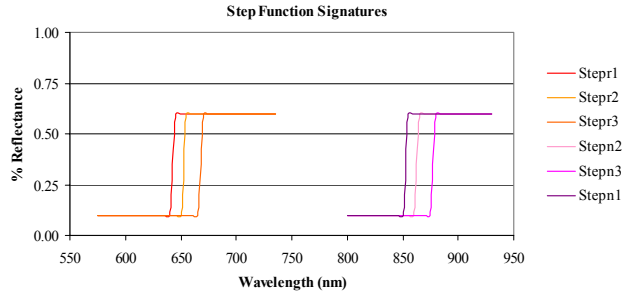

d

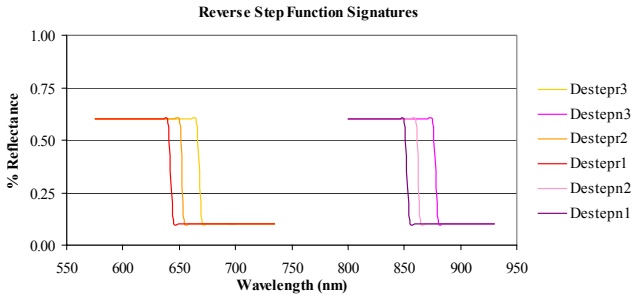

e

Figure 15. Theoretical target signature wavelength characteristics: a, flat; b, increasing; c, decreasing; d, step function; e, reverse step function

Three different signature slopes were used for the increasing and decreasing functions to understand the effect of slope on measurement values from different response functions. Step functions are represented by a step up and a step down within the bands each at three different locations within the bands.

Functions have been designated as flat, for signatures that have constant reflectance through a spectral band; inc, for signatures that have increasing reflectance with increasing wavelength; and dec, for signatures that decline with increasing wavelength within a spectral band. Step functions that step up in reflectance value with increasing wavelength have been designated as stepr and stepn, for the red and near infrared bands, respectively.

Step functions that step down in reflectance value with increasing wavelength are designated as destepr and destepn, for the red and near infrared bands, respectively, as well. Each signature has a number designator at the end to signify an increasing level of reflectance of the signature, or in the case of the step functions, different areas in the band where the step function occurs. For increasing and flat signatures, 1 indicates the lowest level of reflectance, 2 indicates a medium level of reflectance, and 3 indicates the highest level of reflectance of a signature. The highest reflectance level for decreasing signatures is designated by 1 with the lowest level designated by a 3. For step functions, 1 is for those that start in the beginning of a band, 2 for those in the middle of the band, and 3 step functions that are at the end of a spectral band. Increasing and decreasing signatures

slopes have a designator of 1 to 3 for as slopes increase in magnitude from the lowest at 1 to the maximum at 3.

Surface Reflectance

RSRs were then convolved with the NEWKUR solar spectrum (AFRL, 1999) and target reflectance signatures and divided by bandwidth to yield sensor specific red and near infrared band radiance measurements, L_{band}, for each signature (Equation 6).

$$\mathbf{L_{band}} = \frac{\mathbf{\Sigma\ (RSR_{\lambda} * Solar\ Irradiance_{\lambda} * Target\ Reflectance_{\lambda})} * \mathbf{\Delta\lambda}}{\mathbf{Bandwidth_{band}}} \qquad \text{Equation 6}$$

$\mathbf{L_{band}}$ = **Band Radiance** ($W\ m^{-2}\ \mu m^{-1}$)
$\mathbf{RSR_{\lambda}}$ = wavelength dependent spectral response (%)
Target Reflectance$_{\lambda}$ = wavelength dependent target reflectance (%)
Solar Irradiance $_{\lambda}$ = Exo-atmospheric solar spectrum ($W\ m^{-2}\ \mu m^{-1}$)
$\Delta\lambda$ = defined wavelength spectral interval (μm)
$\mathbf{Bandwidth_{band}}$ = FWHM bandwidth (μm)

L_{band} are in units of $Wm^{-2}\mu m^{-1}$ and equal to $\pi * L_{\lambda}$ in Equation 2. For the purpose of this model, factors that account for effects of Earth-sun distance, d, and solar zenith angle, cos(θs) can be set equal to one. Because no intervening atmospheric effects were manifest in this research, planetary and surface reflectance, $\rho_{s,}$ were equal (Equation 7).

$$\mathbf{\rho_p = \rho_s} = \frac{\mathbf{L_{band}}}{\mathbf{ESUN_{band}}} \qquad \text{Equation 7}$$

$ESUN_{band}$ values for the Theoretical Model were calculated using Equation 3 and are provided in Table 4 for the red band and Table 5 for the near infrared band. Because

theoretical bands are all based on the same FWHM spectral characteristics, band center, bandwidth, band minimum at FWHM, and band maximum at FWHM are the same for all theoretical RSRs for each red and near infrared bands.

Red Band Characteristics	Square	Gaussian	SW Biased	LW Biased
ESUN (W m-2 µm-1)	1,573.2	1,572.7	1,553.1	1,598.0
Band Width (nm)	50.0	50.0	50.0	50.0
Band Center (nm)	655.0	655.0	655.0	655.0
Band Min @ FWHM (nm)	630.0	630.0	630.0	630.0
Band Max @ FWHM (nm)	680.0	680.0	680.0	680.0

Table 4. Theoretical model red band characteristics

NIR Band Characteristics	Square	Gaussian	SW Biased	LW Biased
ESUN (W m-2 µm-1)	945.0	950.1	938.5	965.6
Band Width (nm)	40.0	40.0	40.0	40.0
Band Center (nm)	865.0	865.0	865.0	865.0
Band Min @ FWHM (nm)	845.0	845.0	845.0	845.0
Band Max @ FWHM (nm)	885.0	885.0	885.0	885.0

Table 5. Theoretical model rear infrared band characteristics

Maximum differences ((Max $ESUN_{band}$ – Min $ESUN_{band}$) / Min $ESUN_{band}$) in $ESUN_{band}$ values for the four theoretical band spectral response functions are 2.2% for the red band and 2.9% for the near infrared band. When compared to the square wave relative response function $ESUN_{band}$ ((Square Wave $ESUN_{band}$ - Max Difference $ESUN_{band}$) / Square Wave $ESUN_{band}$) difference values were 1.6% for the red band and 2.2% for the near infrared band. The amount of energy acquired by all four RSRs, is therefore, similar. However, energy obtained by these different RSRs comes from different parts of the solar spectrum spectral because response functions differ in profile ranging from short-wave biased to long-wave biased response.

Results and Discussion

Calibration

Best fit linear regressions considering error in both coordinates were determined for each RSR comparison. The regression slopes and offsets used for calibration (Table 6).

RSR	Slope	Intercept	Correlation Coefficient
Square vs. Guassian			
Red	0.9661	0.0000	1.0000
NIR	0.9414	0.0008	1.0000
Square vs. Shortwave Biased			
Red	0.9405	0.0055	0.9986
NIR	0.9445	0.0006	0.9984
Square vs. Longwave Biased			
Red	0.9574	-0.0018	0.9975
NIR	0.9279	0.0069	0.9976
Gaussian vs. Shortwave Biased			
Red	0.9735	0.0054	0.9986
NIR	1.0034	-0.0003	0.9985
Gaussian vs. Longwave Biased			
Red	0.9911	-0.0019	0.9979
NIR	0.9858	0.0061	0.9979
Shortwave Biased vs. Longwave Biased			
Red	1.0181	-0.0074	0.9954
NIR	0.9824	0.0064	0.9957

Table 6. Theoretical model regression data for the red and near infrared band cross-sensor calibration.

Red Band

Relative Differences Between Sensors

Relative differences in post cross-sensor calibration measurements for the six red band RSR comparisons were determined. Initial examination reveals measurement discrepancies for the 3inc1 signature for all comparisons (Table 7). Discrepancies between SRF measurements were also found in about one third of the step function signatures. These differences can be observed in the adjusted, or calibrated, data

scatterplots and relative difference plots as illustrated in Figure 16 for the red band square wave vs. Gaussian RSR.

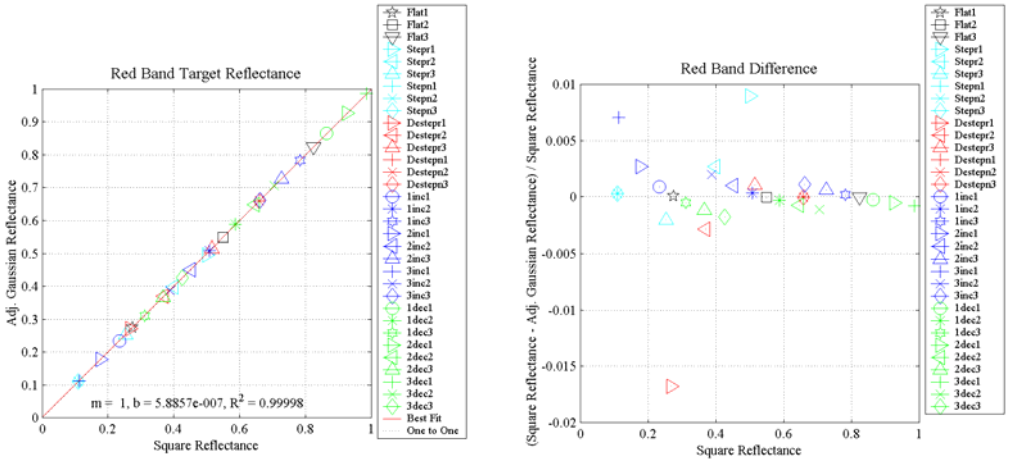

Figure 16. Scatterplots and relative difference plots of red band square vs. Gaussian RSR

Sensor relationships generally appeared to be one-to-one as shown in Figure 16 for the square vs. Gaussian responses. These findings are consistent with those of Stevens (2003). However, examination of relative difference plots (Figure 16) revealed differences between sensors for specific signatures. The maximum difference in calibrated red band reflectance for all signatures for all comparisons was 0.059. If step function signatures and the 3inc1 signature errors are excluded, the maximum difference was 0.023. Most differences were an order of magnitude lower in value. These calibrated differences lead to relative differences between sensors as high as 22.37%. While relative difference plots were initially helpful in evaluating differences between sensors, the non linear mathematics of normalizing to the first sensor in the comparisons was problematic, particularly at low reflectance levels.

Red Band						
Signature	Square vs. Gaussian	Square vs. Shortwave	Square vs. Longwave	Gaussian vs. SW Biased	Gaussian vs. LW Biased	SW vs. LW Biased
Flat 1	0.01%	0.93%	-0.30%	-1.93%	-0.31%	-1.22%
Flat 2	0.00%	-0.13%	0.04%	-1.94%	0.04%	0.17%
Flat 3	0.00%	-0.48%	0.16%	-1.95%	0.16%	0.64%
Stepr1	0.90%	0.34%	11.77%	-2.49%	10.97%	11.34%
Stepr2	0.27%	-2.41%	6.97%	-4.92%	6.71%	9.03%
Stepr3	-0.21%	-18.10%	0.77%	-21.03%	0.97%	15.67%
Stepn1	0.03%	4.10%	-1.32%	-1.91%	-1.38%	-5.39%
Stepn2	0.03%	4.10%	-1.32%	-1.91%	-1.38%	-5.39%
Stepn3	0.03%	4.10%	-1.32%	-1.91%	-1.38%	-5.39%
Destepr1	-1.68%	0.29%	-22.37%	-0.93%	-20.36%	-22.25%
Destepr2	-0.29%	3.28%	-7.75%	1.27%	-7.44%	-11.22%
Destepr3	0.11%	9.36%	-0.53%	7.45%	-0.64%	-10.77%
Destepn1	0.00%	-0.31%	0.10%	-1.94%	0.10%	0.40%
Destepn2	0.00%	-0.31%	0.10%	-1.94%	0.10%	0.40%
Destepn3	0.00%	-0.31%	0.10%	-1.94%	0.10%	0.40%
1inc1	0.09%	0.27%	0.86%	-3.05%	0.76%	0.57%
1inc2	0.04%	-0.52%	0.60%	-2.46%	0.57%	1.11%
1inc3	0.02%	-0.75%	0.53%	-2.28%	0.51%	1.27%
2inc1	0.27%	-1.24%	3.46%	-5.54%	3.19%	4.48%
2inc2	0.10%	-1.21%	1.59%	-3.36%	1.49%	2.73%
2inc3	0.06%	-1.20%	1.14%	-2.83%	1.08%	2.29%
3inc1	0.70%	-4.87%	9.72%	-11.55%	9.05%	13.23%
3inc2	0.20%	-2.26%	3.10%	-4.74%	2.91%	5.17%
3inc3	0.11%	-1.82%	1.98%	-3.58%	1.87%	3.70%
1dec1	-0.03%	-0.24%	-0.18%	-1.64%	-0.15%	0.06%
1dec2	-0.03%	0.21%	-0.44%	-1.50%	-0.41%	-0.64%
1dec3	-0.05%	1.45%	-1.18%	-1.10%	-1.13%	-2.62%
2dec1	-0.05%	0.08%	-0.61%	-1.26%	-0.56%	-0.68%
2dec2	-0.07%	0.62%	-1.04%	-0.96%	-0.97%	-1.65%
2dec3	-0.12%	2.00%	-2.13%	-0.20%	-2.01%	-4.15%
3dec1	-0.08%	0.41%	-1.07%	-0.85%	-0.98%	-1.47%
3dec2	-0.11%	1.05%	-1.64%	-0.41%	-1.53%	-2.69%
3dec3	-0.18%	2.52%	-2.97%	0.60%	-2.79%	-5.55%
Average	**0.00%**	**-0.03%**	**-0.10%**	**-2.57%**	**-0.08%**	**-0.25%**

Table 7. Red band relative differences. Values greater than plus or minus one standard deviation in error are highlighted in yellow (plus) and orange (minus).

This was attributed to small absolute band differences becoming large relative differences at very low reflectance levels. Trischenko (2002) also observed this effect of small absolute band differences resulting in large relative band differences for signatures with low NDVI values. Additionally, relative differences between sensor measurements had limited utility because they did not correlate well with their effect on NDVI. To overcome these limitations, a quantitative approach was developed to evaluate absolute band differences between sensors in relation to their effect on NDVI. This section was included to illustrate the inadequacies of this generally accepted use of relative

differences as an analysis tool to evaluate the effect of band measurement discrepancies between sensors in relation to derived metrics.

NDVI Sensitivity to Red Band Changes

Between-sensor measurement discrepancies were examined to understand their absolute value differences and more importantly, their effect on NDVI. Both 0.050 and 0.010 thresholds of differences in NDVI were considered in evaluating Theoretical Model data results. Due to the complexity of simultaneously dealing with multiple variables, the effect on NDVI from variations between sensor in red and near infrared bands were analyzed independently before their combined effect on NDVI was examined.

Differences between sensors in red and near infrared band absolute reflectance values have varying effect on NDVI. As red band and near infrared band measurements decrease, changes in these values have increasing effect on NDVI (Figure 17). This effect on NDVI can be graphed for isoline values of near infrared band reflectance to illustrate the change in NDVI as red band reflectance decreases (Figure 18). For typical vegetation i.e., red band reflectance in the 10% range with a near infrared band reflection of 50%, a 0.01 difference in red band reflectance leads to a 0.02 - 0.03 change in NDVI. As both red and near infrared band reflectance drop, the 0.01 change in red reflectance can lead to increased changes of NDVI, as high as 0.06 for vegetation.

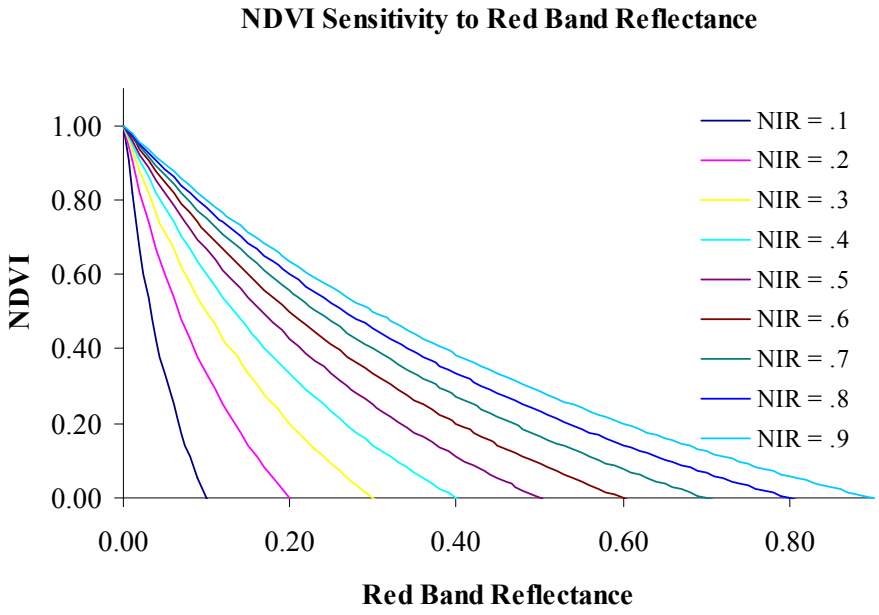

Figure 17. NDVI sensitivity to red band reflectance.

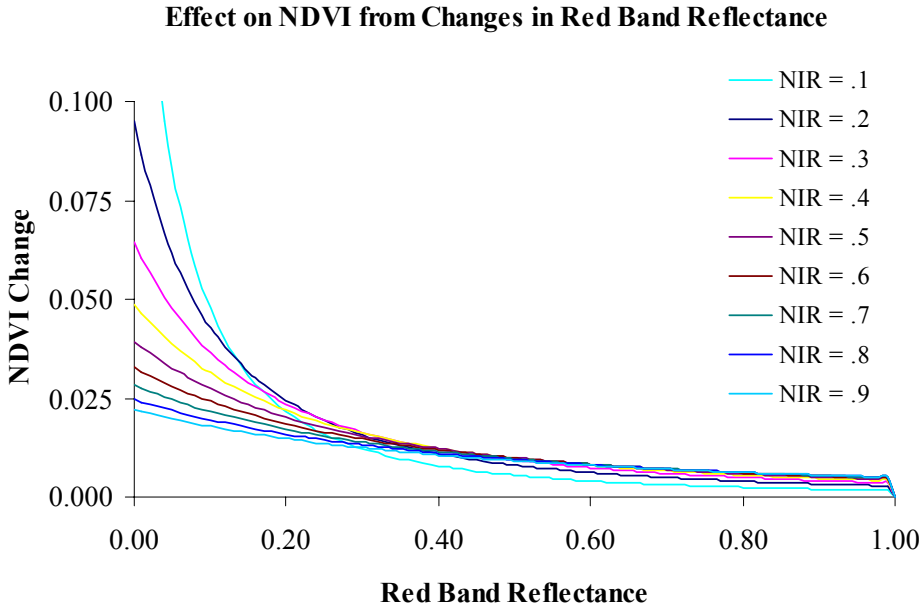

Figure 18. Red band effect on NDVI.

The varying effect on NDVI can also be plotted in red-near infrared space to show what red band difference between sensor measurements lead to a 0.01 change in NDVI (Figure 19).

As red band reflectance levels decrease, differences between sensors have an increasing effect on NDVI values. In order to have precise NDVI measurements of green vegetation within one percent, reflectance measurement discrepancies between sensors, therefore, needs to be generally less than 0.004 for the red band. This requirement is at a similar level to the 0.0039 radiometric precision of 8 bit data, which is employed on sensors such as Landsat 7 ETM+.

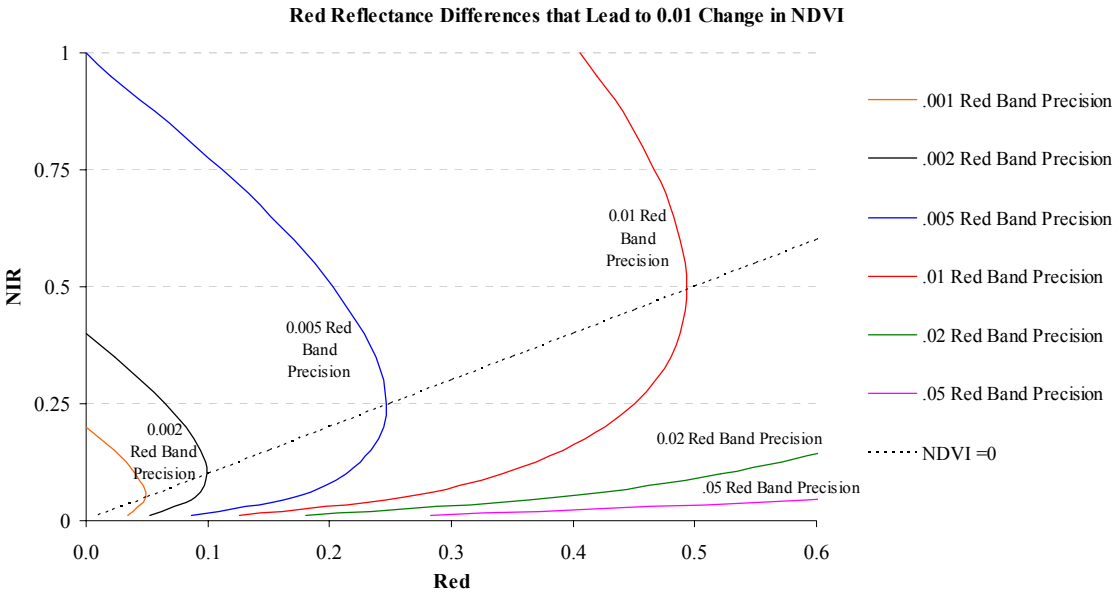

Figure 19. Red reflectance differences that lead to 1% change in NDVI.

The percent differences of NDVI from a 0.010 difference between sensor measurements can also be plotted in red-near infrared space (Figure 20). The 0.010 difference has an increasing effect on NDVI as red band reflectance decreases. For a 5% difference in NDVI values between sensors, red band measurement discrepancies can be higher, in

general, closer to 0.01 for vegetation, and even higher for non-vegetated surfaces with higher red band reflectance (Figure 20).

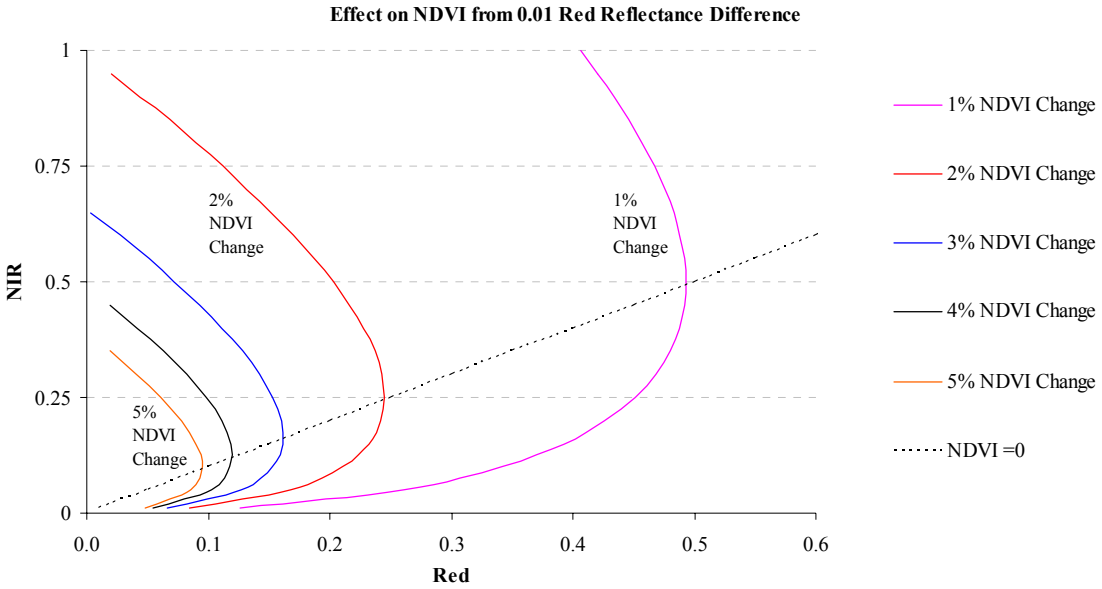

Figure 20. Effect on NDVI from 0.01 red reflectance differences

Effect on NDVI from Red Band Differences

Effect on NDVI from red band differences depends on corresponding near infrared band values. The Theoretical Model was not based on realistic signature profiles for red and near infrared bands, but rather, on signature characteristics that may be found in any one band. Correlation between red and near infrared bands and calculation of NDVI was, therefore, inappropriate. Red band differences between responses in the Theoretical Model were evaluated by signature type and effect on NDVI through a range of NDVI values.

Reflectance signatures used in the Theoretical Model comparisons provide the basis for data extrapolation to cover the wide range of red band values and their differing effect on

NDVI. Red band reflectance differences of 0.0050 and 0.010 were chosen as thresholds to assist in evaluating the effect on NDVI. The 0.005 was used because it is the outer limit of change in red band reflectance that leads to a 0.01 change in NDVI. The 0.010 limit was chosen because red band differences at this level can be used to determine the percent effect on NDVI. Calibrated red band differences between theoretical band responses are provided in Table 8, along with square wave red band reflectance. Note the marked difference between this table of absolute difference effect on NDVI and Table 7 where relative differences were the basis of comparison. Of all comparisons, only the square wave vs. Gaussian wave had no significant differences between sensor measurements.

Flat Signatures

Pre-calibrated signature differences for all sensor comparisons increased as reflectance levels increased. For all comparisons, calculated reflectance values were over estimated compared to reflectance values of defined flat signatures. This surprising result was due to the mathematical method of determination. A standard method for reflectance determination is the ratio of measured band radiance averaged to FWHM bandwidth divided by average band pass, ESUN, the total maximum integrated radiance normalized to the known integrated, or weighted, spectral response (Taylor, 2005).

Red Band							
Signature	Square Red Reflectance	Square vs. Gaussian	Square vs. Shortwave	Square vs. Longwave	Gaussian vs. SW Biased	Gaussian vs. LW Biased	SW vs. LW Biased
Flat 1	0.275	0.000	0.003	-0.001	0.002	-0.001	-0.003
Flat 2	0.549	0.000	-0.001	0.000	-0.001	0.000	0.001
Flat 3	0.824	0.000	-0.004	0.001	-0.004	0.001	0.005
Stepr1	0.502	0.005	0.002	0.059	-0.003	0.053	0.054
Stepr2	0.400	0.001	-0.010	0.028	-0.010	0.026	0.035
Stepr3	0.253	-0.001	-0.046	0.002	-0.044	0.002	0.045
Stepn1	0.110	0.000	0.005	-0.001	0.004	-0.001	-0.006
Stepn2	0.110	0.000	0.005	-0.001	0.004	-0.001	-0.006
Stepn3	0.110	0.000	0.005	-0.001	0.004	-0.001	-0.006
Destepr1	0.268	-0.004	0.001	-0.060	0.005	-0.054	-0.057
Destepr2	0.370	-0.001	0.012	-0.029	0.013	-0.027	-0.038
Destepr3	0.516	0.001	0.048	-0.003	0.046	-0.003	-0.048
Destepn1	0.659	0.000	-0.002	0.001	-0.002	0.001	0.003
Destepn2	0.659	0.000	-0.002	0.001	-0.002	0.001	0.003
Destepn3	0.659	0.000	-0.002	0.001	-0.002	0.001	0.003
1inc1	0.234	0.000	0.001	0.002	0.000	0.002	0.001
1inc2	0.509	0.000	-0.003	0.003	-0.003	0.003	0.005
1inc3	0.784	0.000	-0.006	0.004	-0.006	0.004	0.009
2inc1	0.178	0.000	-0.002	0.006	-0.003	0.005	0.008
2inc2	0.452	0.000	-0.005	0.007	-0.006	0.007	0.012
2inc3	0.727	0.000	-0.009	0.008	-0.009	0.008	0.016
3inc1	0.113	0.001	-0.006	0.011	-0.006	0.010	0.015
3inc2	0.388	0.001	-0.009	0.012	-0.009	0.011	0.020
3inc3	0.662	0.001	-0.012	0.013	-0.012	0.012	0.024
1dec1	0.865	0.000	-0.002	-0.002	-0.002	-0.001	0.001
1dec2	0.588	0.000	0.001	-0.003	0.001	-0.002	-0.004
1dec3	0.311	0.000	0.005	-0.004	0.005	-0.003	-0.008
2dec1	0.927	0.000	0.001	-0.006	0.001	-0.005	-0.006
2dec2	0.647	0.000	0.004	-0.007	0.004	-0.006	-0.010
2dec3	0.367	0.000	0.007	-0.008	0.008	-0.007	-0.014
3dec1	0.986	-0.001	0.004	-0.011	0.005	-0.009	-0.014
3dec2	0.706	-0.001	0.007	-0.012	0.008	-0.010	-0.018
3dec3	0.426	-0.001	0.011	-0.013	0.011	-0.012	-0.022

Table 8. Cross-sensor calibrated red band reflectance differences between sensors. Highlighted in yellow are values above 0.005 and in orange are values greater than 0.010.

The ratio of these normalized values for the square wave response lead to a constant factor of 1.1 in actual signature reflectance vs. calculated values. This was due directly to the averaging methods of signature reflectance and ESUN and resulted in increasing error between sensor measurements as reflectance levels increase. The magnitude of this effect varied for all sensor comparisons and by signature type. This error is avoided in the Landsat 7 ETM+ conversion to planetary reflectance as calibration coefficients are used that inherently account for the weighted integrated response, and is consistent with the calculated ESUN values (LPSO, 1998). To avoid the error associated with

conversion to planetary reflectance in future cross-sensor comparisons, consistent values and methods must be used in the normalization of band irradiance and in ESUN calculations.

Calibration caused shifts in pre-calibrated difference values, such as the adjustment of the Flat3 pre-calibrated difference of -0.002 to 0.005 for the shorter wavelength biased vs. longer wavelength biased response comparison. Inter-response linear calibration lead to slightly non one-to-one correlation for some comparisons between responses, particularly those vs. the shorter wavelength biased response. This resulted in increased error between calibrated sensor measurements as some values depart from the one-to-one relationship. For example, the calibrated flat signature data linear regression has a slope of 0.984 with an intercept of 0.007 for the shorter wavelength biased and longer wavelength biased comparison. At a red band reflectance of approximately 45%, the difference between sensor measurements was 0.000. However, as red band values increase to 0.8 and above or to 0.15 and below, differences became larger than 0.005. Response calibration was based on linear regression of the full pseudo-signature data set for each sensor comparison. Therefore, all data influenced the regression fit and skewed calibrated data slightly away from the one-to-one line for some signatures. This calibration error is sensor and data specific and affects some comparisons more than others.

No differences in calibrated red band reflectance between sensors were above 0.0050 for flat signatures.. Calibration error in this study implies that signatures with very high

reflectance such as snow or very low reflectance such as water could lead to increased measurement error for certain signatures. These differences would most likely only have a significant on NDVI at lower red band values since smaller differences in reflectance here have a greater effect on NDVI. Calibration could be an important factor to consider if based on data that includes significant outliers that are of little interest in studies that use data from different systems. Differences of 0.002 or less could lead to significant changes of NDVI at the 1%. Larger changes could lead to NDVI error beyond 5%.

Increasing Signatures

No trend was observed in the effect of increasing slope on the pre-calibrated differences between sensors. The convolution of the wavelength dependent RSR, signature reflectance and solar irradiance lead to case by case differences between sensors.

Pre-calibrated spectral band measurement differences between sensors of signatures with increasing reflectance slope generally increased with increasing signature reflectance magnitude; however exceptions to this were found in some comparisons with the shorter wavelength biased response. These results were similar to flat signatures findings where differences between sensor responses are maximized at maximum reflectance.

It was also assumed that the method of conversion to planetary reflectance lead to similar error in increasing and other signature measurements as found for flat signatures. Methods on how to address this error are discussed further in Chapter 5.

Differences of cross-sensor calibrated red band measurements became greater as signature slope increased and as reflectance level increased. Differences were generally greater for comparisons with the longer wavelength response with a maximum difference of 0.024 between the most extreme response cases. Differences that exceeded 0.010 were mainly associated with the highest slope signatures.

Calibration also had an effect on data values, especially for the 3inc signatures. For example, the square wave and longer wavelength comparisons to the shorter wavelength biased response for 1inc3 were above 0.0050 for calibrated data, while pre-calibrated differences were below this threshold. The effect of calibration complicated data analysis and was cross-sensor and scene specific.

Of the fifty four sensor red band comparisons of increasing signatures, twenty resulted in significant differences between sensors beyond 0.005 and an additional twelve above 0.010. Increasing signatures through the red band are most often associated with soil type signatures at low to mid reflectance levels. The greater differences between sensors due to increased signature reflectance and slope suggest that for signatures such as soil, red band differences are likely to affect NDVI at or above 1% as signatures increase in slope and in reflectance. For RSRs that differ significantly or for signatures profiles that have high reflectance and slope, differences could have an effect greater than 5% on NDVI.

Decreasing Signatures

Pre-calibrated differences between sensor measurements of signatures with decreasing red band reflectance slope increased with increasing reflectance levels. Increasing signature slope resulted in increasing differences between sensor measurements except for the square wave and Gaussian vs. longer wavelength biased signatures. In these latter cases, the increased slope preferentially favored the longer wavelength biased response leading to decreasing differences between sensor values.

Generally, calibrated differences between sensor measurements decreased with increasing reflectance. Exceptions could be encountered at the very low and very high reflectance levels were calibration error increases and in some cases where calibration resulted in a change of which sensor recorded the highest radiance and reflectance. This lead to differences that changed in magnitude from high to low as the critical reflectance was reached and from low to high as the reflectance continued to change. . Increasing signature slope resulted in increasing differences between sensor measurements for all calibrated values.

Most of the dual sensor comparisons of decreasing signatures resulted in significant differences beyond 0.005 or 0.010 between sensors. Twelve out of fifty four comparisons of band differences were greater than 0.005 and an additional twelve out of fifty four were greater than 0.010. Differences were below these thresholds for 1dec1 and all but one comparison of the 1dec2 signature. Differences exceeded 0.010 for all of the highest slope signature comparisons with lowest reflectance. Comparisons with the

longer wavelength biases responses lead to these higher differences for signatures with lower reflectance as well, and for some lower slope signatures for the shorter wavelength vs. longer wavelength biased response comparison.

Decreasing signatures in the transition from the green to the red region of the electromagnetic spectrum are typical for green vegetation prior to the sharp increase to high near infrared reflection. Sensor responses often capture different ranges and amounts of these characteristics. The portion of red band measurement due to decreasing signatures in this region may lead to significant differences between sensors, especially at lower reflectance levels for high slope signatures. The lowest decreasing signature red band measurement for the square wave response was .311 with a slope of 0.38 in the Theoretical Model. As reflectance decreases, differences between sensors could increase and with an effect on NDVI greater than 5%. A typical slope for green vegetation is significantly less than this: 0.08 for the Deciduos1 signature. This suggests that differences in red band measurements between sensors due to decreasing signature profiles of green vegetation should have an effect on NDVI less than 5%.

Step Function Signatures

Significant differences from step functions in red band reflectance values were generally due to step function exclusion or preferential masking of a portion of one RSR vs. the other. In some cases, step functions were at a position that accentuates areas of RSRs that are most dissimilar, resulting in large differences between measurements.

Calibration between sensors generally leads to improved correlation between sensors with only a few exceptions. No significant differences between square and Gaussian responses were found for step function signatures. However, many of the red band step functions, Stepr1-3 and Destepr 1-3, resulted in differences at or greater than 0.005 and 0.010 between responses. The step function differences were, in general, much higher than other signature types, with a maximum difference of .060 for the square vs. longer wavelength biased Destepr1 response (Figure 21). In this particular case, the step function cuts off a significant portion of the square wave response, but the rise in the longer wavelength biased response before the band minimum at FWHM is reached was unaffected.

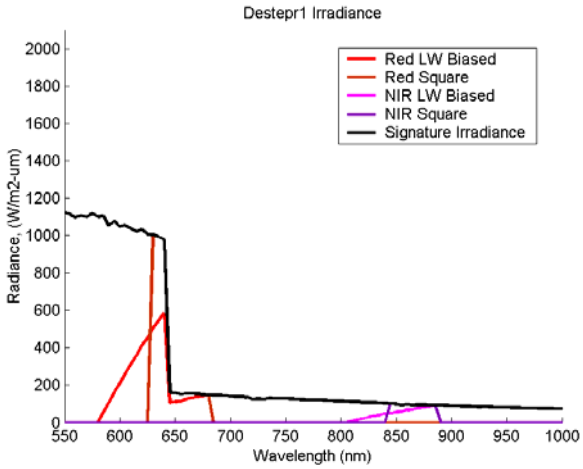

Figure 21. Destepr1 step function cuts off significant portion of square wave response, but does not effect longer wavelength biased response before the band minimum at FWHM.

Differences between sensors increased or decreased with increasing wavelength of step function location. It increased in the square wave vs. shorter wavelength biased comparison because as the step function moves to the right in wavelength, it cuts off

more of the shorter wavelength biased response compared to the square wave. The opposite was true for the square vs. longer wavelength biased response comparison. As the step function moved to the right it cut off less and less of the longer wavelength biased response; resulting in only a .002 difference between sensor measurements for the Stepr3 signature.

The Stepr3 signature that is furthest step function toward the longer wavelength portion of the band is most closely related to the red edge of vegetation that begins to rise at the tail end of the red band. The results determined from the step function data suggest that the contribution in error between sensors due to red band step functions varies depending on band characteristics. In general, sensor differences for step function signatures lead to a significant effect on NDVI for responses that were biased to shorter wavelengths. Comparison with longer wavelength biased signatures did not lead to measurement discrepancies that significantly effect NDVI values.

Near Infrared Band

NDVI Sensitivity to Near Infrared Changes

Differences in near infrared band reflectance have a varying, but generally smaller effect on NDVI values compared to the red band for vegetation depending on red and near infrared band measurements. As near infrared band measurements decrease, differences between sensors have an increasing effect on NDVI (Figure 22). This effect on NDVI can be graphed for values for isolines of red band reflectance to illustrate the change in NDVI as near infrared band reflectance decreases (Figure 23).

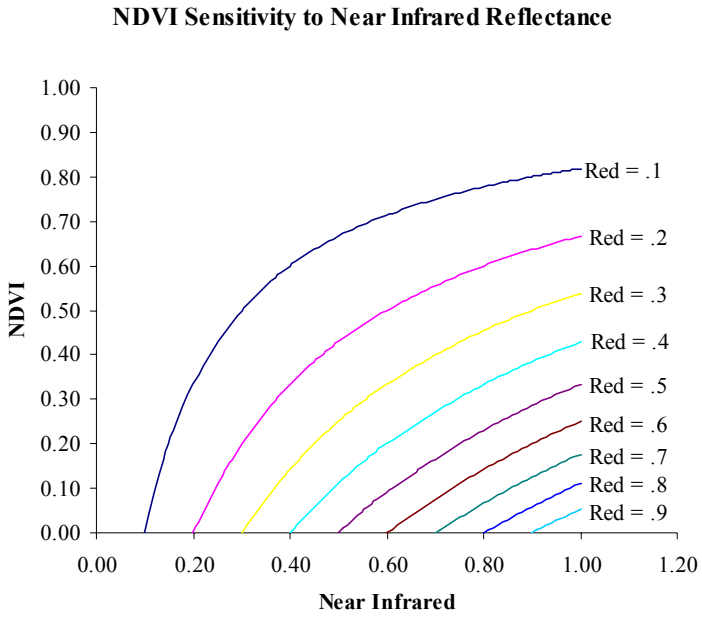

Figure 22. NDVI Sensitivity to near infrared band reflectance

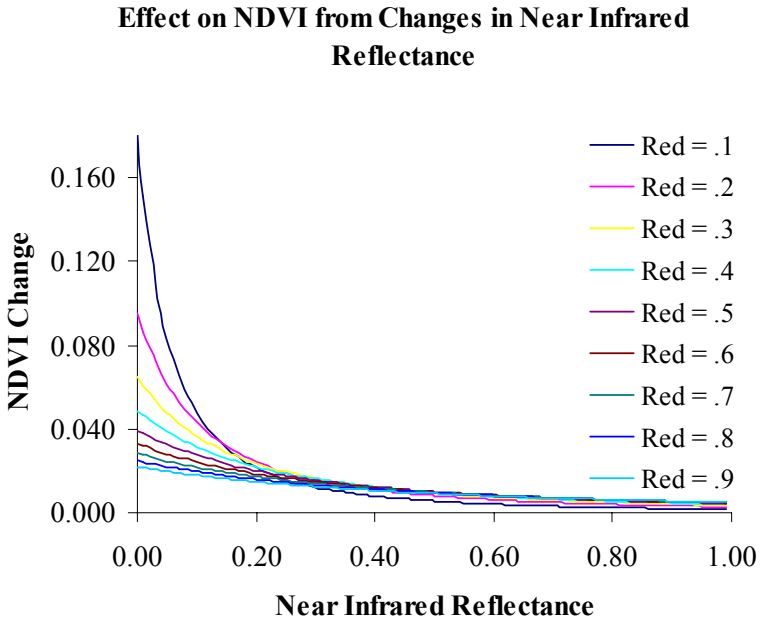

Figure 23. Near infrared band effect on NDVI.

For typical vegetation, a near infrared band reflectance of 50% with a red band reflection of approximately 10%, a 0.01 difference in near infrared band reflectance leads to a 0.005

change in NDVI. As near infrared band reflectance drop, this 0.01 change in near infrared reflectance can lead to increased changes of NDVI, as high as 0.02 for vegetation.

The varying effect on NDVI can also be plotted in red-near infrared space to show what near infrared difference between sensor measurements lead to a 0.01 change in NDVI (Figure 24). As near infrared band reflectance levels decrease, a smaller difference between sensors is needed to maintain a 0.01 effect on NDVI values. In order to have precise NDVI measurements of green vegetation within one percent between sensors, near infrared reflectance measurement discrepancies need to generally be in the range of 0.01 to 0.05. Vegetation signatures with low near infrared reflectance, however, may require measurement discrepancies to be closer to 0.005 (Figure 24) for a one percent or less effect on NDVI.

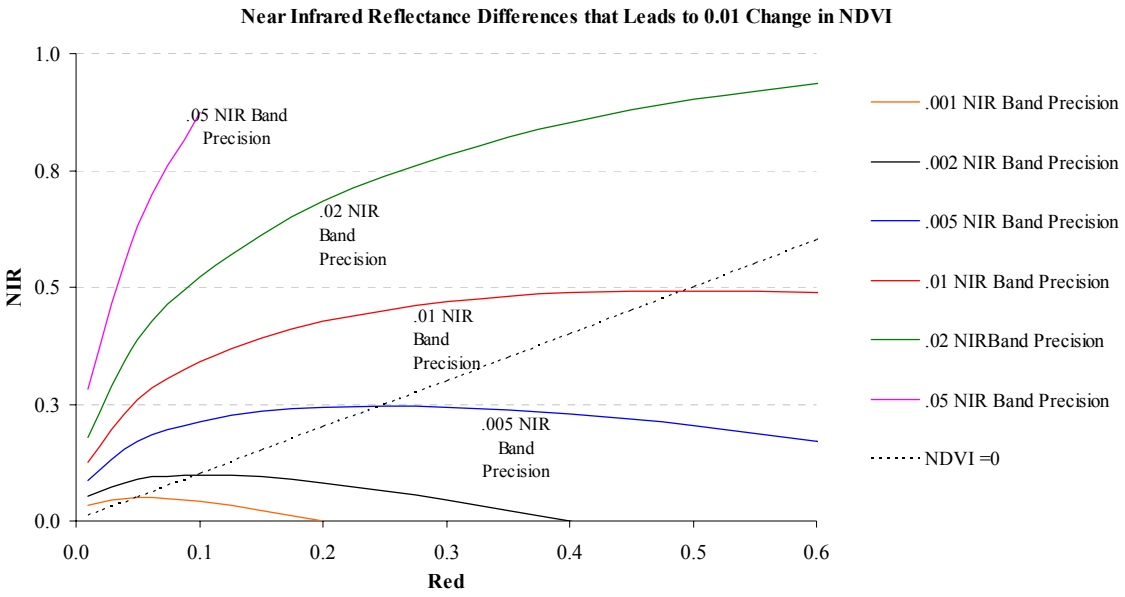

Figure 24. Near Infrared reflectance differences that lead to 1% change in NDVI.

The percent differences of NDVI from a 0.010 difference between sensor measurements can also be plotted in red-near infrared space (Figure 25). The 0.010 difference has an increasing effect on NDVI as near infrared band reflectance decreases. For a 5% difference in NDVI values between sensors, near infrared band measurement discrepancies can be much higher. For green vegetation with near infrared band reflectance greater than 0.25, a 0.01 change in near infrared band reflectance can lead to a maximum effect of 2% on NDVI.

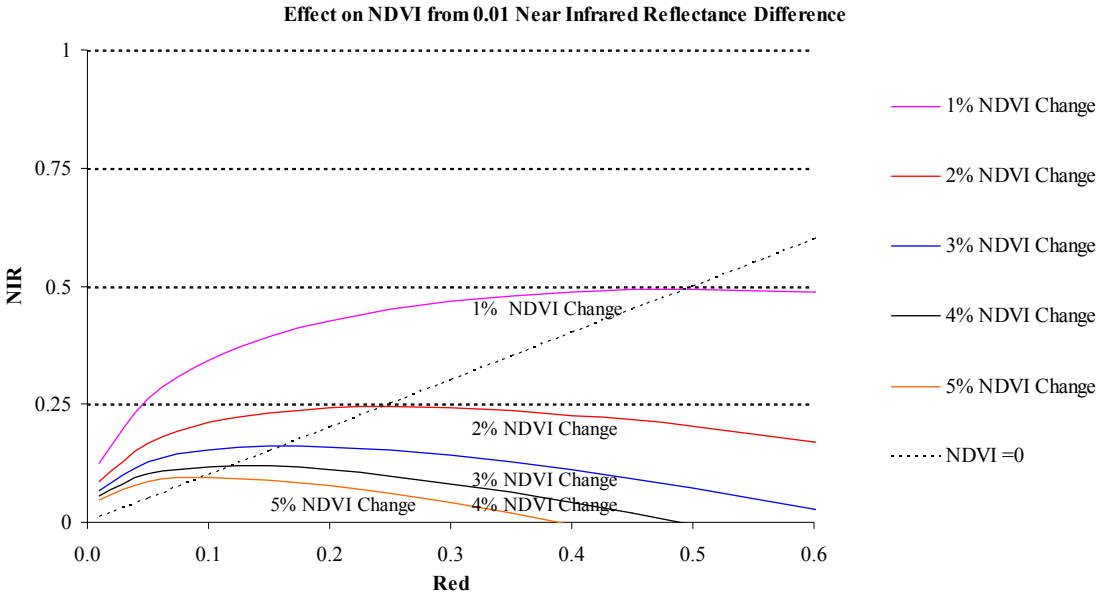

Figure 25. Effect on NDVI from 0.01 near infrared reflectance differences.

Effect on NDVI from Near Infrared Band Differences

Effect on NDVI from near infrared band differences depends on corresponding red band values. Near infrared band differences between responses in the Theoretical Model were, therefore, evaluated by signature type and effect on NDVI through a range of red and

near infrared values. Near infrared band reflectance differences of 0.0050 and 0.010 were chosen as thresholds to assist in evaluating effect on NDVI.

Near Infrared Band							
Signature	Square Near Infrared Reflectance	Square vs. Gaussian	Square vs. Shortwave	Square vs. Longwave	Gaussian vs. SW Biased	Gaussian vs. LW Biased	SW vs. LW Biased
Flat 1	0.285	0.000	0.000	0.003	0.000	0.003	0.003
Flat 2	0.569	0.000	0.000	-0.001	0.000	-0.001	-0.001
Flat 3	0.854	-0.001	0.000	-0.005	0.000	-0.004	-0.004
Stepr1	0.683	0.000	0.000	-0.003	0.000	-0.002	-0.002
Stepr2	0.683	0.000	0.000	-0.003	0.000	-0.002	-0.002
Stepr3	0.683	0.000	0.000	-0.003	0.000	-0.002	-0.002
Stepn1	0.551	0.006	0.004	0.068	-0.002	0.058	0.060
Stepn2	0.424	0.000	-0.008	0.030	-0.008	0.028	0.036
Stepn3	0.237	-0.003	-0.058	0.003	-0.052	0.005	0.058
Destepr1	0.114	0.001	0.000	0.006	0.000	0.005	0.005
Destepr2	0.114	0.001	0.000	0.006	0.000	0.005	0.005
Destepr3	0.114	0.001	0.000	0.006	0.000	0.005	0.005
Destepn1	0.246	-0.006	-0.004	-0.065	0.002	-0.055	-0.057
Destepn2	0.373	0.000	0.009	-0.026	0.008	-0.025	-0.033
Destepn3	0.560	0.003	0.058	0.000	0.052	-0.003	-0.055
1inc1	0.331	0.000	-0.002	0.005	-0.002	0.004	0.006
1inc2	0.616	0.000	-0.002	0.001	-0.002	0.001	0.003
1inc3	0.901	-0.001	-0.002	-0.003	-0.002	-0.003	-0.001
2inc1	0.402	0.000	-0.005	0.007	-0.005	0.006	0.011
2inc2	0.686	0.000	-0.005	0.003	-0.005	0.003	0.008
2inc3	0.971	0.000	-0.005	-0.001	-0.004	-0.001	0.004
3inc1	0.486	0.001	-0.008	0.010	-0.008	0.009	0.017
3inc2	0.770	0.000	-0.008	0.006	-0.008	0.005	0.013
3inc3	1.055	0.000	-0.009	0.002	-0.008	0.002	0.010
1dec1	0.807	-0.001	0.002	-0.007	0.002	-0.006	-0.008
1dec2	0.520	0.000	0.002	-0.003	0.002	-0.002	-0.004
1dec3	0.234	0.000	0.002	0.002	0.002	0.001	0.000
2dec1	0.742	-0.001	0.004	-0.009	0.005	-0.008	-0.013
2dec2	0.453	0.000	0.005	-0.005	0.005	-0.004	-0.009
2dec3	0.163	0.000	0.005	-0.001	0.004	-0.001	-0.005
3dec1	0.653	-0.001	0.008	-0.012	0.008	-0.010	-0.018
3dec2	0.363	0.000	0.008	-0.008	0.008	-0.007	-0.015
3dec3	0.073	0.000	0.008	-0.003	0.008	-0.003	-0.011

Table 9. Near infrared band reflectance differences between sensors. Highlighted in yellow are values above 0.005 and in orange are values greater than 0.010.

The 0.005 was used because it is the outer limit of change in near infrared band reflectance that leads to a 1% change in NDVI. The 0.010 limit was chosen because near infrared band differences at this level can be used to determine the percent effect on

NDVI. Calibrated near infrared band differences between theoretical band responses are provided in Table 10, along with the square wave near infrared band reflectance.

Flat Signatures

Near infrared flat signatures behaved in a similar manner as in the red band for flat signatures. For all comparisons, pre-calibrated differences between sensors increased as reflectance levels increased with a constant factor in the defined signature reflectance vs. calculated values.

Calibration also had a noticeable effect on some of the data as inter-response linear calibrations lead to slightly non one-to-one correlation for most comparisons. Only square wave vs. Gaussian responses lead to a 1.00 slope with a 0.00 intercept. Increasing error between other sensor comparisons as calibrated measurements depart from the one-to-one relationship was observed. For example, flat signature data linear regression has a slope of 0.928 with an intercept of 0.007 for the square wave and longer wavelength biased comparison. At a reflectance of approximately 10%, the difference between sensors measurements is 0.000. However, as values increase to 0.5, differences are 0.029, and for near infrared values of 0.7, differences reach 0.044.

No differences in calibrated near infrared band reflectance of flat signatures between responses were above 0.0050. Comparisons with the longer wavelength response lead to generally higher differences for the flat signatures. For typical flat signatures such as soil with mid red band reflectance, calibration differences should not effect NDVI above 1%.

For flat signatures with near infrared band reflectance above 30% with low red band reflectance, band reflectance differences near 0.005 may be required to limit the effect on NDVI below 1%. For very low reflectance in red and near infrared reflectance, such as water, small differences of .001 could lead to an effect NDVI greater than 1% with effects higher than 5% for differences of 0.01.

Increasing Signatures

Pre-calibrated near infrared measurement differences between RSRs increased with increasing magnitude and slope of signature reflectance. .Calibrated differences increased with increased signature reflectance in most comparisons, but decreased for signature comparisons vs. the longer wavelength biased response.

Fifteen out of the fifty four increasing signature comparisons had near infrared reflectance differences greater than 0.005. In addition, three shorter wavelength biased vs. longer wavelength biased response comparisons lead to a .010 or greater difference in near infrared reflectance. The maximum cross-sensor calibrated near infrared band difference for all increasing reflectance signature comparisons was 0.17. Increasing signatures through the near infrared band are most often associated with soil type or dry vegetation signatures at low to mid reflectance levels. For signatures such as these, near infrared band differences need to be less than 0.01 to not effect NDVI at the 1% level. Signature profiles with high slope and reflectance levels may lead to an increased effect on NDVI, especially as the difference in RSRs increase. Differences of 0.01 in near

infrared band measurements of increasing signatures may lead to differences in NDVI of 2%.

Decreasing Signatures

No trend in pre-calibrated near infrared band differences between sensor measurements of decreasing reflectance signatures was observed. The convolution of wavelength dependent RSR, signature reflectance, and solar irradiance lead to differences that were specific to each comparison. Differences of calibrated near infrared measurements between sensors, on the other hand, generally increased with increasing reflectance and signature slope.

Twenty two of the fifty four decreasing signature comparisons had near infrared band differences greater than 0.005. Six of these signature comparisons had differences greater than 0.010. Half of these were for comparisons of the highest slope, highest reflectance signature (3dec1) with the longer wavelength response. The other highest slope signatures 3dec2 and 3dec3 had elevated difference values, but were under the threshold. For the shorter wavelength biased vs. longer wavelength biased comparison, differences in response function were enough to lead to significant differences in all 3dec1 to 3dec3 signatures. Additionally, 2dec1, the signature with the next highest slope and reflectance level also had differences greater than 0.050. Differences between sensors above 0.050 were also observed in the 1dec1 high reflectance comparisons with the longer wavelength biased response.

Although some vegetation signatures have decreasing characteristics in limited regions of the near infrared band, decreasing signatures in near infrared bands are typical of high reflectance non vegetated surfaces such as snow. Differences between sensor measurements lead to an effect on NDVI beyond the 0.0050 level for some comparisons at all signature reflectance level, which suggests that the effect on NDVI from typically high reflectance signatures will be over 1% in some cases. Unless signature slope is very high, the effect on NDVI should be below 0.010.

Step Function Signatures

As in the case of red band analysis, significant measurement differences between sensors from step functions in near infrared reflectance were generally due to exclusion or preferential masking of a portion of one RSR vs. the other. In some cases, step functions were at a position that accentuates the area of the RSRs that are most dissimilar, resulting in large differences between RSR measurements.

Calibration between sensors generally lead to smaller differences of signature measurements between sensors, but in some cases, differences were higher. Approximately half of near infrared step functions, Stepn1-3 and Destepn1-3, resulted in differences greater than or equal to both 0.005 and 0.010 between responses.

Similarly to the red band step function comparisons, differences between sensors of near infrared step function signatures were, in general, much higher than other signature type

comparisons, with a maximum difference of 0.068 for the square vs. longer wavelength biased Stepn1 response.

Differences between sensors increased or decreased with increasing wavelength of the step function location. It increased in the square vs. shorter wavelength biased comparison because the as the step function moves to the right in wavelength, it cuts off more of the shorter wavelength biased response compared to the square wave. The opposite was true for the square vs. longer wavelength biased response comparison Step functions in near infrared bands are not associated with typical vegetation signatures. The effect on NDVI of step function signatures in the near infrared band is also not typical for land cover targets of primary interest in Earth system science studies.

Summary and Conclusions

A theoretical model was developed using idealized RSRs and reflectance signature characteristics in order to provide qualitative as well as quantitative insight into the effect of differing RSR on band measurements and NDVI. The use of relative measurement differences was found to be inadequate for quantitatively assessing the relationship between RSR, spectral signatures, and their combined effect on NDVI. Instead, a method of examining band differences between sensors in relation to NDVI error was developed and employed based on isolines of NDVI error.

Average band pass, ESUN, values for all RSRs used in this study were similar, with differences of 1.6% and 2.2% relative to the square wave response observed for the red

and near infrared bands, respectively. Signature reflectance characteristics were modeled with step and linear functions. These reflectance signatures were convolved with solar irradiance and RSRs and integrated over each band to provide signature radiance measurements. These values were converted to reflectance values and inter-response calibration was performed. In general, comparison of pre-calibrated and calibrated signature measurement differences between sensors increased with increasing signature reflectance slope and magnitude. However, various exceptions to this were found in a number of circumstances.

Differences between sensor measurements were the smallest for flat reflectance signatures for both red and near infrared bands with maximum differences under 0.005; while step functions lead to the greatest maximum differences between sensor measurements of 0.06. Differences in increasing and decreasing signature reflectance values were around 0.02 for both bands.

Despite the mechanisms that lead to magnitude differences in the various signature measurements between sensors, relationships between sensors were linear and lead to good correlation between sensor responses. This research found that although there was relatively good correlation between sensor measurements, observed measurement discrepancies could result in significant NDVI differences of greater than 0.010 and in some cases 0.050. This is because the sensitivity of NDVI to differences in band measurements between sensors greatly increases as red and near infrared band values

both decrease. For RSRs that were well aligned, such as the square wave and Gaussian responses, the effect of RSR on band measurement was at or below 0.01.

This research also found that the method used to convert radiance to reflectance values lead to measurement error. This small effect, due to the different mathematical averaging methods of band irradiance and average band pass for reflectance determination, was assumed to be a factor in all signature reflectance measurements. While cross-sensor calibration generally resulted in improved correlation between sensors and adjusts for gain and offset differences, it also lead to increased error between sensor measurements for some signatures in certain sensor comparisons.

This theoretical examination of the effect of RSR on NDVI was based on RSRs that were well aligned, which suggests that real sensors with very different RSRs may result in greater band and NDVI differences between sensors.

Chapter 4: Sensor Simulation Study

Introduction

The research in this chapter extends the theoretical quantitative approach developed and employed in Chapter 3 to simulated sensor comparisons, by now integrating actual land cover spectral signatures with actual sensor RSRs in visible and near infrared bands. The RSRs of IKONOS, Landsat 7 ETM+, MODIS, and AVHRR9 were used in this study along with the square wave response from the previous study. The square wave response captures 100% of the energy of land cover signatures and was, therefore, used as a standard for comparison. This square wave response was defined in accordance with the accepted LDCM community standard for continuing the Landsat data record (NASA, 2003) as discussed previously, and was used as the standard for land cover signature measurements. Spectral signatures were selected from a range of land cover types from the PROBE-1 instrument (Secker et al., 1999) and the ASTER Spectral Library (Hook, 1998). Land cover signatures were organized into groups with similar characteristics for analysis and included signatures with flat slopes though spectral bands, such as manmade materials and water; increasing slope signatures typical of soils and dry biomass; and signatures with combined decreasing and step functions common in vegetation. The approach of evaluating differences between sensors in the context of isolines of NDVI error was also used in this study. Signatures were analyzed by band for each of these groups of signature characteristics so that they could be compared to Theoretical Model findings. Analysis by band provided insight into the specific differences in band RSR that leads to measurement and NDVI discrepancies between sensors. Differences in red

and near infrared band measurements were then examined to understand the combined effect on NDVI due to differences in both bands.

Methods

Similarly to the Theoretical Model study, a number of spectral response functions, now from actual sensors, were used in sensor comparisons of actual spectral signatures. Wavelength dependent RSR, signature reflectance, and solar irradiance were integrated over to determine sensor land cover radiance measurements for red and near infrared bands. Values were converted to reflectance and linear regressions that account for error in both data sets were determined to define the regression relationship between sensor band measurements. Regression gain and offsets were then used for cross-sensor calibration and statistics employed in dual sensor comparisons to determine how calibrated RSR measurement values compare. The full data set was used in calibration equation determination and includes manmade, natural non-vegetation, and vegetation signatures. Differences of land cover measurements between sensors were examined in context of Theoretical Model findings in order to evaluate RSR and signature characteristics that effect NDVI.

Relative Spectral Responses

Relative spectral responses of four earth observing sensors were used in this study: IKONOS, Landsat 7 ETM+, MODIS, and AVHRR. The square wave RSR in Chapter 3 was also used as a standard of comparison.

Square Wave

The square wave response captures one-hundred percent of signature radiance within the defined band and serves as a standard for comparison throughout this sensor simulation model. The square wave response function is based on the Landsat Data Continuity Mission (LDCM) Section 4.1, Spectral Band Widths minimum lower and maximum upper band edge data specification (NASA, 2003). The lower and upper band edge is 630 nm and 680, respectively, for the red band, and 845nm and 885nm, respectively, for the near infrared band.

IKONOS

Upon its launch in 1999, the IKONOS satellite sensor represented a significant technical advancement in space-acquired land observation and has provided a major new complement to the multi-scale observations provided by systems such as Landsat, ASTER, SPOT, AVHRR, and MODIS (Zanoni & Goward, 2003).

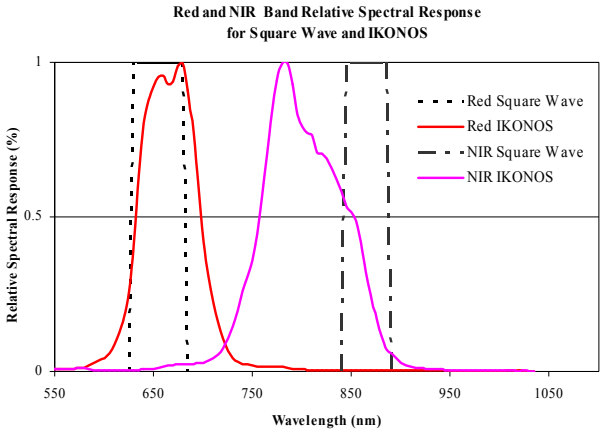

Figure 26. IKONOS and square wave RSR.

The sensor provides four meter resolution multi-spectral data in four bands. Its RSR in the red band has a FWHM bandwidth characteristic that is similar to the square wave response function (Figures 26). The FWHM bandwidth of the IKONOS near infrared band, however, is very different from the square wave response function. The peak of this IKONOS band is at approximately 780nm vs. the initial peak of 845 nm for the square wave function.

Landsat 7 ETM+

The Landsat series of sensors spans almost three decades beginning in 1972. The Landsat data record is important for terrestrial remote sensing because of its relatively fine spatial resolution, extensive terrestrial coverage, and temporal baseline over a time when significant anthropogenic terrestrial change has occurred (Teillet et al., 2001). ETM+ has seven multi-spectral bands from the visible through thermal region of the electro-magnetic spectrum. The spatial resolution of the red and near infrared bands is thirty meters. The ETM+ red band aligns well, although not perfectly, with the square wave RSR (Figure 27).

The near infrared square wave band, however, is much narrower than the ETM+ near infrared band. The ETM+ near infrared band FWHM bandwidth minimum is at 775 nm with a maximum at 900 nm. The first 100nm of the ETM+ near infrared band does not overlap with the square wave near infrared response function

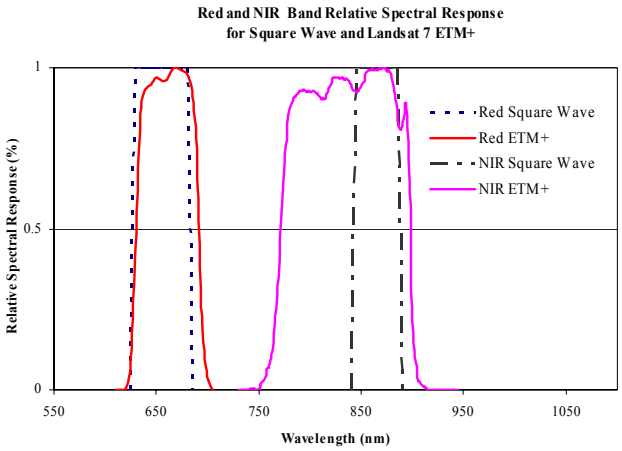

Figure 27. Landsat 7 ETM+ and square wave RSR.

MODIS

The Moderate Resolution Imaging Spectroradiometer (MODIS) was designed in a manner to provide consistent comparisons of global vegetation conditions and is referred to as the "continuity index" to the existing 20+ year NOAA-AVHRR-derived NDVI time series, which could be extended by MODIS data to provide a longer term data record (Huete et al., 2002). The MODIS red and near infrared bands align well, but not perfectly with the square wave RSR (Figure 28).

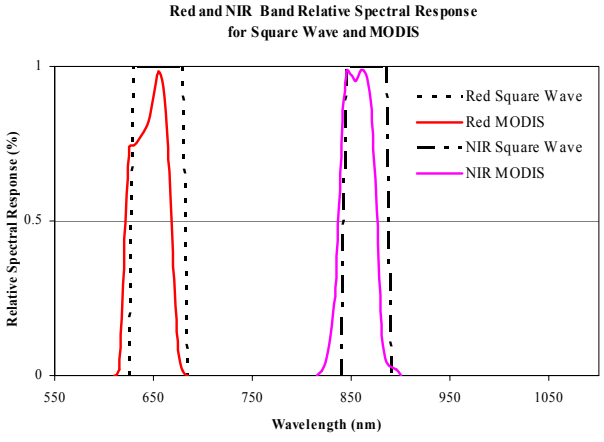

Figure 28. MODIS and square wave RSR.

AVHRR

The AVHRR9 data application is very broad (Trishchenko et al., 2002) and has the widest bandwidth in both the red and near infrared regions (Figure 29). Both channels used in this study contain the region of the square wave RSR, but at varying degrees of responsivity. The AVHRR9 relative response function covers a spectral range that is about twice as large as the square wave spectral region in the red band and almost 7 times larger in the near infrared region.

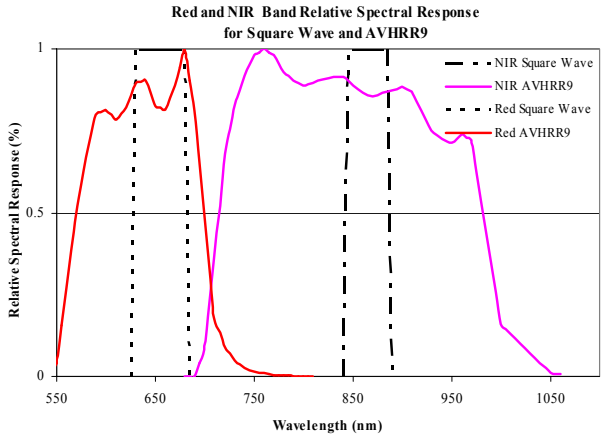

Figure 29. AVHRR9 and square wave RSR.

These sensors were chosen for this study because they cover the span of observation systems widely used in Earth System Science from the past, present, and into the future. All have red and near infrared multi-spectral bands that overlap (Figure 30) and cover a range of spatial resolutions from 4m for IKONOS to the 1 km for AVHRR9. While the bandwidths of all the RSRs used in the Theoretical Model were similar, the wide range of

bandwidths used in this study can be observed in the figure. Similarly to the previous study, response characteristics between sensors vary throughout the bands.

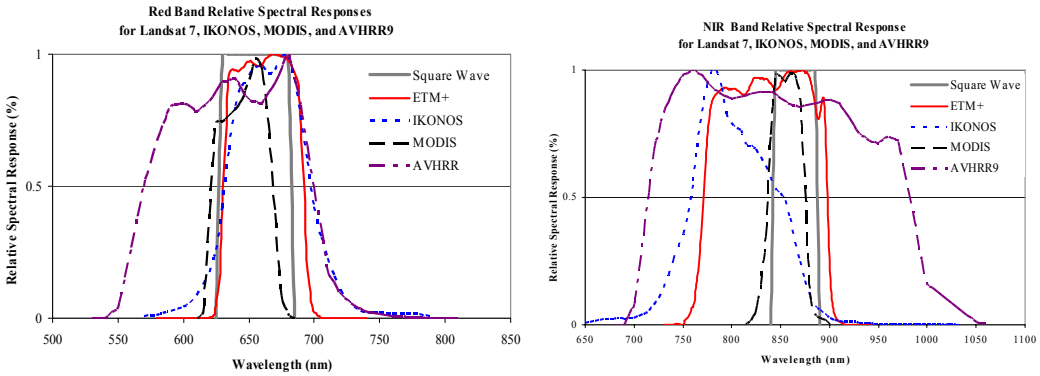

Figure 30. Sensor simulation model spectral response functions for the red and near infrared band.

Surface Object Reflectance Profiles

This study uses a range of target reflectance signature types from the Advanced Spaceborne Thermal Emission and Reflection Radiometer (ASTER) and PROBE1 (Secker et al., 1999) signature profiles. NDVI values for these signatures cover the full range from almost zero to one. Surface object reflectance of these signature profiles have characteristics similar to those used in the Theoretical Model including increasing slopes, decreasing slopes, no slope, or step functions within bands. While measurements of vegetation are the main concern of this research, other manmade and natural objects on the surface of the Earth are of interest and prevalent in remotely sensed data, and were, therefore, included in spectral analyses.

The ASTER spectral library (Hook, 1998) is a compilation of almost 2000 spectra of natural and man made materials and includes data from three other spectral libraries: the Johns Hopkins University (JHU) Spectral Library, the Jet Propulsion Laboratory (JPL) Spectral Library, and United States Geological Survey (USGS – Reston) (Hook, 1998). These spectral signatures were reproduced from the ASTER Spectral Library through the courtesy of the Jet Propulsion Laboratory, California Institute of Technology, Pasadena, California. Copyright © 1999, California Institute of Technology. ALL RIGHTS RESERVED. Spectral data was collected using a number of instruments to measure spectra for each signature. Data from the ASTER JHU spectral library available at the initiation of this research were used in this study and include a total of fifteen signatures: three vegetation, three water, four soils and five manmade signatures. Vegetation signatures cover a range of vegetation types and include conifer, deciduous, and grass signatures. Visible-near infrared spectra of these signatures were simulated canopy measurements based on laboratory spectrometer measurements and were corrected for illuminations sources that depart from solar spectrum. Water signatures of tap water, snow, and ice spectra were also measured in the laboratory and validated through a number of methods. The four soil spectra used in this study, were by no means comprehensive, but cover a number of different types including soils found in level or undulating plains (87P3468 and 87P1087), upland slopes in plateaus or table lands (85P5339), and from mountains and deeply dissected plateaus (87P3665). Sample numbers are those assigned by the Soil Survey Laboratory. Manmade signatures were selected to provide a wide range of common materials and include concrete, asphalt, roof

shingles, and galvanized steel roofing. Details on the ASTER signatures and measurement methods are available from JPL at http://speclib.jpl.nasa.gov.

In addition to laboratory measured ASTER spectral library signatures, seventeen remotely sensed hyper-spectral data signatures were used in this study. This data was obtained with the airborne PROBE-1 hyper-spectral sensor that has 128 spectral bands spanning the wavelength range from 440 nm to 250 nm with 32 bands in each of four spectrometers. The spectral bandwidths in the visible near infrared region are between 11 and 18 nm at FWHM (Secker et al., 1999). Unlike idealized visible-near infrared ASTER data, PROBE-1 data were collected by a real airborne sensor and contains typical noise inherent in remotely sensed data.. In addition to PROBE-1 signatures of Barren Desert, Water, Coarse Granular Snow, and Fresh Snow; thirteen vegetation signatures were used: two different coniferous types, two different deciduous types, Closed Shrub, Open Shrub, Drygrass Savanna, three different low NDVI grass signatures, Grassland, Cropland, and Crop Mosaic.

Use of both data sets provides value in understanding the effect of RSR on measured data both in the laboratory and from remotely sensed data. Signature profiles used in this study include sixteen vegetation, eleven natural non-vegetation, and five manmade types (Figure 31): half of the signatures are non vegetation and half are vegetation. The signatures are listed below based on their profile characteristics as they pass through each band (Table 11).

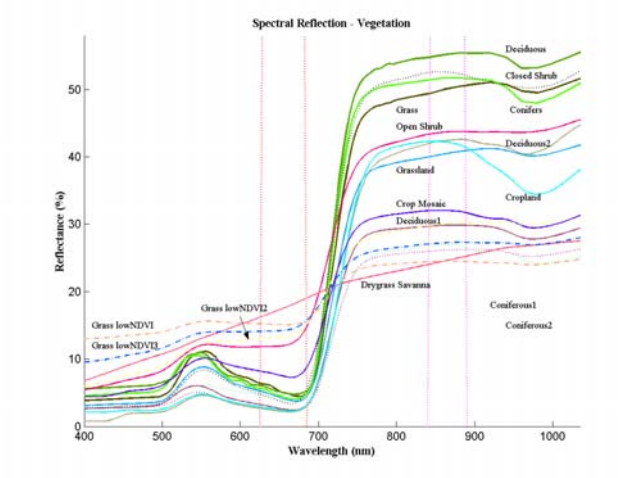

a

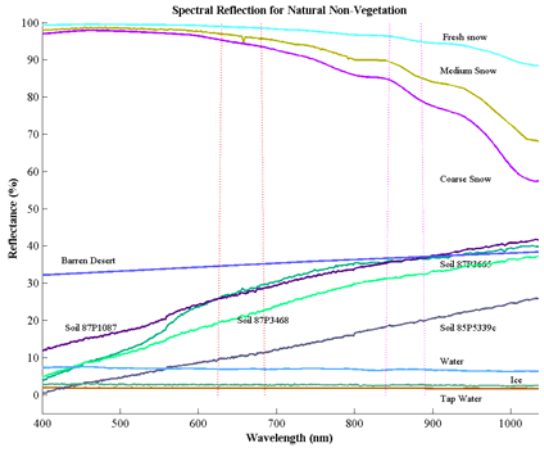

b

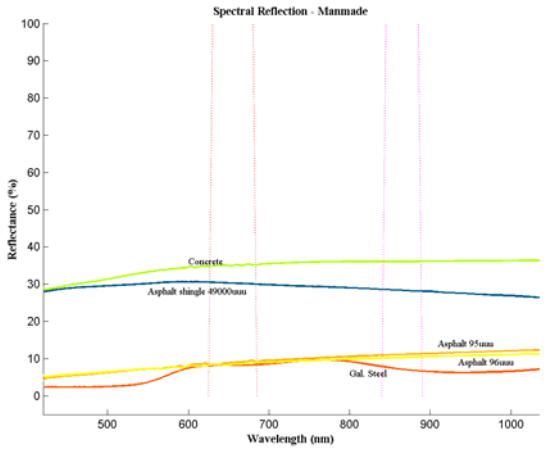

c

Figure 31. Vegetation (A), Natural Non-Vegetation (B), and Manmade (C) Target Signature Characteristics from the ASTER spectral library (Hook, 1998) and PROBE1 data (Secker et al., 1999).

Non vegetation signatures generally have similar characteristics in both their red and near infrared bands; however, Galvanized Steel and the three snow signatures have an overall slight decrease as they pass through the near infrared band compared to flat red band profiles.

Red band vegetation signatures have a characteristic declining slope from the green band region as reflectance drops into the high absorption area of the red band.

These signatures also have a step function increase from red band absorption below 700 nm to the high reflectance portion of the near infrared band beyond 720nm. Vegetation near infrared band characteristics are relatively flat, but are labeled veg in Table 10 because in many cases they deviate from a pure flat signature.

Surface Reflectance

As done in Chapter 3, RSRs and signature reflectance profiles were convolved with the NEWKUR solar spectrum and divided by bandwidth (Equation 6) to yield target signature red and near infrared band radiance measurements for each signature. Signature radiance values for each RSR were then divided by sensor band ESUN values for conversion to signature reflectance,. ETM+ ESUN values were obtained from the Landsat Data Users Handbook (LPSO, 1998) and determined using the same formula (Equation 3) and solar spectrum as used for the determination of ESUN values for IKONOS, MODIS, and AVHRR9. Band characteristics for sensor RSRs used in this study are provided in Table 11 for the red band and Table 12 for the near infrared band.

Signature	Red Band	NIR Band
Ice	Flat	Flat
Tap Water	Flat	Flat
Water	Flat	Flat
Gal Steel Roof 525uuua	Flat	Dec
Asphalt 96uuu	Flat	Flat
Asphalt 95uuu	Flat	Flat
Asphalt shingle 49000uuu	Flat	Flat
Barren Desert	Flat	Flat
Concrete	Flat	Flat
Coarse Granular Snow	Flat	Dec
Medium Snow	Flat	Dec
Fresh snow	Flat	Dec
Soil 85P5339c	Inc	Inc
Drygrass Savanna	Inc	Inc
Soil 87P3468	Inc	Inc
Soil 87P1087	Inc	Inc
Soil 87P3665	Inc	Inc
Deciduous2	Veg	Veg
Coniferous2	Veg	Veg
Cropland	Veg	Veg
Deciduous1	Veg	Veg
Closed Shrub	Veg	Veg
Grassland	Veg	Veg
Coniferous1	Veg	Veg
Conifers	Veg	Veg
Deciduous	Veg	Veg
Grass	Veg	Veg
Crop Mosaic	Veg	Veg
Open Shrub	Veg	Veg
Grass lowNDVI2	Veg	Veg
Grass lowNDVI3	Veg	Veg
Grass lowNDVI	Veg	Veg

Table 10. Simulation study signature characteristics as they pass through the red and near infrared bands (Flat = flat slope profile, Inc = increasing profile with increasing wavelength, Dec = decreasing profile with increasing wavelength, Veg = profile characteristic of vegetation).

Red Band Characteristics	Square	IKONOS	L7 ETM+	MODIS	AVHRR9
ESUN (W/m^2)	1,571.4	1,527.1	1,548.1	1,602.5	1,629.9
Band Width (nm)	50.0	65.8	60.0	40.0	130.0
Band Center (nm)	655.0	664.8	660.0	641.5	635.0
Band Min @ FWHM (nm)	630.0	631.9	630.0	621.6	570.0
Band Max @ FWHM (nm)	680.0	697.7	690.0	661.5	700.0

Table 11. Simulation Model Red Band Characteristics

NIR Band Characteristics	Square	IKONOS	L7 ETM+	MODIS	AVHRR9
ESUN	956.4	1,150.5	1,044.2	976.8	1,026.4
Band Width (nm)	40.0	95.4	125.0	37.7	264.0
Band Center (nm)	865.0	805.0	837.5	855.7	846.4
Band Min @ FWHM (nm)	845.0	757.3	775.0	836.9	714.4
Band Max @ FWHM (nm)	885.0	852.7	900.0	874.6	978.3

Table 12. Simulation Model Near Infrared Band Characteristics

Maximum differences ((Max – Min) / Min) in ESUN values for the four simulation band spectral response functions are 6.7% for the red band and 20.3% for the near infrared band. When compared to the square wave RSR ((Square Wave - Max Difference) / Square Wave) the difference values were 3.7% for the red band and the same 20.3% for the near infrared band. The amount of energy acquired by all five RSRs, is therefore, not too dissimilar for the red band, but differs significantly for the near infrared band. Energy obtained by these different RSRs comes from different parts of the solar spectrum.

RSRs in this sensor simulation study have very different FWHM spectral bandwidth. Band widths range from 264 nm for AVHRR9 to the 37.7 nm bandwidth for MODIS. Band centers range from 805 nm to 865, a 60 nm difference, which is larger than the total bandwidths of some of these sensors.

Results and Discussion

Calibration

Red, near infrared, and NDVI values for each RSR were calculated along with best fit regressions considering error in both coordinates (Table 13). Linear calibration equations were determined based on regression slope and offset to calibrate the first RSR to the other for the red and near infrared band for each comparison (Equation 4).

RSR	Slope	Intercept	Correlation Coefficient
Square vs. Ikonos			
Red	0.9766	0.0118	0.9997
NIR	0.8933	-0.0256	0.9936
NDVI	0.9362	-0.0721	0.9957
Square vs. Landsat 7 ETM+			
Red	0.9075	0.0019	1.0000
NIR	0.8588	-0.0069	0.9995
NDVI	1.0166	-0.0398	0.9987
Square vs. MODIS			
Red	0.9496	-0.0007	1.0000
NIR	0.9214	-0.0028	0.9999
NDVI	1.0052	-0.0147	0.9999
Square vs. AVHRR			
Red	1.6297	0.0094	0.9993
NIR	0.7873	-0.0109	0.9970
NDVI	1.0890	-0.3592	0.9958
Landsat 7 ETM+ vs. Ikonos			
Red	1.0762	0.0097	0.9997
NIR	1.0410	-0.0186	0.9964
NDVI	0.9212	-0.0355	0.9991
Ikonos vs. MODIS			
Red	0.9723	-0.0121	0.9997
NIR	1.0309	0.0237	0.9947
NDVI	1.0737	0.0626	0.9958
Ikonos vs. AVHRR			
Red	1.6684	-0.0102	0.9997
NIR	0.8813	0.0116	0.9988
NDVI	1.1629	-0.2753	0.9980
Landsat 7 ETM+ vs. MODIS			
Red	1.0464	-0.0026	0.9999
NIR	1.0728	0.0046	0.9998
NDVI	0.9888	0.0246	0.9987
Landsat 7 ETM+ vs. AVHRR			
Red	1.7959	0.0060	0.9992
NIR	0.9172	-0.0048	0.9983
NDVI	1.0711	-0.3165	0.9979
MODIS vs. AVHRR			
Red	1.7160	0.0106	0.9996
NIR	0.8548	-0.0086	0.9975
NDVI	1.0833	-0.3433	0.9962

Table 13. Sensor simulation model regression data for the red band, near infrared band, and NDVI.

Red Band

Effect on NDVI from Red Band Differences

The thirty two spectral signatures examined in this study are graphed according to their square wave red and near infrared values in Figure 32 along with the isolines of red band reflectance differences that lead to a 0.01 change in NDVI. Vegetation signatures are displayed in green, manmade in blue, and natural non-vegetation in brown. To have NDVI differences within one percent, vegetation red reflectance signatures measurement differences generally needed to be in the range of 0.002 to 0.005. The coniferous2 signature requires a red band precision less than 0.002 if differences in NDVI between sensors are to be less than or equal to 0.010.

For a 5% difference in NDVI values between sensors, red band measurement discrepancies could be higher. Differences of 0.01 in red band reflectance for green vegetation generally had an effect on NDVI in the 2-4% range. However, for vegetation with red band reflectance below approximately 0.15, a 0.01 change in red band reflectance could lead to an effect of 5% or greater on NDVI (Figure 33).

Effect on NDVI from differences in red band reflectance between sensors is provided in Table 14 for all signatures. Effect on NDVI from differences in red band measurements between sensors was calculated by taking the difference between the second RSR derived NDVI and NDVI calculated using calibrated red band measurements from the first sensor substituted for red band values for each comparison (Equation 8). This resulted in NDVI differences that were associated with only differences in red band measurements.

$$\mathbf{NDVI}_{RSR2} - ((\mathbf{NIR}_{RSR2} - \mathbf{Red}_{Cal\ RSR1})/(\mathbf{NIR}_{RSR2} + \mathbf{Red}_{Cal\ RSR1})) \quad \text{Equation 8}$$

Differences in red band measurements between sensors lead to an effect on NDVI greater than 0.050 for 10% of all signatures and 3% of vegetation. Differences also lead to an effect on NDVI greater than 0.010 for 52% of all signatures and 58% for vegetation.

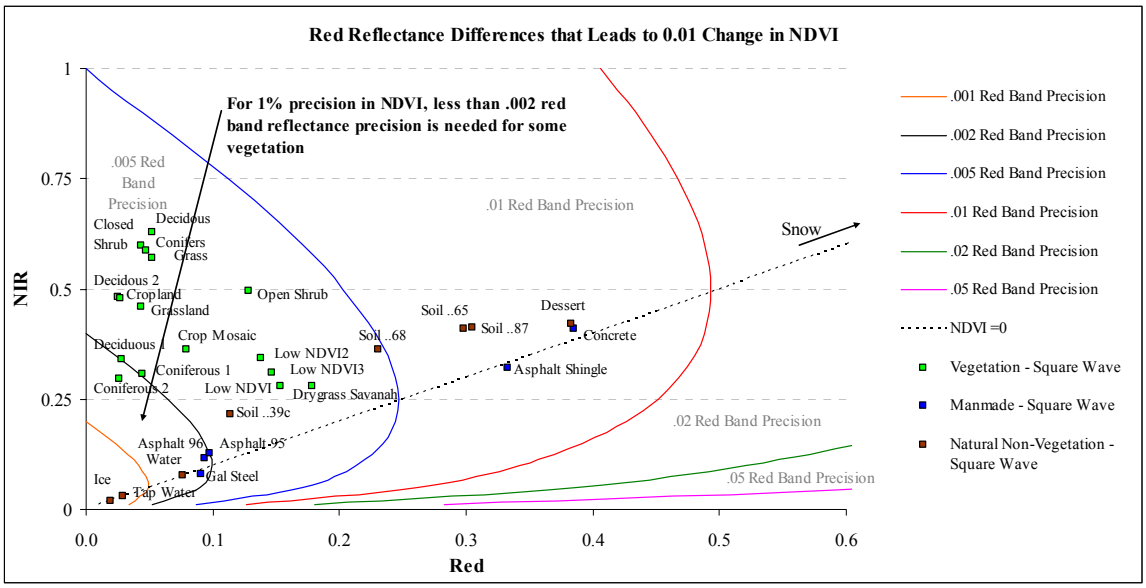

Figure 32. Red reflectance differences that lead to 1% change in NDVI.

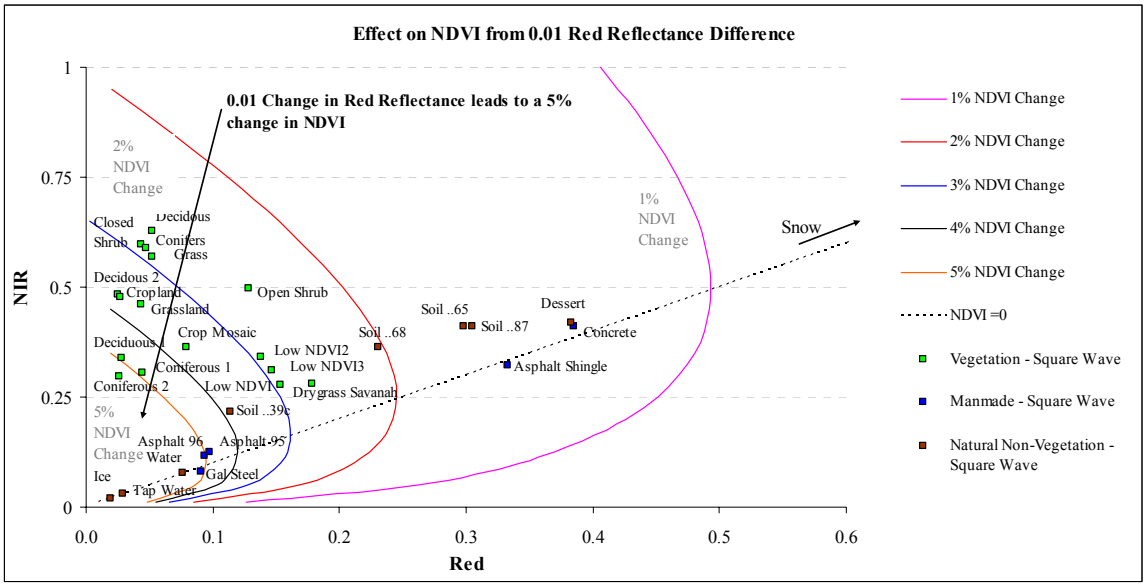

Figure 33. Effect on NDVI from 0.01 red reflectance differences

Effect on NDVI from Differences in Red Band Measurements										
Signature	Square vs. IKONOS	Square vs. Landsat7 ETM+	Square vs. MODIS	Square vs. AVHRR9	Landsat7 ETM+ vs. IKONOS	Landsat7 ETM+ vs. MODIS	Landsat7 ETM+ vs. AVHRR9	IKONOS vs. MODIS	IKONOS vs. AVHRR	MODIS vs. AVHRR
Ice	-0.428	-0.055	0.018	-0.165	-0.332	0.065	-0.098	0.235	0.133	-0.192
Tap Water	-0.247	-0.037	0.008	-0.104	-0.195	0.042	-0.062	0.167	0.092	-0.116
Water	-0.077	-0.013	0.004	-0.033	-0.062	0.017	-0.020	0.068	0.037	-0.038
Gal Steel Roof 525uuua	-0.062	-0.008	0.002	-0.067	-0.052	0.010	-0.057	0.055	-0.005	-0.069
Asphalt 96uuu	-0.052	-0.005	-0.002	-0.042	-0.046	0.003	-0.036	0.045	0.009	-0.040
Asphalt 95uuu	-0.047	-0.004	-0.004	-0.043	-0.043	0.000	-0.039	0.039	0.003	-0.040
Asphalt shingle 49000uuu	-0.012	-0.003	0.002	-0.004	-0.009	0.004	-0.001	0.013	0.008	-0.006
Barren Desert	-0.006	0.000	-0.001	-0.007	-0.006	-0.001	-0.007	0.005	-0.001	-0.006
Concrete	-0.007	-0.001	-0.001	-0.008	-0.006	0.000	-0.007	0.006	-0.001	-0.007
Coarse Granular Snow	0.000	-0.001	0.001	0.004	0.001	0.002	0.005	0.001	0.004	0.003
Medium Snow	0.001	0.000	0.001	0.003	0.001	0.001	0.003	0.000	0.002	0.002
Fresh snow	0.002	0.000	0.000	0.002	0.002	0.000	0.002	-0.002	0.000	0.002
Soil 85P5339c	-0.025	0.002	-0.011	-0.050	-0.028	-0.014	-0.054	0.013	-0.025	-0.040
Drygrass Savanna	-0.009	0.005	-0.010	-0.036	-0.014	-0.015	-0.041	-0.001	-0.026	-0.026
Soil 87P3468	-0.004	0.005	-0.011	-0.038	-0.009	-0.017	-0.044	-0.007	-0.033	-0.027
Soil 87P1087	-0.004	0.004	-0.008	-0.028	-0.007	-0.011	-0.032	-0.004	-0.024	-0.020
Soil 87P3665	-0.004	0.004	-0.010	-0.039	-0.008	-0.014	-0.044	-0.006	-0.035	-0.030
Deciduous2	0.019	0.000	0.004	0.025	0.021	0.004	0.027	-0.018	0.006	0.022
Coniferous2	0.005	-0.005	0.008	0.028	0.010	0.013	0.035	0.003	0.025	0.021
Cropland	0.019	0.000	0.005	0.026	0.021	0.005	0.028	-0.017	0.007	0.022
Deciduous1	0.017	-0.002	0.009	0.039	0.020	0.011	0.043	-0.009	0.024	0.031
Closed Shrub	0.049	0.007	0.005	0.054	0.045	-0.001	0.050	-0.050	0.005	0.050
Grassland	0.021	-0.004	0.011	0.045	0.026	0.016	0.052	-0.011	0.027	0.035
Coniferous1	0.004	-0.001	0.005	0.023	0.005	0.006	0.025	0.001	0.019	0.018
Conifers	0.036	-0.002	0.009	0.048	0.041	0.012	0.053	-0.031	0.013	0.040
Deciduous	0.034	-0.003	0.007	0.042	0.040	0.011	0.047	-0.031	0.008	0.036
Grass	0.024	-0.006	0.012	0.047	0.032	0.019	0.056	-0.014	0.026	0.036
Crop Mosaic	0.020	0.003	0.005	0.033	0.018	0.002	0.031	-0.016	0.013	0.028
Open Shrub	0.029	0.010	-0.006	0.010	0.020	-0.017	0.000	-0.038	-0.020	0.017
Grass lowNDVI2	0.006	0.005	-0.005	-0.007	0.000	-0.011	-0.012	-0.011	-0.013	-0.001
Grass lowNDVI3	0.001	0.004	-0.004	-0.004	-0.003	-0.008	-0.008	-0.004	-0.005	0.000
Grass lowNDVI	-0.008	0.000	0.001	-0.001	-0.008	0.001	-0.001	0.008	0.007	-0.002
Average	-2.19%	-0.32%	0.13%	-0.78%	-1.64%	0.42%	-0.33%	1.22%	0.88%	-0.92%

Table 14. Effect on NDVI from red band measurement discrepancies between sensors. Highlighted in yellow are red band differences that have greater than a 0.010 effect on NDVI and highlighted in orange are values that have greater than a 0.050 effect on NDVI.

Flat Signatures

Twelve of the signature reflectance profiles had relatively constant reflectance values through the red band region for the RSRs used in this study. These signatures are related mostly to snow, ice, water, and man made materials but also include Barren Desert. Snow signature profiles had a very slight decrease through the red band but were included in the flat signature analysis.

No band measurement effect on NDVI beyond 5% was found in comparisons of MODIS and square wave responses for flat signatures. Only the very low reflectance of Ice lead to an error greater than 5% for the comparisons of Landsat 7 ETM+ vs. MODIS and the square wave responses. Error beyond 5% was found in some signatures for all other comparisons for reflectance square wave values less than 0.098. Maximum square wave NDVI was 0.128 for an Asphalt signature and most were significantly lower.

Signature	Square Wave Red Band Reflectance	Landsat ETM+ vs. IKONOS Cal. Red Band Difference	
Fresh Snow	1.084	-.004	
Medium Snow	1.058	-.003	
Coarse Granular Snow	1.037	-.002	
Concrete	.385	.004	
Barren Desert	.383	.004	
Asphalt shingle 49000uuu	.333	.006	
Asphalt 95uuu	.098	.007	>.010 Effect
Asphalt 96uuu	.093	.008	on NDVI
Gal Steel Roof 525uuua	.090	.008	>.050 Effect
Water	.076	.008	on NDVI
Tap Water	.029	.009	
Ice	.020	.009	

Table 15. Flat signature red band reflectance and calibrated differences for Landsat 7 ETM+ and IKONOS sensors.

Flat signatures (Table 15) are listed in order of highest to lowest red band reflectance for the square wave along with absolute calibrated band measurement differences between Landsat 7 ETM+ and IKONOS sensors. Red band differences that lead to greater than 1% and 5% change in NDVI are noted. Consistent with the Theoretical Model, all pre-calibrated differences in red band flat signatures increased with increasing reflectance; and the effect on NDVI increased as reflectance decreased. This was mostly due to the fact that smaller differences at lower red band reflectance lead to a greater effect on NDVI. As in the Theoretical Model, calibration error was also observed in many comparisons and its effect can be observed in Table 16 as differences between sensors transition from negative to positive values.

For signatures with higher red band reflectance, such as Barren Desert differences in band measurements did not lead to significant differences in NDVI beyond 0.010. The differences between sensor measurements for these signatures were slightly lower and at a red and near infrared reflectance level that allows greater band differences for NDVI differences of 0.01.

Reflectance values were greater than one for all three square wave red band snow signature values. This mathematical artifact of converting to reflectance was observed and explained in the Theoretical Model and due to different averaging methods used to determine sensor radiance vs. ESUN in reflectance calculations. For the near maximum reflectance case of Fresh Snow, this error was 0.09 for the IKONOS RSR and -0.002 for

Landsat 7 ETM+ when compared to the average reflectance of the signature through corresponding FWHM bandwidth.

Increasing Signature

Five of the simulation study signatures had increasing slopes in the red band region. These signatures were four soil types and Drygrass Savanna. No significant differences were found in the square wave vs. Landsat 7 ETM+ signature comparisons. Of all comparisons, 64% had differences that lead to a greater than 0.010 effect on NDVI. Signatures with higher reflectance values tended to have a lesser effect on NDVI. The IKONOS comparisons with square wave and MODIS responses only lead to NDVI differences greater than 0.01 for the lowest reflectance soil signature, 85P5339c. Red band differences that lead to a greater than 0.050 effect on NDVI were found only in the AVHRR9 comparisons of this same soil signature to the square wave and Landsat 7 ETM+ responses; and these values were 0.0504 and 0.0540, respectively. This soil signature had much lower red band reflectance than the other soils and Drygrass Savanna signatures. This soil, found in upland slopes of plateaus or table lands also has the lowest near infrared reflectance of all signatures. This puts the signature at a position that requires red reflectance measurement differences between sensors to be less than approximately 0.003 to have an effect on NDVI of one percent. For similar changes in NDVI, Drygrass Savanna signature differences need to be less than 0.005 and for other signatures a difference of 0.005 is sufficient.

Signature	Square Wave Red Band Reflectance	Square Wave vs. AVHRR9 Cal. Red Band Difference	
Soil 87P3665	0.305	0.024	> 0.010 effect on NDVI
Soil 87P3468	0.230	0.018	
Soil 87P1087	0.298	0.017	
Drygrass Savanna	0.193	0.014	
Soil 85P5339c	0.114	0.012	> 0.050 effect on NDVI

Table 16. Increasing signature red band reflectance and calibrated differences for square wave and AVHRR9 sensors.

Increasing signatures are listed in Table 16 in order of highest to lowest slope along with respective square wave red band reflectance and calibrated difference with AVHRR9. As signature slope increased so did measurement variance between sensors, which is consistent with Theoretical Model findings.

Differences generally became greater as reflectance levels increased as well. The exception to this was the increased difference for the higher slope Soil 87P3468 over the higher square wave reflectance signature Soil 87P1087. This was due to a greater effect at this reflectance level of slope compared to reflectance.

Vegetation Signatures

Theoretical Model study step functions were specifically used to represent the "red edge" of vegetation as their high red band absorption transitions to high near infrared band reflection. Fifteen vegetation signatures were used in this study and include three low NDVI signatures. All RSRs capture some portion of the step function with MODIS capturing only the very beginning of some signatures, followed by the square wave that captures the initial rise of additional signatures. ETM+ captures more of the red edge

with IKONOS and AVHRR capturing about one third of the rise. Additionally, AVHRR9 captures a significant portion of the red band below 600nm compared to the other sensors. Vegetation signatures generally also have a decreasing profile in transition from the green to the red region of the electro-magnetic spectrum. The combination of decreasing slope and step function in red band vegetation profiles was considered in the following analyses.

No significant differences were found in Grass LowNDVI2 and Grass LowNDVI3 signatures values for all sensor comparisons due to the relatively flat characteristics in the band. Only five signature comparisons lead to differences beyond the 0.050 effect on NDVI and all were in comparisons with AVHRR9: Closed Shrub for both the square wave and ETM+ comparison; and Grassland, Conifers, and Grass for comparison with ETM+. These differences were due to increases in reflectance for these signatures in the 550nm range which is captured only by the AVHRR9 sensor. This effect can be observed in the conifer radiance profile and band profiles as high radiance decreases from 550 nm to the red band region for the Conifers signature (Figure 34).

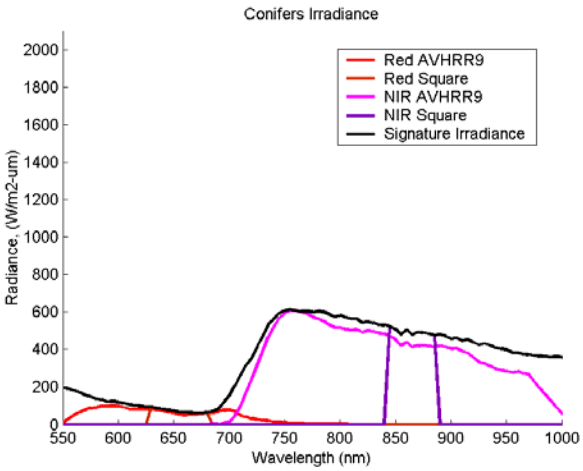

Figure 34. Increased radiance below 600nm in the conifer radiance profile.

Other signatures increased in this region as well, but to a lesser degree and at lower reflectance levels.

Fifty eight percent of comparisons between responses of vegetation signatures effected NDVI measurements beyond 0.010 including at least one signature in each of the response comparisons. Vegetation signature measurement differences that effect NDVI in this range were consistent with both Theoretical Model results of red band decreasing and step function signatures. This holds true if slopes of decreasing signatures are small and if response functions are not biased towards shorter wavelengths. This was precisely the case for virtually all vegetation signatures and response functions of IKONOS, ETM+, MODIS, and AVHRR9 which are biased toward longer wavelengths. Exceptions are cases, as noted above, where the broadband AVHRR9 response function captures vegetation variation at around 550 nm.

Near Infrared Band

Effect on NDVI from Near Infrared Differences

The thirty two spectral signatures examined in this study are graphed according to their square wave red and near infrared values in Figure 35 along with the isolines of near infrared band reflectance differences that lead to a 0.01 change in NDVI. Vegetation signatures are displayed in green, manmade in blue and natural non-vegetation in brown. To have NDVI differences within one percent, vegetation near infrared reflectance signatures measurement differences generally needed to be in the range of 0.01 or greater, except for signatures with low red and near infrared reflectance, which required differences to be closer to 0.005.

For a 5% difference in NDVI values between sensors, near infrared band measurement discrepancies could be much higher. Differences of 0.01 in near infrared band reflectance for green vegetation generally had an effect on NDVI in the 2% or less range (Figure 36).

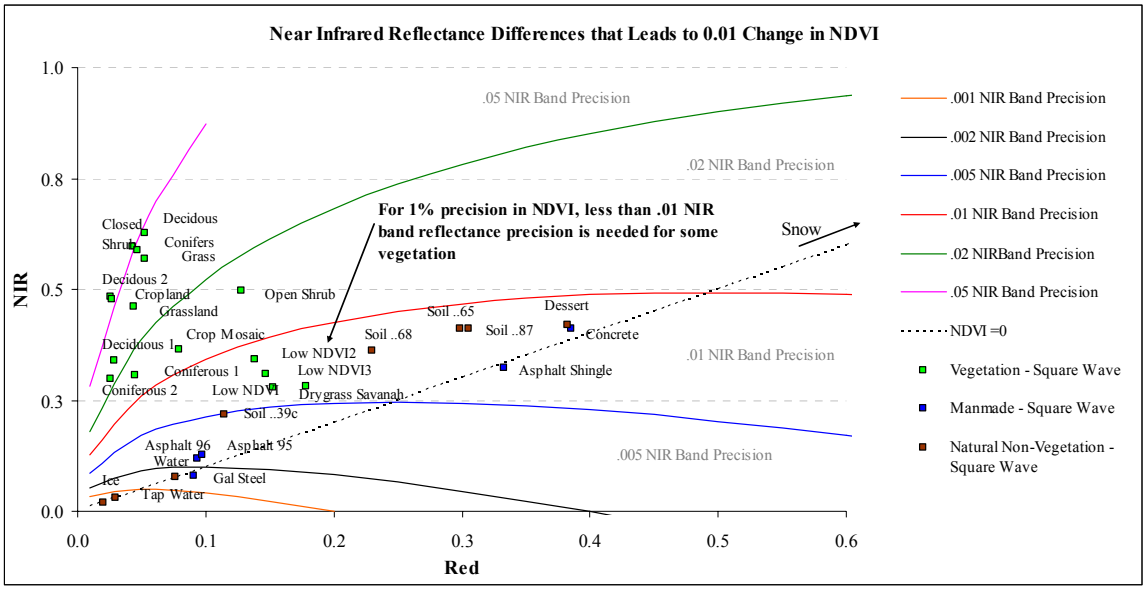

Figure 35. Near Infrared reflectance differences that lead to 1% change in NDVI.

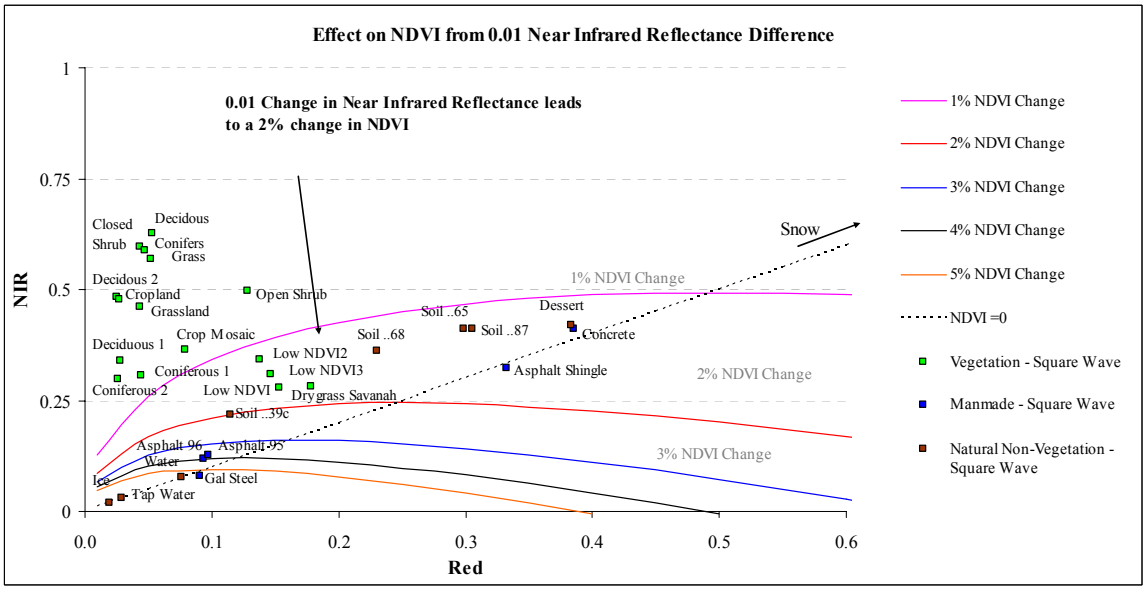

Figure 36.Effect on NDVI from 0.01 near infrared reflectance differences.

Effect on NDVI from Differences in NIR Band Measurements										
Signature	Square vs. IKONOS	Square vs. Landsat7 ETM+	Square vs. MODIS	Square vs. AVHRR9	Landsat7 ETM+ vs. IKONOS	Landsat7 ETM+ vs. MODIS	Landsat7 ETM+ vs. AVHRR9	IKONOS vs. MODIS	IKONOS vs. AVHRR	MODIS vs. AVHRR
Ice	-0.416	-0.165	-0.068	-0.262	-0.350	0.145	-0.141	1.731	0.560	-0.224
Tap Water	-0.319	-0.110	-0.041	-0.187	-0.266	0.092	-0.101	0.752	0.319	-0.163
Water	-0.151	-0.041	-0.013	-0.082	-0.122	0.032	-0.046	0.201	0.098	-0.073
Gal Steel Roof 525uuua	-0.212	-0.103	-0.032	-0.134	-0.120	0.078	-0.035	0.247	0.105	-0.107
Asphalt 96uuu	-0.074	-0.016	-0.006	-0.046	-0.063	0.011	-0.033	0.090	0.036	-0.042
Asphalt 95uuu	-0.063	-0.013	-0.005	-0.041	-0.055	0.009	-0.031	0.077	0.028	-0.038
Asphalt shingle 49000uuu	-0.045	-0.012	-0.003	-0.029	-0.033	0.010	-0.018	0.046	0.017	-0.027
Barren Desert	-0.014	0.001	0.001	-0.016	-0.015	0.001	-0.017	0.017	-0.001	-0.017
Concrete	-0.021	-0.003	0.000	-0.019	-0.018	0.004	-0.016	0.022	0.002	-0.020
Coarse Granular Snow	-0.035	-0.011	-0.005	-0.018	-0.024	0.006	-0.007	0.031	0.017	-0.013
Medium Snow	-0.025	-0.007	-0.003	-0.015	-0.018	0.004	-0.008	0.023	0.010	-0.012
Fresh snow	-0.010	-0.001	0.001	-0.011	-0.009	0.001	-0.011	0.011	-0.001	-0.012
Soil 85P5339c	0.029	0.022	0.005	0.002	0.007	-0.018	-0.022	-0.029	-0.033	-0.004
Drygrass Savanna	0.003	0.008	0.003	-0.010	-0.005	-0.005	-0.020	0.000	-0.016	-0.014
Soil 87P3468	0.023	0.013	0.004	0.001	0.010	-0.009	-0.013	-0.021	-0.025	-0.003
Soil 87P1087	0.017	0.012	0.004	-0.004	0.005	-0.008	-0.016	-0.014	-0.023	-0.008
Soil 87P3665	0.008	0.004	0.002	-0.008	0.004	-0.002	-0.013	-0.007	-0.018	-0.010
Deciduous2	0.010	0.002	0.000	0.008	0.009	-0.002	0.007	-0.017	-0.003	0.008
Coniferous2	0.003	0.000	0.000	0.003	0.003	0.000	0.004	-0.005	0.001	0.003
Cropland	0.008	0.001	0.000	0.010	0.008	-0.001	0.011	-0.014	0.004	0.011
Deciduous1	0.004	0.000	0.000	0.004	0.004	0.000	0.005	-0.006	0.000	0.004
Closed Shrub	0.009	0.001	0.000	0.006	0.009	-0.001	0.006	-0.016	-0.005	0.006
Grassland	0.011	0.002	0.001	0.007	0.010	-0.001	0.006	-0.016	-0.006	0.007
Coniferous1	0.006	0.001	0.000	0.010	0.006	-0.002	0.010	-0.010	0.005	0.011
Conifers	0.009	0.001	0.001	0.006	0.009	-0.001	0.006	-0.014	-0.004	0.006
Deciduous	0.011	0.002	0.001	0.007	0.010	-0.001	0.005	-0.016	-0.006	0.006
Grass	0.013	0.003	0.001	0.008	0.011	-0.002	0.006	-0.018	-0.008	0.007
Crop Mosaic	0.005	0.000	0.000	0.005	0.006	0.000	0.006	-0.008	0.000	0.006
Open Shrub	0.019	0.005	0.001	0.009	0.015	-0.004	0.005	-0.022	-0.012	0.008
Grass lowNDVI2	0.008	0.004	0.001	0.002	0.004	-0.003	-0.002	-0.008	-0.007	0.001
Grass lowNDVI3	-0.003	0.000	0.000	-0.004	-0.004	0.000	-0.005	0.004	-0.001	-0.004
Grass lowNDVI	-0.017	-0.004	-0.001	-0.011	-0.014	0.003	-0.007	0.019	0.007	-0.010
Average	-0.038	-0.013	-0.005	-0.025	-0.031	0.010	-0.015	0.095	0.033	-0.022

Table 17. Effect on NDVI from near infrared band measurement discrepancies between sensors. Highlighted in yellow are red band differences that have greater than a 0.010 effect on NDVI and highlighted in orange are values that have greater than a 0.050 effect on NDVI.

The effect on NDVI from differences in near infrared band reflectance between sensors is provided in Table 17 for all signatures. Effect on NDVI from differences in near infrared band measurements between sensors was calculated by taking the difference between the second RSR derived NDVI and NDVI calculated using calibrated near infrared band measurements from the first sensor substituted for near infrared band values for each comparison (Equation 9). This resulted in NDVI differences that were associated with only differences in near infrared band measurements.

$$\mathbf{NDVI}_{RSR2} - \mathbf{((NIR}_{Cal\ RSR1} \mathbf{-\ Red}_{RSR2}\mathbf{)/(NIR}_{Cal\ RSR1} \mathbf{+\ Red}_{RSR2}\mathbf{))} \qquad \text{Equation 9}$$

Differences in near infrared band measurements between sensors lead to an effect on NDVI greater than 0.050 for 12% of all signatures with none for vegetation. Differences also lead to an effect on NDVI greater than 0.010 for 44% of all signatures and 15% for vegetation.

Flat Signatures

Eight of the signature reflectance profiles had relatively constant reflectance values through the near infrared band. These signatures were ice, water, and man made materials and included Barren Desert. Consistent with previous findings, near infrared signature reflectance values were over estimated for some flat signatures and calibration error had some effect on data. Near infrared band measurement differences that lead to changes greater than 0.05 NDVI were found for at least one flat signature below a reflectance level of 0.15 for all comparisons. The comparison of MODIS vs. the square wave response was consistent with Theoretical Model predictions. Only differences of very low reflectance signatures resulted in an effect on NDVI greater than 1% with the difference of the very lowest reflectance signature of Ice resulting in an effect grater than 5% (Table 18). Similar to the Theoretical Model RSRs, the square wave and MODIS responses are similar. All other response differ considerably in response, bandwidth, band center and average band pass.

The differences in responses lead to significant differences between sensor measurements and on NDVI for many of the comparisons of flat signatures. However, all comparisons

followed the same general trend of a higher effect on NDVI as reflectance levels decrease as can be seen in the comparison of MODIS with AVHRR9 (Table 19).

Signature	Square Wave NIR Band Reflectance	Square wave vs. MODIS Cal. NIR Band Difference	
Concrete	.411	.000	
Barren Desert	.420	.001	
Asphalt shingle 49000uuu	.322	-.002	
Asphalt 95uuu	.126	-.001	
Asphalt 96uuu	.118	-.001	
Water	.077	-.002	>1% Effect on NDVI
Tap Water	.030	-.003	
Ice	.020	-.003	>5% Effect on NDVI

Table 18. Flat signature near infrared band reflectance and calibrated differences for square wave and MODIS sensors.

Measurement differences between these two sensors were considerably higher than in previously comparisons, however, as predicted their effect on NDVI was still below 0.05 for signatures with higher band reflectance values..

Signature	Square Wave NIR Band Reflectance	MODIS vs. AVHRR9 Cal. NIR Band Difference	
Concrete	.411	-.02	
Barren Desert	.420	-.02	>1% Effect
Asphalt shingle 49000uuu	.322	-.03	on NDVI
Asphalt 95uuu	.126	-.04	
Asphalt 96uuu	.118	-.04	
Water	.077	-.07	
Tap Water	.030	-.016	>5% Effect
Ice	.020	-.022	on NDVI

Table 19. Flat signature near infrared band reflectance and calibrated differences for MODIS and AVHRR9 sensors.

Increasing Signature

Five of the simulation study signatures had increasing slopes in the near infrared band region. These signatures were the same four soil types and Drygrass Savanna as for the red band. No near infrared band differences resulted in greater than a 0.050 effect on NDVI, however, 25% lead to differences effecting NDVI at 0.010. The maximum absolute difference in near infrared band reflectance for increasing signatures for all RSRs was 0.033, with an average difference of 0.004. These results are consistent with the Theoretical Model that predicts significant differences that effect NDVI at the 1% level due to significantly different RSRs and that the effect on NDVI would be below 5%.

Increasing signatures are listed in Table 20 in order of highest to lowest slope along with respective square wave near infrared band reflectance and calibrated differences between ETM+ and IKONOS. No significant differences between increasing signatures was found for the ETM+ and IKONOS comparison, even though some response differences were noticeable.

Signature	**Square Wave NIR Band Reflectance**	**ETM+ vs. IKONOS Cal. NIR Band Difference**
Soil 85P5339c	0.217	0.002
Soil 87P1087	0.411	0.004
Soil 87P3468	0.363	0.006
Soil 87P3665	0.412	0.003
Drygrass Savanna	0.280	-0.003

Table 20. Increasing signature near infrared band reflectance and calibrated differences for ETM+ and IKONOS sensors.

This is consistent with Theoretical Model findings that near infrared band differences are unlikely to effect NDVI values at or above the 0.01 level unless RSRs are significantly different. Near infrared band RSRs are significantly different for a number of comparisons such as the square wave vs. IKONOS and Landsat ETM+ vs. AVHRR9. In these cases, differences between sensors lead to an effect on NDVI greater than 1%, and all were below an effect of 5%.

Decreasing Signature

Four of the simulation study signatures had decreasing slopes in the near infrared band region and included three snow signatures and Galvanized Steel Roof. For the snow signatures, 56% of all comparisons had in an effect on NDVI greater than 1% and none for greater than 5%. For Galvanized Steel, all signatures had and effect on NDVI greater than 5% except for the square wave vs. MODIS and ETM+ vs. AVHRR which had an effect greater than 1%. Signatures with near infrared band differences that lead to greater than 1% and 5% change in NDVI are shown in Table 21 in order of highest to lowest band reflectance for the square wave along with absolute calibrated band measurement difference for Landsat 7 ETM+ and MODIS sensors. Near infrared band differences that lead to greater than 5% change in NDVI are noted. Decreasing signatures covered a range of slopes similar to those in the Theoretical Model.

Consistent with Theoretical Model results, no significant differences between sensors was found in comparisons of snow signatures for sensors with similar RSRs, such as ETM+ vs. MODIS, and Square wave vs. MODIS. In cases where RSRs differed

significantly, differences that effect NDVI below the 5% were observed. Only comparisons of Galvanized Steel Roof signature resulted in significant differences between sensors that effect NDVI greater than 5%. This is because the Galvanized Steel signature has very low red and near infrared reflectance that requires near infrared spectral measurements to be less than 0.002 in order not to have an effect on NDVI at the 1% level; and a 0.01 difference for these low reflectance signatures can lead to measurement discrepancies that effect NDVI beyond the 5% level.

Signature	Square Wave NIR Band Reflectance	ETM+ vs. MODIS Cal. NIR Band Difference	
Fresh Snow	1.088	.003	
Medium Snow	.994	.007	
Coarse Granular Snow	.932	.010	
Gal Steel Roof 525uuua	.081	-.011	>5% Effect on NDVI

Table 21. Decreasing signature square wav near infrared band reflectance and calibrated differences for MODIS vs. AVHRR9 sensors.

Reflectance values were also greater than one for the Fresh Snow signature square wave near infrared band values. For the case of Fresh Snow, this error was 2.1% between the square wave and IKONOS RSR. This effect is consistent with Theoretical Model findings that is a result of the different averaging method used for sensor radiance and average band pass for reflectance calculations.

Vegetation Signatures

Fifteen vegetation signatures were used in this study and include three different low NDVI grass signatures. Real vegetation near infrared signatures have a combination of characteristics investigated in the Theoretical Model and are mainly described by flat and

step functions characteristics. There is also considerable variation of these signatures throughout the near infrared band region from the red edge and beyond, and include slightly increasing and decreasing characteristics at different parts of the band. Theoretical Model results suggest that differences for flat signatures in the near infrared band should not significantly effect NDVI at the 1% level. However, Theoretical Model results for step functions, increasing, and decreasing profiles lead to differences between RSRs that resulted in significant effects on NDVI values under certain conditions.

For the sensors studied, significant differences in RSR indeed exist. The AVHRR9 RSR captures almost the entire red edge while the IKONOS and ETM+ RSR capture only the tail end. MODIS and square wave responses do not capture the red edge, only the near infrared plateau beyond 830 nm. Additionally, AVHRR9 captures a large spectral range beyond approximately 900nm compared to other sensors. Signature variation increases in this area compared to the initial plateau region around 800 nm. The IKONOS near infrared RSR has a shorter wavelength biased response compared to ETM+, MODIS, and square wave responses. AVHRR9 also has a shorter wavelength bias, but it is not as pronounced and the wide bandwidth appears to reduce the overall effect of the bias.

No near infrared signature measurement differences between sensors lead to a greater than 5% difference in NDVI. Fifteen percent of vegetation signatures comparisons affected NDVI measurements beyond 0.010. No significant differences were found in Conifesous2, Deciduous 1, Crop Mosaic, Grass LowNDVI2 or Grass Low NDVI3 signatures for all sensor comparisons. The maximum differences observed had an effect

on NDVI of 0.022. All but five of the comparisons that lead to an effect on NDVI below 5% were associated with the IKONOS sensor. This was attributed to its pronounced shorter wavelength biased response. All other significant differences had an effect on NDVI of 0.010. While the significant differences in near infrared band RSRs used in this study might imply a significant effect on NDVI due to increasing, decreasing and step function signature characteristics of vegetation, the effect of the flat characteristic of the near infrared "plateau" on measurement discrepancies between sensors dominated the resulting differences between sensors

NDVI

NDVI Sensitivity to Red and Near Infrared Changes

This section extends the red and near infrared band analyses to the combined effect on NDVI from both red and near infrared band measurement discrepancies between sensors. The thirty two spectral signatures examined in this study were graphed using their square wave red and near infrared values (Figure 37) along with the isolines of red and near infrared band reflectance differences that lead to a 0.01 change in NDVI. Vegetation signatures are displayed in green, manmade in blue and natural non-vegetation in brown. Low red band reflectance and high near infrared band reflectance of vegetation signatures are in the red and near infrared space that is more sensitive to differences in red band measurements. For an effect on NDVI less than 0.01, red band measurement differences in signatures of Low NDVI targets need to be in the range of 0.003 to 0.004 and even lower for some vegetation signatures. For a similar effect, corresponding near infrared

band measurements can be from 0.006 to 0.008 for low NDVI signatures, and much higher for most vegetation signatures.

For a 5% difference in NDVI between sensors, red and near infrared band measurement discrepancies can be much higher (Figure 38). A change in near infrared band reflectance of 0.01 leads to a maximum effect on NDVI of less than 2% for even low NDVI vegetation signatures. Similar differences in red band measurements for these same signatures result in an effect on NDVI of approximately 3%. For green vegetation with low near infrared and very low red band reflectance, such as the Coniferous1, Coniferous2, and Deciduous1 signatures, the 0.01 change in red band reflectance leads to a larger effect on NDVI, around 5%. The same difference in near infrared band reflectance leads to an effect on NDVI less that 1%.

The effect on NDVI from differences in red and near infrared band reflectance between sensors is provided in Table 22. Differences in red and near infrared band measurements between sensors lead to an effect on NDVI greater than 0.050 for 23% of all signatures and 11% for vegetation. Differences also lead to an effect on NDVI greater than 0.010 for an additional 55% of all signatures and 25% for vegetation. These significant differences account for 77.5% of all signature comparisons.

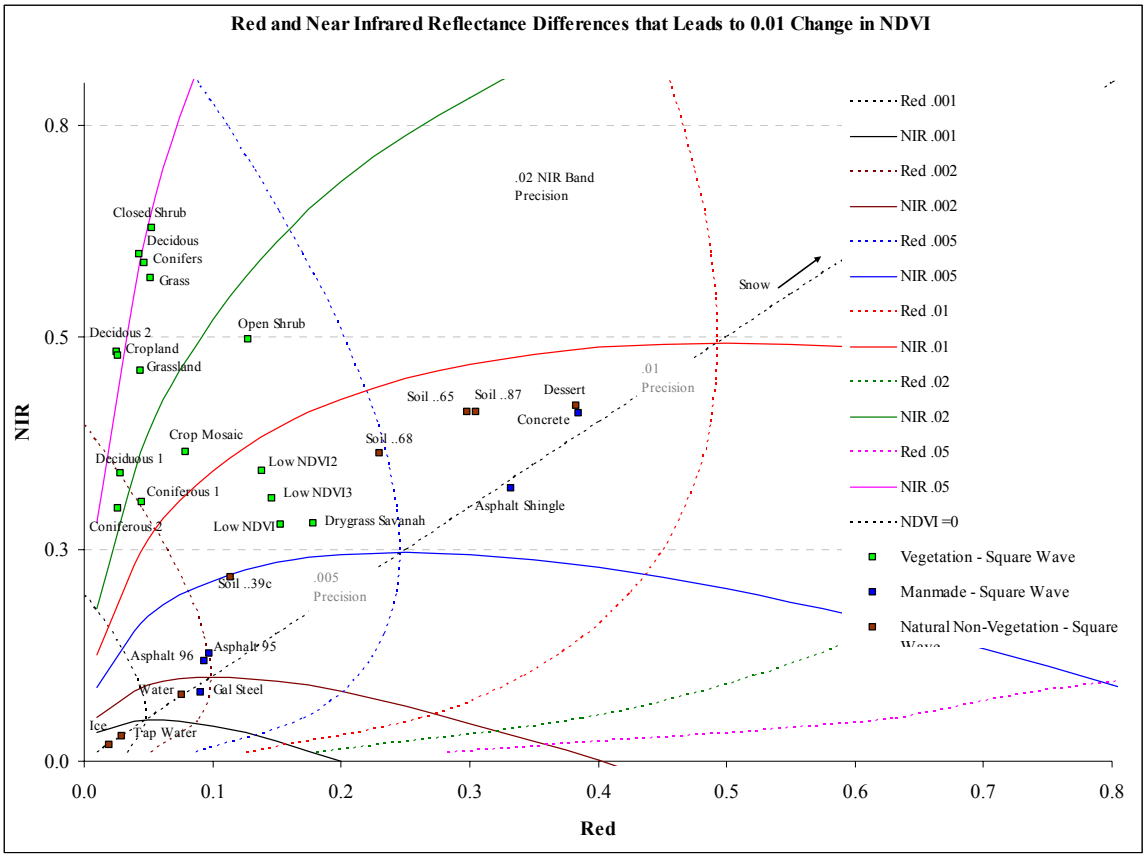

Figure 37. Red and near infrared reflectance differences that lead to 1% change in NDVI.

The differences in NDVI are the result of the combined effect of sensor differences in both the red and near infrared band. In most cases the combined effect on NDVI from the two bands results in a cumulative and higher effect on NDVI. For example, the Deciduous2 signature comparison between Landsat 7 ETM+ and IKONOS had a red band effect of 0.009 and near infrared band effect of 0.021 and lead to a total error of 0.031. In some cases, the differences in each band compensated for individual band error and resulted in an NDVI difference between sensors lower than the higher error in each band. The Landsat 7 ETM+ comparison with MODIS reduced the effect on NDVI from the 0.011 effect in the near infrared band with the -0.002 effect in the red band.

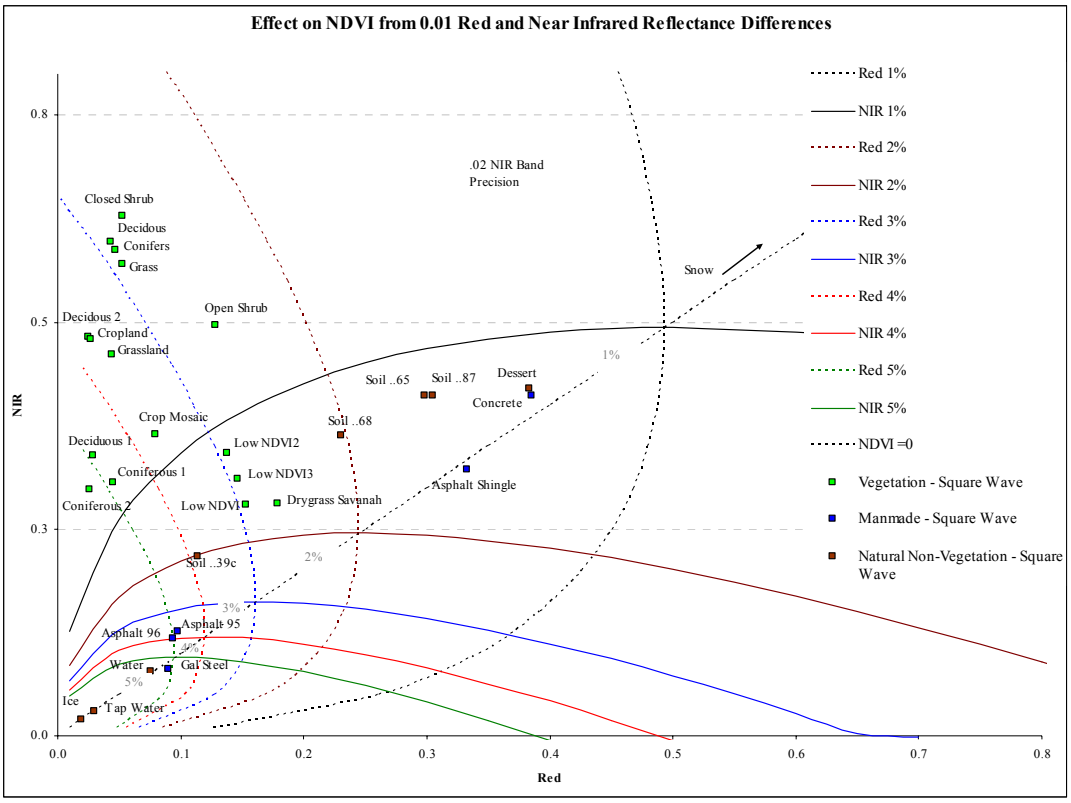

Figure 38. Effect on NDVI from 0.01 red and near infrared reflectance differences.

Effect on NDVI from Differences in Red and Near Infrared Band Measurements										
Signature	Square vs. IKONOS	Square vs. Landsat7 ETM+	Square vs. MODIS	Square vs. AVHRR9	Landsat7 ETM+ vs. IKONOS	Landsat7 ETM+ vs. MODIS	Landsat7 ETM+ vs. AVHRR9	IKONOS vs. MODIS	IKONOS vs. AVHRR	MODIS vs. AVHRR
Ice	-0.715	-0.218	-0.051	-0.409	-0.616	0.208	-0.237	1.366	0.638	-0.400
Tap Water	-0.523	-0.147	-0.032	-0.285	-0.441	0.133	-0.162	0.806	0.396	-0.274
Water	-0.225	-0.055	-0.009	-0.115	-0.183	0.049	-0.066	0.264	0.134	-0.110
Gal Steel Roof 525uuua	-0.272	-0.111	-0.030	-0.201	-0.171	0.087	-0.092	0.298	0.100	-0.175
Asphalt 96uuu	-0.124	-0.021	-0.008	-0.088	-0.109	0.014	-0.069	0.135	0.045	-0.082
Asphalt 95uuu	-0.109	-0.017	-0.009	-0.084	-0.097	0.009	-0.070	0.115	0.031	-0.077
Asphalt shingle 49000uuu	-0.057	-0.015	-0.001	-0.033	-0.042	0.015	-0.019	0.059	0.024	-0.033
Barren Desert	-0.020	0.000	0.000	-0.023	-0.021	0.000	-0.024	0.022	-0.003	-0.023
Concrete	-0.027	-0.004	0.000	-0.027	-0.024	0.004	-0.023	0.028	0.000	-0.027
Coarse Granular Snow	-0.035	-0.012	-0.004	-0.014	-0.023	0.009	-0.002	0.032	0.021	-0.010
Medium Snow	-0.024	-0.007	-0.002	-0.012	-0.017	0.005	-0.005	0.023	0.012	-0.010
Fresh snow	-0.008	0.000	0.001	-0.010	-0.007	0.001	-0.009	0.009	-0.002	-0.011
Soil 85P5339c	0.003	0.024	-0.006	-0.049	-0.021	-0.032	-0.075	-0.015	-0.058	-0.043
Drygrass Savanna	-0.006	0.013	-0.007	-0.046	-0.020	-0.021	-0.060	-0.001	-0.042	-0.040
Soil 87P3468	0.019	0.018	-0.007	-0.037	0.001	-0.026	-0.056	-0.028	-0.058	-0.030
Soil 87P1087	0.013	0.016	-0.004	-0.032	-0.002	-0.019	-0.048	-0.018	-0.047	-0.028
Soil 87P3665	0.004	0.009	-0.007	-0.047	-0.004	-0.016	-0.057	-0.012	-0.053	-0.040
Deciduous2	0.031	0.002	0.004	0.035	0.031	0.002	0.036	-0.034	0.004	0.032
Coniferous2	0.008	-0.005	0.008	0.032	0.014	0.014	0.039	-0.002	0.026	0.025
Cropland	0.028	0.000	0.004	0.038	0.030	0.004	0.040	-0.030	0.012	0.034
Deciduous1	0.021	-0.002	0.009	0.044	0.025	0.012	0.049	-0.015	0.024	0.036
Closed Shrub	0.061	0.008	0.006	0.062	0.056	-0.003	0.057	-0.063	0.000	0.058
Grassland	0.033	-0.002	0.012	0.054	0.037	0.014	0.059	-0.026	0.021	0.043
Coniferous1	0.011	0.000	0.005	0.033	0.011	0.004	0.035	-0.009	0.025	0.029
Conifers	0.047	-0.001	0.009	0.056	0.051	0.011	0.060	-0.043	0.009	0.048
Deciduous	0.047	-0.001	0.008	0.050	0.051	0.009	0.054	-0.045	0.002	0.043
Grass	0.039	-0.003	0.013	0.057	0.045	0.017	0.063	-0.031	0.017	0.045
Crop Mosaic	0.026	0.003	0.005	0.039	0.024	0.001	0.037	-0.024	0.013	0.035
Open Shrub	0.049	0.015	-0.005	0.020	0.035	-0.021	0.005	-0.059	-0.032	0.025
Grass lowNDVI2	0.014	0.009	-0.004	-0.005	0.005	-0.014	-0.015	-0.019	-0.020	-0.001
Grass lowNDVI3	-0.003	0.004	-0.004	-0.008	-0.007	-0.008	-0.013	0.000	-0.005	-0.004
Grass lowNDVI	-0.025	-0.004	-0.001	-0.012	-0.022	0.004	-0.008	0.027	0.014	-0.011
Average	-0.054	-0.016	-0.003	-0.032	-0.044	0.015	-0.018	0.085	0.039	-0.031

Table 22. Effect on NDVI from red and near infrared band measurement discrepancies between sensors. Highlighted in yellow are red band differences that have greater than a 0.010 effect on NDVI and highlighted in orange are values that have greater than a 0.050 effect on NDVI.

Flat and Decreasing Signatures

Signatures with flat reflectance signatures through both the red and near infrared band are representative of desert, water, ice, and manmade materials and have low NDVI values. For these land cover types, the combined band effect of differences between sensors generally had a significant effect on NDVI beyond 0.010 or 0.050. Only 15% of the signature comparisons had an effect on NDVI below this level. Most of these were from the very well aligned RSRs such as the square wave vs. MODIS comparisons. Of the eighty five percent of signatures that had an effect on NDVI greater than 0.010, fifty one percent were above a 0.050 effect on NDVI. Table 23 shows the Flat signature square

wave NDVI value and the difference in NDVI between Landsat 7 ETM+ and IKONOS. The effect these differences have on NDVI is also noted. Generally, differences between sensors had an increasing effect on NDVI as red and near infrared band values decrease following the NDVI equal to zero line.

Signature	Square Wave NDVI	ETM+ vs. IKONOS Cal. NDVI Difference	
Concrete	.032	-.024	
Barren Desert	.046	-.021	>1% Effect
Asphalt shingle 49000uuu	-.016	-.042	on NDVI
Asphalt 95uuu	.128	-..097	
Asphalt 96uuu	.115	-.109	>5% Effect
Water	.010	-.183	on NDVI
Tap Water	.010	-.441	
Ice	.006	-.616	

Table 23. Flat signature square wave NDVI and calibrated differences for ETM+ and IKONOS sensors.

Results for signatures with a flat or slightly decreasing profile in the red band and decreasing profiles in the near infrared band were similar to the flat signatures above (Table 24). These low NDVI signatures also lead to a significant effect on NDVI as red and near infrared band values decrease.

Signature	Square Wave NDVI	ETM+ vs. MODIS Cal. NDVI Difference	
Fresh Snow	.002	.001	
Medium Snow	-.031	.005	
Coarse Granular Snow	-.053	.009	
Galvanized Steel Roof	-.052	.087	>5% Effect on NDVI

Table 24. Square wave NDVI and calibrated differences for ETM+ and MODIS of signatures with flat red and decreasing near infrared profiles.

These results are generally consistent with the independent findings for both the red and near infrared band analyses for the Theoretical Model, which predicted increasing error in band measurements as red and near infrared reflectance decreases.

Increasing Signature

Signatures with increasing profiles through both the red and near infrared band are representative of soils and dry vegetation, and have low NDVI values. For these low NDVI land cover types, the combined band effect of differences between sensors had a significant effect on NDVI beyond 0.010 for seventy two percent of the comparisons. For comparisons or RSRs with very different characteristics, such as AVHRR9 vs. Landsat 7 ETM+ and IKONSOS, differences exceeded an effect on NDVI greater than 0.050.

NDVI differences became larger as the absolute value of NDVI increased (Table 25). These findings are consistent with previous investigations of red and near infrared bands that resulted in significant sensor response differences for all signatures; and with Theoretical Model results that predicted significant differences in the 1% or greater effect on NDVI between sensors.

These differences were attributed mostly to differences to the increased sensitivity to red band differences for theses signatures, especially as red and near infrared band measurements drop along the NDVI equal to zero line.

Signature	Square Wave NDVI	ETM+ vs. MODIS Cal. NDVI Difference	
Soil 85P5339c	0.311	-0.032	> 0.010 effect
Soil 87P3468	0.223	-0.026	on NDVI
Drygrass Savanna	0.186	-0.021	
Soil 87P1087	0.159	-0.019	
Soil 87P3665	0.149	-0.016	

Table 25. Increasing signature square wave NDVI and calibrated differences for ETM+ and MODIS sensors.

Vegetation Signatures

Vegetation signatures have significant variation in red and near infrared band characteristics. Vegetation signatures used in this study span the range of NDVI values and reflectance levels observed in Earth observations. For these cover types, the combined band effect of differences between sensors had a significant effect on NDVI beyond 0.050 for eleven percent of the comparisons. Sixty four percent of all vegetation signatures comparisons had differences that lead to an effect on NDVI greater than 0.010. All sensor comparisons had at least one signature that resulted in a significant difference. Most of the signatures that had an effect on NDVI less than 0.010 were comparisons of RSRs with very similar characteristics, specifically the square wave vs. MODIS and ETM+.

All signatures that resulted in greater than 5% effect on NDVI had near infrared values above approximately 0.4. As discussed previously, these high differences were mostly related to an increase in signature radiance in the red band 550 nm range. In addition to effect on NDVI from red band measurements, the additional effect on NDVI from near infrared band measurements of Closed Shrub, Grassland, Conifers, and Grass signatures

resulted in some deciduous and open shrub signature comparisons to be above the 5% effect on NDVI. Half of these signatures were from the ASTER spectral Library and the other half from the remotely sensed hyper-spectral PROBE-1 data including Open Shrub, Closed Shrub, and Grassland. Over half of the differences that lead to the greater than 0.050 effect on NDVI were from comparisons with AVHRR9, which is to be expected given the very different red and near infrared band RSRs compared to the other sensors.

The effect on NDVI from differences between sensors was mostly due to discrepancies in red band measurements, however, near infrared band discrepancies contributed as well. For the wide range of RSRs examined in this study, it can be expected that vegetation NDVI discrepancies will generally be less than 0.050, but will exceed this in some cases.

Summary and Conclusions

Mirroring the methodology used in Chapter 3, a sensor simulation study was conducted using real sensor RSRs and real land cover reflectance signatures. Quantitative differences between sensor band measurements were examined in relation to their effect on NDVI and based on isolines of NDVI error. Generally, close agreement was found between the Theoretical Model and Sensor Simulation study results.

RSRs were very different for the sensors used in this study with differences observed in average band pass values as high as of 3.7% and 20.3% relative to the square wave response for the red and near infrared bands, respectively.

Land cover types were examined in relation to their signature reflectance characteristics as modeled in the Theoretical Model study. These reflectance signatures were convolved with solar irradiance and RSRs and integrated over each band to provide signature radiance measurements. These values were converted to reflectance values and inter-response calibration was performed.

As observed in the Theoretical Model, small measurement error due to conversion of radiance to reflectance values was observed in some signature comparisons of between sensors. Cross-sensor calibration generally resulted in improved correlation between sensors and adjusted for gain and offset differences, however, for some signatures it lead to increased error between sensor measurements.

Despite the mechanisms that lead to magnitude differences in the various signature measurements between sensors, relationships between sensors were linear and lead to good correlation between sensor responses. This study validated the findings of the Theoretical Model study that found that although there was relatively good correlation between sensor measurements, observed measurement discrepancies could result in significant NDVI differences of greater than 0.010 and in some cases 0.050. This is because the sensitivity of NDVI to differences in band measurements between sensors greatly increases as red and near infrared band values both decrease. Maximum differences between sensors for all signature reflectance comparisons were 0.024 and 0.068 for the red and near infrared band, respectively. Band measurement differences resulted in a maximum effect on NDVI of 0.428 and 1.73 for the red and near infrared

band, respectively. These large effects were associated with water, ice, asphalt, and galvanized steel signatures that all had very low reflectance and NDVI values. For all other signatures, differences in red or near infrared band measurements alone did not lead to NDVI differences greater than 0.050 except for in some isolated signature comparisons with AVHRR9. The effect on NDVI from the combined differences in red and near infrared band was generally less than 0.050 as well, however, a number of signature comparisons between sensors lead to an effect on NDVI greater than this, including 11% of vegetation signatures. This was due to several contributing factors, i.e. RSR, artifacts of NDVI calculations, calibration, and more importantly measurement sensitivity of NDVI to band measurement differences at low reflectance levels.

Chapter 5: Summary and Conclusions

Introduction

This study examined the variability in spectral measurements due to RSR differences in different remote sensing systems and the implications of these measurement variations on the accuracy and consistency of NDVI. Excellent agreement between a theoretical model and sensor simulations provided insights into the factors that contribute to differences in spectral measurements and NDVI between different remote sensing systems.

The primary findings of this research were that differences in RSR did not lead to significant differences in band measurement values between sensors; but under certain conditions, these small band differences could result in significant differences of up to 6% in NDVI; and that NDVI is increasingly sensitive to band measurement differences as reflectance levels decrease. Maximum differences between sensors for all signature reflectance comparisons were 0.024 and 0.068 for the red and near infrared band, respectively. Except for signatures with very low reflectance, differences in red or near infrared band measurements alone did not lead to NDVI differences greater than 0.050 except for in some isolated signature comparisons with AVHRR9.

Study Implications

While observations from different remote sensing systems generally provide consistent measurements of vegetation, differences between sensor RSRs can have an effect on

band measurements that result in significant differences in NDVI for studies that require NDVI at higher levels of precision. However, the good news from this study is that as long as appropriate cautions are taken in comparing vegetation spectral measurements between sensors, the effect of RSR on band measurements and NDVI is relatively small compared to other error factors, and that similarly comparable measurements of vegetation from different sensors can be obtained. For example, El Saleous, et al. (2000) found that individual effects from ozone, Rayleigh scattering, and aerosols on AVHRR data lead to differences of up to 0.12 for red band and .083 for near infrared band measurements. Effects of water vapor were as high as 4.4% and 25% for the red and near infrared band, respectively. These atmospheric effects lead to individual effects on NDVI up to 0.12 and 0.23 for soils and deciduous forest, respectively.

Researchers should take the following precautions when using or comparing spectral measurements from different sensors:

- Appropriately account for effects of atmosphere on band measurements
- Appropriately account for land cover dynamics between images
- Use consistently derived surface reflectance values as the basis for comparison
- Use a standard solar spectrum for average band pass (ESUN) determination
- Cross-calibrate band data based on two-directional estimated line fits and only with data types of interest
- Perform cross-calibration on band measurements prior to NDVI derivation
- Avoid, or at least understand, effects of comparing RSRs that have large fundamental differences
- Understand the effect of differences in band measurements on NDVI in context of isolines of NDVI error

This study should provide guidance for future research that depends on reflectance measurements from a number of different sensor systems to derive and use NDVI for a variety of investigations of land cover and vegetation. Using the results detailed in this

study, researches are now in a position to quantitatively evaluate differences in spectral band measurements and their subsequent effect on the accuracy and precision of NDVI derived from those measurements.

The results of this study show that NDVI measures from the 40+ year archive of remotely sensed data generally provide a consistent record of vegetation, but not always within a precision of 5% in NDVI. Additionally, it suggests that sensors in the future may be used to maintain a land cover data record even if relative spectral responses are somewhat different. It also demonstrates that the 1% precision in NDVI needed for accurate assessments of certain biophysical variables is achievable when considering only the effect of sensor RSR, but is unlikely given the combined sensor and scene error inherent in remotely sensed land cover measurements. Design of new sensors for Earth observation should take into consideration the implied need for standardization of spectral response if higher levels of NDVI precision are to be realized.

Research Questions Addressed

Factors of Variation

Question 1: what are the factors that contribute to variation in red and near infrared band measurements of land cover and vegetation due to relative spectral response? The factors that contribute to the variation in red and near infrared band measurements of land cover and vegetation due to RSR are quite complex and, therefore, no single relationship can be derived which explains their effects for all cases. This is because variation between sensors of land cover signature reflectance is due to the wavelength dependent

convolution of signature reflectance, solar irradiance, and RSR. Variation in these factors between sensor measurements differs for each comparison. However, the mechanisms that lead to red and near infrared cross-sensor measurement discrepancies can generally be understood to explain how data from different sensors compare. Several general conclusions can be drawn and predictions made regarding the effect of RSR on measurement differences and NDVI derived from different remote sensing systems. Land cover types generally have reflectance characteristics that can be used to group similar signatures to understand the effect of RSR on spectral band measurements. Groupings include signatures that have flat, increasing, decreasing, or step functions profiles within bands, as well as classifications such as manmade materials, soil, water, snow, and vegetation. Generally, for most signature groupings, differences between sensors increased with increasing slope and magnitude of land cover reflectance signatures, but exceptions to this were observed. Examination of signature by characteristic or classification type provided an understanding of the level of error that can be expected between band measurements from different sensors.

Reflectance Determination

Conversion of band radiance to reflectance values minimizes differences between sensor measurements; however, the inconsistencies in conversion methods can result in a small induced error if reflectance value determination is not performed correctly. This was observed in the data analysis in this study. A small error was introduced in planetary reflectance calculations due to the different mathematical averaging methods employed in reflectance calculations between sensor radiance in the numerator and average band pass

of the RSR in the denominator. This error increased as averaged convolved signature, RSR, and solar irradiance deviated from the average spectral band response. The resulting error is small compared to the error introduced by differences in RSR between sensors if not accounted for by conversion to planetary reflectance. The error, generally appears to be less than 1% between sensor measurements for typical vegetation types, but can be greater for very high reflectance signatures such as snow. These errors for vegetation signatures did not have a significant effect on NDVI differences between sensors. It has a minor effect due to the over estimation of some bright targets, which leads to a shift in signature red and near infrared reflectance in relation to isolines of NDVI error. To avoid this error in future sensor comparisons, caution must be taken in converting to reflectance values and methods need to be internally consistent for each sensor and between sensors as well.

Two approaches can be used that effectively address this error (Liang, 2005; Markham, 2005). One approach is to normalize the numerator in Equation 6 with the integrated response (Equation 10) instead of by bandwidth for reflectance calculations (Equation 2).

$$\rho_p = \frac{\pi * L_{band} * d^2}{ESUN_{band} * \cos(\theta s)} \qquad \text{Equation 2}$$

$$L_{band} = \frac{\Sigma\,(RSR_\lambda * \text{Solar Irradiance}_\lambda * \text{Target Reflectance}_\lambda) * \Delta\lambda}{\text{Bandwidth}_{band}} \qquad \text{Equation 6}$$

$$L_{band} = \frac{\Sigma\,(RSR_\lambda * \text{Solar Irradiance}_\lambda * \text{Target Reflectance}_\lambda) * \Delta\lambda}{\Sigma(RSR_\lambda)} \qquad \text{Equation 10}$$

Another method to address this error is to obtain reflectance values by using the total irradiance values (the numerator) in Equation 6 for L_{band} as long as only the numerator in $ESUN_{band}$ calculations is used in the determination of (Equation 3).

$$\mathbf{ESUN_{band}} = \frac{\mathbf{\Sigma(RSR_\lambda * Solar\ Irradiance_\lambda) * \Delta\lambda}}{\mathbf{\Sigma\ (RSR_\lambda) * \Delta\lambda}} \qquad \text{Equation 3}$$

In this case, both at sensor irradiance and ESUN values are in terms of W m^{-2} not normalized to wavelength (W $m^{-2}\mu m^{-1}$). This results in using the following definitions of L_{band} (Equation 11) and $ESUN_{band}$ (Equation 12) in reflectance calculations (Equation 2).

$$\mathbf{L_{band} = \Sigma\ (RSR_\lambda * Solar\ Irradiance_\lambda * Target\ Reflectance_\lambda) * \Delta\lambda} \qquad \text{Equation 11}$$

$$\mathbf{ESUN_{band} = \Sigma(RSR_\lambda * Solar\ Irradiance_\lambda) * \Delta\lambda} \qquad \text{Equation 12}$$

Cross-Sensor Calibration

Cross-sensor calibration generally lead to reduced differences in the range of land cover signature measurements between sensors, however, this was not true in all cases as some cross-sensor calibrated signature value differences became greater.

Quantitative Effects on Accuracy and Consistency of NDVI

Question 2: what are the quantitative effects of these factors on the accuracy and consistency of NDVI measurements of vegetation from different remote sensing sensors? Despite the factors of RSR that interact in a complex way and contribute to measurement

discrepancies between different sensors, nevertheless, result show that a surprisingly large number of signature comparisons resulted in NDVI differences of less than 0.050. Only when RSRs were extremely different and red or near infrared values were very low, did differences between RSRs lead to measurement discrepancies that effected NDVI greater than 0.050. The average error between all sensors for all vegetation types was 0.023. All sensor comparisons lead to measurement discrepancies greater than 0.010 for at least one very low NDVI signature and beyond 0.0050 for at least one other signature.

The quantitative effect of RSR factors on the accuracy and consistency of NDVI measurements of vegetation from different remote sensing sensors is directly related to the red and near infrared band values of signatures in relation to isolines of NDVI error (Figure 37 and Figure 38). While the effect of RSR and coupled factors of error varied throughout reflectance comparisons; the effect on NDVI error consistently increased between sensors as red and near infrared band values decreased. This factor was dominant and could be used to predict the general effect of differences in NDVI values from band measurement discrepancies between different remote sensing systems.

Significance of Differences in RSR on NDVI

Question 3: How significant are differences in RSR to measurement variability of NDVI between a range of standard Earth observation sensors in use today as well as systems in the future? The significance of variation in system RSRs in conjunction with land cover type was analyzed in depth in this study. The null hypothesis posed in Chapter 2 that the magnitude of the effect of differing RSR on NDVI measurements of vegetation derived

from different sensors is below 0.050 uncertainty was shown to be invalid. However, differences between sensors, even with very different RSRs, resulted in an effect on NDVI less than this 0.050 for 60% of the vegetation signatures studied in this investigation. The combination of very different RSRs in conjunction with sensitivity of NDVI error to certain signature red and/or near infrared band differences between sensors was the cause of errors greater than 0.050.

This research has shown that it is possible to have and effect on NDVI equal to or less than 0.01 when sensor spectral response profiles are extremely well aligned, as in the theoretical square wave response vs. the actual MODIS and Landsat 7 ETM+ responses. For direct comparisons of actual sensors such as Landsat 7 ETM+ and MODIS with similar but not identical response functions, error between sensor measurements for a number of vegetation types fall between 1 and 2%.

Comparison with Previous Studies

The results of this study are consistent with findings of previous research related to the effect of the RSR on NDVI, and provide additional insights into these studies. This research differed from most previous empirical studies, in that it examined the theoretical basis for differences in NDVI between sensors. Mechanisms that lead to differences in band measurements were identified and their effect on NDVI quantified based on NDVI sensitivity to band measurements. Theoretical findings were validated in a sensor simulation study.

Gallo and Daugherty (1987a) observed greater variability between minimum values of NDVI for both ground and satellite observations. This variability was attributed to differences in RSR. The current study demonstrates that the sensitivity of NDVI to differences at lower red and near infrared reflectance values, generally related to low NDVI values, was a significant factor in these elevated differences at low NDVI. The 1987 study also found that based on agronomic variables, AVHRR9 could estimate NDVI of Landsat 5 multi-spectral scanner (MSS) as effectively as direct use of MSS. This was attributed to similar RSRs of these two sensors. AVHRR9, on the other hand, did not estimate well NDVI for the SPOT and Landsat 5 Thematic Mapper (TM) sensors that had very different RSRs. These study results are completely consistent with the current study findings.

Teillet et al. (1997) found that bandwidths greater than 50nm, particularly in the red band, had a significant effect on vegetation index values of forested regions attributed to spectral band capture of the red edge and a portion of the green edge. The current study supports this finding and adds that small differences in measurement values between sensors can have a significant effect on NDVI due to NDVI sensitivity to low red reflectance values typical of forested areas.

Stevens et al.(2003) concluded that vegetation indices may be inter-converted to a precision of 1-2% for a wide range of sensors based on examination of two cultivated crops. For a similar range of sensors, the current study resulted in maximum error between sensors as high as 4% for the Cropland and Crop Mosaic signatures. The

average error for all vegetation determined in the current study was 2.3% and errors for other land cover signatures were higher in a number of cases, which indicates that the precision of NDVI error between sensors could be higher for other inter-comparison of other land cover types.

The current study findings are also consistent with the investigation of the effects of spectral response function on NDVI measured with moderate resolution satellite sensors by Trishchenko et al. (2002). The suite of sensors used in their study included both MODIS and AVHRR9. They found higher differences between sensors, up to 25% in red band reflectance, compared to a maximum of 4% for the near infrared band. This phenomenon of higher relative red band differences between sensors was observed in this current study as small absolute differences became large relative differences as reflectance levels decreased. Their findings of -0.02 to 0.06 effect on NDVI due to RSR match well with the current study findings of an average RSR effect on NDVI of 0.023 with a maximum difference of up to 0.06.

Delimitations

This study examined the isolated factor of the effect of RSR differences on land cover measurements and their effect on NDVI. The effects of other factors that contribute to error between sensor measurements, such as sensor calibration, Earth-sun-sensor geometry, spatial resolution, MTF, or atmospheric effects were not considered in this study. The effect of different pre-processing steps of sensor data was also not considered in this study. Additionally, the effect on NDVI from measurement discrepancies between

sensors of mixed pixels was not examined; only pure target signatures were used. Alternative metrics to NDVI were also not investigated and does not preclude the possibility that other vegetation indices or metrics may be less sensitive to the vagaries of measurement differences between sensors.

Suggestions for Future Research

A number of interesting research questions were suggested by the results of this study. First, while the error due to the method of conversion of planetary reflectance used in this study is small, future research that eliminates this error could provide improved error estimates between sensor measurements due to RSR differences. Second, what is the quantitative effect on band measurement differences between sensors with improved calibration techniques? Inter sensor calibration was based on full signature data measurements between sensors which lead to increased band differences for some land cover signatures. Calibration based on only land cover types of interest, i.e. only green vegetation, may lead to improved relationships between sensor band measurements and subsequent measures of NDVI. Lastly, can a reference RSR be established in order to provide a better standard of comparison for past, present, and future multi-spectral systems? Uncorrected substantial differences between sensor systems lead to significantly biased estimates of any biophysical parameters derived from them (Steven et al., 2003). This is why cross-sensor calibration is performed. However, it was observed in the course of this research that cross-sensor calibration only removed the bias between sensor responses with no reference to a true standard. As sensor systems come and go; only cross-sensor studies will provide relationships between specific sets of

sensors. As techniques and capabilities in data processing improve, and the number of remote sensing systems and available data increase, a reference standard could provide a basis of comparison and common spectral metric for remotely sensed data. The definition of mutually agreed upon standards has been key in the progress of science and could potentially benefit the long history and future record of remotely sensed data application. This concept is not unlike the development of the universal standard for temperature measurement. Previous to the defined standard, different scale divisions, often based on different reference points, made it impossible to accurately convert temperature measurements and at times, impossible to compare temperatures of different places (Middletons, 1966).

Bibliography

AFRL (1999) MODTRAN. Air Force Research Laboratories (AFRL), Space Vehicles Directorate, Albuquerque.

Bailey, G.B., Lauer, D.T., & Carneggie, D.M. (2001) International collaboration: the cornerstone of satellite land remote sensing in the 21st century. *Space Policy*, *17*, 161-169.

Bannari, A., Morin, D., Bonn, F., & Huete, A.R. (1995) A review of vegetation indices. *Remote Sensing Reviews*, *13*, 95-120.

Baret, F. & Guyot, B. (1991) Potentials and limits of vegetation indices for LAI and APAR assessment. *Remote Sensing of Environment*, *35*, 161-173.

Billings, W.D. & Morris, R.J. (1951) Reflection of visible and infrared radiation from leaves of different ecological groups. *American Journal of Botany*, *38*(5), 327-331.

Brown, M.E., Pinzon, J.E., Morisette, J.T., Didan, K., & Tucker, C.J. (2005) Inter-sensor validation of long-term NDVI time series from AVHRR, SPOT-Vegetation, SeaWIFS, MODIS, and Landsat ETM+. *IEEE Transactions Geoscience and Remote Sensing*, *in review*.

Bruzzone, H. & Moreno, C. (1998) When errors in both coordinates make a difference in the fitting of straight lines by least squares. *Measurement Science and Technology*, *9*, 2007-2011.

Cahoon, D.R., Stocks, B.J., Alexander, M.E., Baum, B.A., & Goldammer, J.G. (2000) Wildland fire detection from space: theory and application, pp 151-169. Kluwer Academic Publishers, Boston.

Chander, G., Meyer, D.J., & Helder, D.L. (2004) Cross calibration of the Landsat-7 ETM+ and EO-1 ALI Sensor. *IEEE Transactions Geoscience and Remote Sensing*, *42*(12), 2821-2831.

Chaurasia, S. & Dadhwal, V.K. (2004) Comparison of principal component inversion with VI-empirical approach for LAI estimation using simulated reflectance data. *International Journal of Remote Sensing*, *25*(14), 2881-2887.

Chilar, J. (2000) Land cover mapping of large areas from satellites: status and research priorities. *International Journal of Remote Sensing*, *21*(6&7), 1093-1114.

Chilar, J., Tcherednichenko, I., Latifovic, R., Li, Z., & Chen, J. (2001) Impact of variable atmospheric water vapor content on AVHRR data corrections over land. *IEEE Transactions on Geoscience and Remote Sensing*, *39*(1), 173-180.

Choudhury, B.J. (1987) Relationships between vegetation indices, radiation absorption, and net photosynthesis evaluated by a sensitivity analysis. *Remote Sensing of Environment*, *22*, 209-233.

Colwell, R.N. (1960) Manual of photographic interpretation, pp 868. American Society of Photogrammetry, Washington, DC.

Curran, P.J. (1983) Multispectral remote sensing for the estimation of green leaf area index. *Philosophical Transactions of the Royal Society, Series A*, *309*, 257-270.

Deering, D.W. & Haas, R.H. (1980). Using Landsat Digital Data for Estimating Green Biomass, Rep. No. TM-80727. NASA, Greenbelt.

Deering, D.W., Rouse, J.W., Jr., Haas, R.H., & Schell, J.S. (1975). Measuring forage production of grazing units from Landsat MSS data. In *Proceedings 10th International Symposium Remote Sensing Environment*, pp. 1169-1178. Environmental Research Institute of Michigan, Ann Arbor, Michigan.

DeFries, R.S. & Belward, A.S. (2000) Global and regional land cover characterization from satellite data: an introduction to the Special Issue. *International Journal of Remote Sensing*, *21*(6), 1083-1092.

Digital-Globe (2004) QuickBird Imagery Products, Product Guide, Vol. 2004.

Dinguirard, M. & Slater, P.N. (1999) Calibration of space-multispectral Imaging Sensors: A Review. *Remote Sensing of Environment*, *68*, 194-205.

Dymond, J.R., Shepherd, J.D., & Qi, J. (2001) A simple physical model of vegetation reflectance for standardising optical satellite imagery. *Remote Sensing of Environment*, *77*, 230-239.

El Saleous, N.Z., Vermote, E.F., Justice, C.O., Townshend, J.R.G., Tucker, C.J., & Goward, S.N. (2000) Improvements in the global biospheric record from the Advanced Very High Resolution Radiometer (AVHRR). *International Journal of Remote Sensing*, *21*(6&7), 1251-1277.

Forshaw, M.R.B., Haskell, A., Miller, P.F., Stanley, D.J., & Townshend, J.R.G. (1983) Spatial resolution of remotely sensed imagery. A review paper. *International Journal of Remote Sensing*, *4*(3), 497-520.

Gallo, K.P. & Daughtry, C.S.T. (1987a) Differences in vegetation indices for simulated Landsat-5 and TM, NOAA-9 AVHRR and SPOT-1 sensor systems. *Remote Sensing of Environment*, *23*(439-452).

Gallo, K.P. & Daughtry, C.S.T. (1987b) Differences in vegetation indices for simulated landsat-5 and TM, NOAA-9 AVHRRa nd SPOT-1 sensor systems. *Remote Sensing of Environment*, *23*(439-452).

Gamon, J.A., Huemmrich, K.F., Peddle, D.R., Chen, J., Fuentes, D., Hall, F.G., Kimbal, J.S., Goetz, S., Gu, J., McDonald, K.C., Miller, J.R., Moghadam, M., Rahman, A.F., Roujean, J.-L., Smith, E.A., Walthall, C.L., Zarco-Tejada, P., Hu, B., Fernandes, R., & Chilar, J. (2004) Remote Sensing in BOREAS: Lessons learned. *Remote Sensing of Environment*, *89*, 139-162.

Gates, D.M., Keegan, H.J., Schleter, J.C., & Weidner, V.R. (1965) Spectral properties of plants. *Applied Optics*, *4*, 11-20.

Goetz, S.J. (1997) Multi-sensor analysis of NDVI, surface temperature and biophysical variables at a mixed grassland site. *International Journal of Remote Sensing*, *18*(1), 71-94.

Goward, S.N., Davis, P.E., Fleming, D., Miller, L., & Townshend, J.R. (2003) Empirical comparison of Landsat 7 and IKONOS multispectral measurements for selected Earth Observation System (EOS) validation sites. *Remote Sensing of Environment*, *88*, 80-99.

Goward, S.N., Dye, D.G., Turner, S., & Yang, J. (1993) Objective assessment of the NOAA Global Vegetation Index data product. *International Journal of Remote Sensing*, *14*(18), 3365-3394.

Goward, S.N. & Hummerrich, K.F. (1992) Vegetation canopy PAR absorptance and the Normalized Difference Vegetation Index: An assessment sing the SAIL model. *Remote Sensing of Environment*, *39*, 119-140.

Goward, S.N., Markham, B., Dye, D.G., Dulaney, W., & Yang, J. (1991) Normalized difference vegetation index measurements from the advanced very high resolution radiometer. *Remote Sensing of Environment*, *35*, 257-277.

Guyot, G. & Gu, X.F. (1994) Effect of radiometric corrections on NDVI-determined from SPOT HRV and Landsat TM data. *Remote Sensing of Environment*, *49*, 169-180.

Harrison, L.C., Berndt, J.L., Kiedron, P.W., Michalsky, J.J., Min, Q., & Schlemmer, J. (2003) Extraterresrial solar spectrum 360-1050 nm from rotating shadowband spectroradiometer measurements at the Southern Great Plains (ARM) site. *Journal of Geophysical Research*, *108*(D14), 4424.

Hastings, D.A. & Emery, W.J. (1992) The Advanced Very High Resolution Radiometer (AVHRR): A Brief Reference Guide, Vol. 2005. NOAA.

Hook, S.J. (1998) ASTER Spectral Library, Vol. 2002. JPL.

Huete, A., Didan, K., Miura, T., Rodriguez, E.P., Gao, X., & Ferreira, L.G. (2002) Overview of the radiometric and biophysical performance of the MODIS vegetation indices. *Remote Sensing of Environment*, *83*, 195-213.

Huete, A.R. (1988) A Soil-Adjusted Vegetation Index (SAVI). *Remote Sensing of Environment*, *25*, 295-309.

Hummrich, K.F. & Goward, S.N. (1997) Vegetation canopy PAR absorptance and NDVI: An assessment for ten tree species with the SAIL model. *Remote Sensing of Environment*, *61*, 254-269.

Jackson, R.D. (1983) Spectral indices in n-space. *Remote Sensing of Environment*, *13*, 1401-1429.

Jacobsen, A., Heidebrecht, K.B., & Goetz, A.F.H. (2000) Assessing the quality of the radiometric and spectral calibration of CASI data and retrieval of surface reflectance factors. *Photogrammetric Engineering & Remote Sensing*, *66*(9), 1083-1091.

Jensen, J.R. (1996) Introductory digital image processing: a remote sensing perspective, 2nd edn., pp 318. Prentice-Hall, Inc, Upper Saddle River.

Jordan, C.F. (1969) Derivation of leaf area index from quality of light on the forest floor. *Ecology*, *50*(4), 663 - 666.

Justice, C., Belward, A., Morisette, J., Lewis, P., Privette, J., & Baret, F. (2000) Developments in the 'validation' of satellite sensor products for the study of the land surface. *International Journal of Remote Sensing*, *21*(17), 3383-3390.

Kahane, L.H. (2001) Regression Basics, pp 201. Sage Publications, Inc, Thousand Oaks.

Kaufman, Y. & Tanré, D. (1992) Atmospherically Resistant Vegetation Index (ARVI). *Institute for Electrical and Electronics Engineers Transactions on Geosciences and Remote Sensing*, *30*(2), 261-270.

Kauth, R.J. & Thomas, G.S. (1976). The tasseled cap - a graphic description of the spectral-temporal development of agricultural crops as seen by Landsat. In *10th Symposium on Machine Processing of Remotely Sensed Data*, pp. 41-51. Purdue University, West Lafayette, Indiana.

Kramer, H.J. (1996) Observation of the Earth and Its Environment, Survey of Missions and Sensors, 3rd edn., pp 960. Springer, Berlin.

Liang, S. (2004) Quantitative Remote Sensing of Land Surfaces, pp 534. John Wiley & Sons, New Jersey.

Liang, S. (2005) Radiance to Reflectance Calculations, College Park.

LPSO (1998) Landsat-7 Science Data User's Handbook, Vol. 2004. Landsat Project Science Office.

Marburger III, J.H. (2004). Landsat Data Continuity Strategy. Executive Office of the President, Office of Science and Technology Policy, Washington, D.C.

Markham, B. (2005) Radiance to Reflectance Conversion, Greenbelt.

Masek, J.G., Honzak, M., Goward, S.N., Liu, P., & Pak, E. (2001) Landsat-7 ETM+ as an observatory for land cover Initial radiometric and geometric comparisons with Landsat-5 Thematic Mapper. *Remote Sensing of Environment*, *78*, 118-130.

Middletons, W.E.K. (1966) A History of the Thermometer and its Use in Meteorology, pp 249. Johns Hopkins Press, Baltimore.

NASA (2003). Landsat Data Continuity Mission (LDCM) Implementation Phase, Data Specification, Rep. No. 427-14-01-003. NASA, Goddard Space Flight Center, Greenbelt.

Nieke, J. & Fukushima, H. (2001) Selection of a solar reference spectrum for GLI's reflective bands. *Applied Optics*, *Draft to be submitted*.

NOAA (2004) Advanced Very High Resolution Radiometer (AVHRR): Overview, Vol. 2004.

Pagnutti, M., Ryan, R.E., kelly, M., Holekamp, K., Zanaoni, V., Thome, K., & Schiller, S. (2003) Radiometric characterization of IKONOS multispectral imagery. *Remote Sensing of Environment*, *88*, 53-68.

Pearson, K. (1901) On lines and planes of closest fit to systems of points in space. *Philos. Mag.*, *6*(2), 559-572.

Peltzer, E.T. (2000) Matlab shell-scripts for linear regression analysis, Model II regressions, Vol. 2002. www.mbari.org/~etp3/regressindex.htm.

Perry, C.R., Jr. & Lautenschlager, L.F. (1984) Functional equivalence of spectral vegetation Indices. *Remote Sensing of Environment*, *14*, 169-182.

Pinty, B., Leprieur, C., & Verstraete, M.M. (1993) Towards a quantitative interpretation of vegetation indices. Part 1: Biophysical canopy properties and classical indices. *Remote Sensing Reviews*, *7*, 127-150.

Press, W.H., Teukolsky, S.A., Vetterling, W.T., & Flannery, B.P. (1992) Numerical recipes in fortran 77, the art of scientific computing, 2 edn., pp 934. Cambridge University Press, Cambidge.

Price, J.C. (1987) Calibration of satellite radiometers and the comparison of vegetation indices. *Remote Sensing of Environment*, *21*, 15-27.

Qin, W., Gerstl, S.A.W., Deering, D.W., & Goel, N.S. (2002) Characterizing leaf geometry for grass and crop canopies from hotspot observations: A simulation study. *Remote Sensing of Environment*, *80*, 100-113.

Rao, C.R.N. & Chen, J. (1995) Inter-satellite calibration linkages for the visible and near-infrared channels of the Advanced Very High Resolution Radiometer on the NOAA 7, -9, -11 spacecraft. *International Journal of Remote Sensing*, *16*, 1931-1942.

Reeves, R.G., ed. (1975) Manual of Remote Sensing, 1st edn, pp 2123. American Society of Photogrammetry, Falls Church, Virginia.

Richards, J.A. & Jia, X. (1999) Remote Sensing Digital Image Analysis, An Introduction, 3rd edn., pp 363. Springer-Verlag, New York.

Rondeaux, G., Steven, M.D., & Baret, F. (1996) Optimization of soil adjusted vegetation indices. *Remote Sensing of Environment*, *55*(95-107).

Rouse, J.W., Haas, R.H., Schell, J.A., & Deering, D.W. (1973). Monitoring vegetation systems in the great plains with ERTS. In *Third ERTS Symposium*, Vol. I, pp. 309-317. NASA.

Sample, N.O.L.S. (2004) The Landsat Program, Vol. 2005. NASA.

Schott, J.R. (1997) Remote Sensing, The Image Chain Approach, pp 394. Oxford University Press, New York.

Secker, J., Staenz, K., Budkewitsch, P., & Neville, R.A. (1999). A vicarious calibration of the Probe-1 hyperspectral sensor. In *4th International airborne remote sensing conference and exhibition / 21st Canadian symposium on remote sensing*, pp. 21-24, 75-82, Ottawa, Ontario, Canada.

Sinclair, T.R., Hoffer, R.M., & Schreiber, M.M. (1971) Reflectance and internal structure of leaves from several crops during a growing season. *Agron. J.*, *63*, 864-868.

Slater, P.N. (1979) A re-examination of the Landsat MSS. *Photogram. Eng. Remote Sens.*, *45*, 1479-1495.

Space-Imaging (2004) Ikonos Imagery Products and Product Guide, Vol. 2004.

Steven, M.D., Malthus, T.J., Baret, F., Xu, H., & Chopping, M.J. (2003) Intercalibration of vegetation indices from different sensor systems. *Remote Sensing of Environment*, *88*, 412-422.

Taylor, M. (2005) IKONOS Planetary Reflectance and mean Solar Exoatmospheric Irradiance, Vol. 2005. Space Imaging.

Teillet, P.M., Barker, J.L., Markham, B.L., Irish, R.R., Fedosejevs, G., & Storey, J.C. (2001) Radiometric cross-calibration of the Landsat-7 ETM+ and Landsat-5 TM sensors based on tandem data sets. *Remote Sensing of Environment*, *78*, 39-54.

Teillet, P.M., Staenz, K., & Williams, D.J. (1997) Effects of spectral, spatial, and radiometric characteristics of remote sensing vegetation indices of forest areas. *Remote Sensing of Environment*, *61*(1), 139-149.

Townshend, J.R.G., Huang, C., Kalluri, S.N.V., DeFries, R.S., & Liang, S. (2000) Beware of per-pixel characterization of land cover. *International Journal of Remote Sensing*, *21*(4), 839-843.

Trishchenko, A.P., Cihlar, J., & Li, Z. (2002) Effects of spectral response function on surface reflectance and NDVI measured with moderate resolution satellite sensors. *Remote Sensing of Environment*, *81*, 1-18.

Tucker, C.J. (1979) Red and photographic infrared linear combinations for monitoring vegetation. *Remote Sensing of Environment*, *8*, 127-150.

Tucker, C.J. & Garratt, M.W. (1977) Leaf optical system modeled as a stochastic process. *Applied Optics*, *16*, 635-642.

Turner, D.P., Cohen, W.B., Kennedy, R.E., Fassnacht, K.S., & Briggs, J.M. (1999) Relationships between leaf area index and Landsat TM spectral vegetation indices across three temperate zone sites. *Remote Sensing of Environment*, *70*(1), 52-68.

USGS (2004) Earthshots: Satellite Images of Environmental Change, Vol. 2004.

Vogelmann, J.E., Helder, D., Morfitt, R., Choate, M.J., Merchant, J.W., & Bulley, H. (2001) Effects of Landsat 5 Thematic Mapper and Landsat 7 Enhanced Thematic Mapper Plus radiometric and geometric calibrations and corrections on landscape characterization. *Remote Sensing of Environment*, *78*, 55-70.

Wiegand, C.L. & Richardson, A.J. (1984) Leaf area, light interception and yield estimates from spectral components analysis. *Agron. J.*, *76*, 543-548.

Wooley, J.T. (1971) Reflectance and transmittance of light by leaves. *Plant Physiology*, *47*, 656-662.

Zanoni, V.M. & Goward, S.M. (2003) A new direction in Earth observations from space: IKONOS. *Remote Sensing of Environment*, *88*, 1-2.